NASA TECHNICAL MEMORANDUM

NASA TM X-1469

NASA TM X-1469

WIND-TUNNEL INVESTIGATION OF THE FLOW FIELD BENEATH THE FUSELAGE OF THE X-15 AIRPLANE AT MACH NUMBERS FROM 4 TO 8

by Earl J. Montoya and Murray Palitz

Flight Research Center
Edwards, Calif.

NATIONAL AERONAUTICS AND SPACE ADMINISTRATION • WASHINGTON, D. C. • NOVEMBER 1967

NASA TM X-1469

WIND-TUNNEL INVESTIGATION OF THE FLOW FIELD BENEATH THE FUSELAGE OF THE X-15 AIRPLANE AT MACH NUMBERS FROM 4 TO 8

By Earl J. Montoya and Murray Palitz

Flight Research Center
Edwards, Calif.

NATIONAL AERONAUTICS AND SPACE ADMINISTRATION

For sale by the Clearinghouse for Federal Scientific and Technical Information
Springfield, Virginia 22151 – CFSTI price $3.00

WIND-TUNNEL INVESTIGATION OF THE FLOW FIELD BENEATH THE FUSELAGE OF THE X-15 AIRPLANE AT MACH NUMBERS FROM 4 TO 8

By Earl J. Montoya and Murray Palitz
Flight Research Center

SUMMARY

Wind-tunnel data were obtained on the local flow field beneath the fuselage of a model of the X-15 airplane approximately 5 to 8 fuselage diameters aft of the model nose from the model surface to the bow shock. Multiple-tube rakes, model surface pressure orifices, and a cone probe were used to survey the flow field. The cone probe was used to obtain Mach numbers in the flow field up to a free-stream Mach number of 6 and to obtain flow angularity up to a Mach number of 8. Test results were obtained at free-stream Mach numbers from 4 to 8 and angles of attack from -3° to 20° and were compared with theory and flight data.

Results indicate that Mach number, impact pressure, and flow-angularity gradients exist between the vehicle's surface and the bow shock. These gradients generally become larger with both increased angle of attack and Mach number. Good agreement with theoretical results at zero angle of attack was obtained.

Mass flow through a proposed hypersonic ramjet engine inlet positioned beneath the X-15 was determined by using both a two-dimensional oblique-shock-wave assumption and wind-tunnel results. The two-dimensional oblique-shock assumption predicted a larger inlet mass flow than was obtained from the wind-tunnel data. The local-flow-field gradients across the assumed inlet are discussed.

INTRODUCTION

The successful development of future hypersonic vehicles (see refs. 1 to 3) in which air-breathing propulsion systems will be used will, in part, depend on an understanding of three-dimensional vehicle flow fields and an ability to predict these flow fields. To attain the necessary high propulsion-system efficiencies and to properly integrate the airframe and propulsion system on these vehicles, flow-field information will be required (refs. 4 to 6). At present, very little three-dimensional flow-field information is available on bodies that may be representative of present or future vehicles.

This lack of flow-field information was brought to light on a research program involving the X-15 airplane in which a ramjet engine will be flight tested at Mach numbers from 4 to 8 (ref. 7). The ramjet will be mounted on the modified lower ventral fin of the airplane and, thus, will be affected by the flow field of the airplane. Knowledge of this flow field will assist in the design of the inlet and other portions of the ramjet and will help in interpreting flight data from this experiment. Since the required X-15 flow-field information was not available, a series of wind-tunnel tests was conducted at the Arnold Engineering Development Center (AEDC) and the NASA Langley Research Center (LRC) to obtain the local-flow-field Mach numbers, flow angles, and impact pressures in the region ahead of the X-15 ventral fin at zero angle of sideslip. In addition, schlieren photographs were obtained from tests at the NASA Jet Propulsion Laboratory (JPL) and the Langley Research Center.

This paper presents some of the results of these studies not previously reported in references 8 and 9 and extends the analysis to parameters that may be useful in the X-15 ramjet program. The wind-tunnel data are compared with theoretical results and X-15 flight data.

SYMBOLS

The units used for the physical quantities in this paper are given in U. S. Customary Units and parenthetically in the International System of Units (SI). Factors relating the two systems are presented in reference 10.

A	area, feet^2 (meters^2)
D	maximum fuselage diameter of one-fifteenth-scale model, 3.73 inches (9.48 centimeters)
M	free-stream Mach number
m	mass flow, pounds/second (kilograms/second)
N_{Re}	Reynolds number
p	static pressure, pounds per square inch absolute (meganewtons per meter^2)
p_a, p_b, p_c, p_d	cone static pressure at orifices a, b, c, and d, respectively (see fig. 5)
$\bar{p}_c$	average cone static pressure, $\frac{p_a + p_b + p_c + p_d}{4}$, pounds per square inch absolute (meganewtons per meter^2)
p_i	total pressure behind the normal shock, pounds per square inch absolute (meganewtons per meter^2)
p_t	total pressure, pounds per square inch absolute (meganewtons per meter^2)

$\Delta p_c = \frac{p_a - p_c}{2}$, pounds per square inch absolute (meganewtons per meter^2)

$\Delta p_{\sigma} = \frac{p_b - p_d}{2}$, pounds per square inch absolute (meganewtons per meter^2)

x — longitudinal distance (station) from model nose, inches (centimeters)

y — lateral distance from plane of symmetry, inches (centimeters)

z — normal (perpendicular to centerline) distance from fuselage lower surface (see fig. 2(b)), inches (centimeters)

α — angle of attack, degrees

β — angle of sideslip, degrees

θ — shock-wave angle, degrees

ϵ — angle of upwash with respect to horizontal plane of model, degrees (see fig. 13)

σ — angle of sidewash with respect to vertical plane of model, degrees (see fig. 13)

Subscripts:

1 — rake probe on centerline

2,3,4,5 — first to fourth rake probes off centerline

l — local

∞ — free stream

MODELS

Flow-field pressure surveys at the Arnold Engineering Development Center and the Langley Research Center were conducted about a one-fifteenth-scale X-15 heat-transfer and pressure model. This model is 39.28 inches (99.79 centimeters) long and has flush surface orifices which are connected to pressure sensors. All fuselage surface pressure data were obtained with this model. Figure 1 shows the locations of the static-pressure orifices used. References 11 and 12 give additional information on the model.

Schlieren photographic data were obtained with a one-fifteenth-scale X-15 force model (refs. 13 and 14) and several one-fiftieth-scale X-15 models (refs. 15 to 17). The models differed in full-scale airplane length by 29 inches (73.66 centimeters). The schlieren data were adjusted to correct for this difference.

WIND TUNNELS

The following table summarizes important characteristics of the wind-tunnel facilities used to obtain flow-field pressure surveys in this study. More detailed information on the tunnels is presented in reference 18 (AEDC) and reference 19 (LRC).

	von Kármán Gas Dynamics Facility		Langley 4- by 4-foot Unitary Plan tunnel, test section 2
	Tunnel A	Tunnel B	
Type	Continuous flow, closed circuit, variable density	Continuous flow, closed circuit, variable density	Continuous flow, asymmetric sliding block
Test-section shape	Square	Circular	Square
Test-section dimensions	40 in. (101.7 cm)	50 in. diameter (127 cm)	4 ft (122 cm)
Mach number range	1.5 to 6.0	8	2.29 to 4.65

Schlieren photographic data were obtained from the 20-inch (50.8 centimeters) supersonic tunnel and the 21-inch (53.3 centimeters) hypersonic tunnel at the Jet Propulsion Laboratory. The construction and operating conditions of these tunnels are described in reference 20. Schlieren photos were also obtained from the LRC tests; reference 21 describes the system used.

TESTS

Pressure surveys at several longitudinal locations on the models were made at AEDC (M = 4, 6, and 8) and at LRC (M = 4.65). The average tunnel test conditions were as follows:

M	Stagnation pressure, psia (MN/m^2)	Stagnation temperature, °R (°K)	N_{Re} per foot (meter)	Impact pressure (free stream), psia (MN/m^2)	Static pressure (free stream) psia (MN/m^2)
4	40.4 (0.279)	560 (311)	3.50×10^6 (1.15×10^7)	5.60 (0.0386)	0.266 (0.0018)
4.65	54 (.372)	760 (422)	3.40 (1.12)	4.39 (.0303)	.155 (.0011)
6	140 (.965)	710 (394)	3.46 (1.14)	4.15 (.0286)	.089 (.0006)
8	800 (5.52)	1350 (750)	3.40 (1.12)	6.79 (.0469)	.082 (.0006)

Static pressures were measured along the bottom centerline of the model (locations shown in fig. 1). In addition, the probes illustrated in figure 2(a) were used to survey the flow field beneath the model (fig. 2(b)). The two-probe rake was used in the LRC tests and the other probes in the AEDC tests. The probes could be moved forward and rearward and upward and downward and could also be pitched to maintain the same angle of attack as the model. The surveys were extended past the bow shock, when possible, to measure the free-stream impact pressure. Figure 3 shows a typical model installation in the AEDC von Kármán Gas Dynamics Facility Tunnel A. The following table shows the relative positions at which the probe measurements were made. The tests were at zero angle of sideslip.

M	Probe	y/D	x/D, α, deg					
			-3	0	5	10	14.5	20
4	Five-probe rake	-----	----	5.36	5.36	5.36	5.36	----
		-----	----	6.43	6.43	6.43	6.43	----
		-----	----	7.77	7.77	7.77	7.77	----
	Cone	0	5.36	5.36	5.36	----	----	----
		0	6.43	6.43	6.43	6.43	----	----
		0	7.37	7.37	7.37	7.37*	----	----
		0.536	7.37	7.37	7.37	7.37	----	----
4.65	Two-probe rake	0	----	6.16	6.16	6.16	----	6.16
		0	----	7.77	7.77	7.77	----	7.77
		0.401	----	6.16	----	6.16	----	6.16
		.401	----	7.77	----	7.77	----	7.77
		0.804	----	6.16	----	6.16	----	----
		.804	----	7.77	----	7.77	----	----
6	Five-probe rake	-----	----	5.36	5.36	5.36	----	----
		-----	----	6.43	----	6.43	6.43	----
		-----	----	7.37	7.37	----	----	----
		-----	----	7.77	7.77	7.77	7.77	----
	Cone	0	----	5.36	5.36	5.36	5.36	----
		0	6.43	6.43	6.43	6.43	6.43	----
		0	7.37	7.37	7.37	7.37	7.37	----
		0.268	----	6.43	6.43	6.43	6.43	----
		.268	----	7.37	7.37	7.37	7.37	----
		0.536	----	6.43	6.43	6.43	----	----
		.536	7.37	7.37	7.37	7.37	7.37	----
8	Four-probe rake	-----	6.16	6.16	6.16	6.16	----	6.16
		-----	6.96	6.96	6.96	6.96	----	6.96
		-----	7.77	7.77	7.77	7.77	----	7.77
	Cone	0	----	6.16	6.16	6.16	----	6.16
		0	----	6.96	6.96	6.96	----	6.96
		0	7.37	7.37	7.37	----	----	7.37
		0.268	5.36	5.36	5.36	----	----	----
		.268	----	6.16	6.16	----	----	----
		.268	6.96	6.96	6.96	----	----	----
		.268	----	7.37	7.37	----	----	----

*α = 10.5°

Schlieren photographs were obtained from tests in the LRC tunnel at M = 3, 4, and 4.65 and in the tunnels at JPL at M = 6.6 and 8. For the LRC tests (one-fifteenth-scale model), angles of attack were from -4° to 20° and Reynolds number was 2.0×10^6 per foot (6.56×10^6 per meter). Details on the JPL tests with the one-fiftieth-scale model are presented in references 22 and 23. Angle of sideslip was zero for the schlieren tests.

DATA REDUCTION

Shock Structure

Figures 4(a) to 4(d) show typical schlieren photographs obtained in the JPL facilities. The schlieren analysis was limited to five shock waves, which appear in the lower aft region of the X-15 airplane. These were the bow, side fairing, wing leading edge, wing trailing edge, and landing-skid shock waves. The model schlieren shock-wave data were adjusted to correspond to the basic X-15 airplane coordinates as discussed in the Models section (page 3). This adjustment affected the wing leading edge, wing trailing edge, and landing-skid shock waves. The basic X-15 airplane shock-wave coordinates were then plotted and lines were faired through the data points.

Impact Pressure

The impact pressures were normalized with respect to calculated wind-tunnel free-stream impact pressure. The free-stream impact pressure could not be measured at low Mach numbers and angles of attack because of traverse limitations of the probes.

Flow Angles

The flow angles were obtained by taking pressure differences between opposite orifices on the 40° included-angle cone and using the cone calibration data obtained at AEDC (fig. 5). A detailed description of this technique is given in reference 24.

Mach Number and Total-Pressure Recovery

Local Mach numbers were determined by three different methods:

1. Pressure measurements from the 40° included-angle cone probe were used along with the curve (theory, ref. 25) presented in figure 6 to obtain the local Mach numbers for free-stream Mach numbers up to 6.

2. Schlieren photographs, for which the free-stream Mach numbers were known, were used to obtain the local bow shock-wave angles. The local Mach numbers immediately behind the bow shock were determined by using reference 26.

3. By assuming the measured model surface static pressure to be constant through the boundary layer and slightly past it, and knowing the local impact pressures, local Mach numbers were determined using the Rayleigh pitot equation (ref. 27).

From the three local Mach numbers discussed above and from the theoretical local Mach number results (ref. 28), total-pressure recoveries were calculated as follows: For each local Mach number source except the schlieren bow shock, the free-stream Mach number M, the local Mach number M_l, and the ratio of local impact to free-stream pressure $\frac{p_{il}}{p_{i\infty}}$ were obtained. From M and M_l the ratio of impact to total pressure $\frac{p_{i\infty}}{p_{t\infty}}$ and $\frac{p_{il}}{p_{tl}}$ was determined (ref. 27). Total pressure recovery was then calculated by using the relationship

$$\frac{p_{tl}}{p_{il}} \frac{p_{il}}{p_{i\infty}} \frac{p_{i\infty}}{p_{t\infty}} = \frac{p_{tl}}{p_{t\infty}}$$

The total-pressure recovery for the schlieren bow-shock results was obtained directly from reference 26, since the free-stream Mach number and the bow-shock-wave angle were known.

ACCURACY

The absolute levels of accuracy of the schlieren shock-system coordinates, pressures, flow angle, and Mach numbers are difficult to establish because of the combined effects of the many possible error sources. The shock-system coordinates are repeatable within ±1.0°. This accuracy is based on an analysis of data from many different photographs.

Pressures were measured with the standard pressure systems of the AEDC and LRC tunnels, which are described in references 18 and 21. The AEDC Tunnel A and B pressure data are accurate to ±0.015 psi ($\pm 1.03 \times 10^{-4}$ MN/m^2) and ±0.006 psi ($\pm 4.13 \times 10^{-5}$ MN/m^2), respectively (refs. 9 and 18). The LRC pressures are accurate within 1 percent of the full-scale range used or less than 2 percent for individual measurements (ref. 21). When the data were available, the measured free-stream impact pressure was compared to the calculated free-stream impact pressure. This comparison showed a 2-percent to 5-percent discrepancy as M increased from 4 to 8, respectively.

The error in determining flow angles (fig. 5) is estimated to be ±0.5°. The relative scale of cone probe to model diameter was large (0.134). Flow angles measured near the model surface and bow shock were affected by the presence of the probe; therefore, data close to the model surface and the bow shock are not presented. Probe alinement relative to the wind-tunnel centerline is considered to be accurate within ±0.5° (ref. 9). At a Mach number of 4, a cone-probe misalinement of about 1° between the model and probe centerlines in the vertical plane ϵ is believed to have existed. (The data have not been corrected for this possible misalinement.) The calibration curve in figure 5 is valid for all local flow angles (ϵ or σ) from 0° to ±5°.

Inasmuch as the basic Mach number calibration curve (fig. 6) becomes insensitive with increasing Mach number, local Mach numbers at $M = 8$ are not presented. The following table shows the estimated pressure-ratio error and the resultant local Mach number error:

M	Estimated error in $\frac{\bar{p}_c}{p_{il}}$, percent	Resultant error in -	
		M_l, percent	Variation of M_l
4	±1.3	±2.3	±0.09
6	±1.9	±6.4	±.38
8	±2.4	±12.3	±.98

Although the cone-determined local Mach numbers may be in error, because of the calibration, their trends in the flow field agree favorably with local Mach numbers determined from the other data sources.

As a further check on the M_l results, the total-pressure recoveries were calculated and compared. A 1-percent error in Mach number causes a 3.4-percent to 5.5-percent variation in total-pressure recovery over the Mach number range of 4 to 8 covered by these tests. Variation of impact-pressure ratio by 1 percent causes an approximate 1-percent error in total-pressure recovery.

RESULTS AND DISCUSSION

Tables

Results of an analysis of schlieren photographs and a survey of rake and cone pressures are presented in tables I to IV:

Table I - Coordinates for Shock System From Schlieren Photographs

Table II - AEDC Rake Survey Results

Table III - LRC Rake Survey Results

Table IV - AEDC Cone Survey Results

Height corrections were necessary in table II for the data from the AEDC five-probe rake (used only at $M = 4$ and 6) because the fourth and fifth probes (see fig. 2(a)) are at a different height than the first three probes. The correct z/D for $\frac{p_{i4}}{p_{i\infty}}$ and $\frac{p_{i5}}{p_{i\infty}}$ is shown in table II. For the LRC probes, which are in the same vertical plane, lateral-plane surveys were made at $y/D = 0$, $y/D = 0.410$, and $y/D = 0.804$ and are identified as $\frac{p_{i1}}{p_{i\infty}}$, $\frac{p_{i2}}{p_{i\infty}}$, and $\frac{p_{i3}}{p_{i\infty}}$, respectively. These values are tabulated in table III.

Shock Structure

Figure 7 shows the X-15 shock system as determined from schlieren photographs at $M = 4.65$. The bow, side fairing, wing leading edge, wing trailing edge, and the landing-skid shock waves are shown. As expected, all the shock lines tend to become straight at large distances from the origin of the point of disturbance on the model. At low angles of attack, these shock lines are parallel; at high angles of attack they tend to converge. The bow shock-wave angle is larger than the Mach line angle, as expected, which indicates that the bow shock has not yet reached its final state. This trend was observed for all the Mach numbers and angles of attack covered.

Additional schlieren data at $M = 3, 4, 4.65, 6.6$, and 8 at angles of attack of 0° and 10° are presented in table I.

Model Surface Static Pressures

Model surface static pressures along the fuselage bottom centerline are presented in figures 8(a) to 8(d). Also shown are flight data from reference 29 and theoretical results from reference 28. The theoretical calculations are based on a combination of two methods: the linearized characteristics theory and the tangent-body method for axisymmetric bodies. The X-15 shape was approximated by a blunt nose followed by an ogive cylinder. Only the plane-of-symmetry flow was studied.

Angle of attack and Mach number effects on the model surface static-pressure ratios are also shown in figure 8. The theoretical and the experimental results agree and suggest that a constant static-pressure ratio exists from $x/D = 3.5$ to about 6 for small angles of attack over the free-stream Mach number range covered. Surface static-pressure ratio for $x/D > 3.5$ decreases only slightly with Mach number at zero angle of attack and has a value slightly less than unity (p_l slightly smaller than p_∞). Increasing angle of attack at any Mach number and x/D value caused the surface static-pressure ratio to increase, as expected.

Flight and wind-tunnel data agree at a Mach number of 4 (fig. 8(a)); however, at $M = 6$ (fig. 8(c)) the flight data show considerably higher pressures than the wind-tunnel results for $x/D < 2.0$.

Impact Pressures

Typical wind-tunnel impact pressures from tables II and III are presented in figures 9(a) to 9(d) and 10(a) to 10(d) for Mach numbers of 4, 4.65, 6, and 8 at angles of attack of 0° and 10°. Theoretical data (ref. 28) are also shown in figure 10. The wind-tunnel data are presented at the plane of symmetry and at a lateral plane at each Mach number.

At zero angle of attack in figure 9 ($x/D = 6.16$ and 6.43) the intermediate stations show slightly more variation in impact-pressure ratio than does the downstream station in figure 10 ($x/D = 7.77$) for z/D from 0.2 to 1.0. Impact-pressure ratio increases as the bow shock is approached and decreases abruptly to unity after passing through the bow shock. Data obtained from the lateral-plane surveys generally show higher values of impact-pressure ratio than those obtained in the plane of symmetry. Bow-shock curvature is also evident. Theory provides reasonable predictions of the slope and magnitude of impact-pressure ratio (figs. 10(a), (c), and (d)).

In figures 9 and 10 at an angle of attack of 10°, the wind-tunnel data show generally the same trends with increasing Mach number as do the zero angle-of-attack data. The level of impact-pressure ratio increased substantially at M = 6 and 8. Differences in impact-pressure ratio between the upstream and downstream stations are evident at M = 6 and 8. Comparison of the data for the lateral-plane surveys and the plane of symmetry generally shows the same trends as for zero angle of attack.

The quasi-steady-state flight data shown in figure 11 cover Mach numbers from about 4 to 6.3 and were obtained from two X-15 flights. Impact-pressure ratio is plotted against Mach number for several angles of attack and is seen to be a strong function of both variables. The wind-tunnel data have been interpolated and extrapolated for $z/D = 0.411$ and $x/D = 8.20$. Flight and wind-tunnel data agree.

Figure 12 compares bow-shock locations as determined from schlieren, rake, and theoretical (ref. 28) data. These data are for the plane of symmetry. Reference 28 data at M = 4 and 6 were cross-plotted to obtain the theoretical M = 4.65 result shown. Good agreement between the various data sources was obtained. The bow shock is linear as x/D increases beyond about 6 for all Mach numbers and angles of attack considered.

For each of the flow parameters, the gradient across a proposed hypersonic ramjet engine inlet which is 18 inches (45.72 centimeters) in diameter and has its centerline located approximately at $x/D = 7.77$, $y/D = 0$, and $z/D = 0.4$ can be determined from the tables and figures. The impact-pressure-ratio gradient across this inlet varies from 0.05 at M = 4 and $\alpha = 0°$ to 0.18 at M = 8 and $\alpha = 10°$.

Flow Angles

Two flow angles, upwash ϵ and sidewash σ, were measured with the cone probe; both angles were measured with respect to the model centerline. Positive values of ϵ and σ indicate flow toward the model. The flow-angularity results from the AEDC tests at zero sideslip are presented in table IV. The values of upwash and sidewash at Mach numbers of 4, 6, and 8 and $\alpha = 0°$ and 10° are also shown in figures 13(a) to 13(c). The upwash angle shows evidence of outflow as the bow shock is approached at zero angle of attack in the plane of symmetry. This effect becomes more pronounced as Mach number is increased from 4 to 8. The aft stations show less trend toward outflow ($-\epsilon$) than the forward stations at any Mach number.

At M = 4 in figure 13(a) both the magnitudes and trends of the upwash data in the lateral and symmetry planes agree for $\alpha = 0°$. At M = 6 (fig. 13(b)) the magnitudes disagree slightly, although the trend is the same for these data. At M = 8 (fig. 13(c)) both the magnitude and trend of the symmetry-plane data disagree with the lateral-plane data, the latter tending toward an inflow ($+\epsilon$) as the bow shock is approached. Theory (ref. 28) agrees with the experimental results in both level and trend.

At $\alpha = 10°$ in figure 13 there appears to be inflow instead of outflow as the bow shock is approached. This inflow tends to increase as the bow shock is approached. The amount of inflow tends to increase with increasing aft station. Off-centerline upwash data generally give larger inflow values than plane-of-symmetry data at $\alpha = 10°$ for the Mach numbers covered.

On the centerline, a negligible sidewash angle was expected at $M = 6$ and 8 but not at $M = 4$ because of the possible cone misalinement mentioned earlier. Figure 13(a) indicates that this 1° misalinement existed, and figures 13(b) and 13(c) show a negligible sidewash at $M = 6$ and 8. Off the centerline, there is also a negligible sidewash angle at $\alpha = 0°$ for all stations and Mach numbers covered. However, when $\alpha = 10°$, a pronounced negative sidewash angle is noted at the Mach numbers covered.

Table IV and figure 13 provide the local-flow-angle gradient across the proposed ramjet inlet (see p. 10). This gradient varies from 0.3° at $M = 4$ and $\alpha = 0°$ to 2.7 at $M = 8$ and $\alpha = 10°$.

Local Mach Numbers

Figures 14(a) to 14(c) show local Mach number as obtained from schlieren photographs and rake surveys as a function of free-stream Mach number, angle of attack, and flow-field position. Theoretical calculated values from reference 28 are shown at zero angle of attack.

At a Mach number of 4 and $\alpha = 0°$ and 10° (fig. 14(a)), the local Mach number profile is relatively independent of flow-field position. This profile tends to become less uniform at an angle of attack of 10° as Mach number increases to 6 (fig. 14(b)) and 8 (fig. 14(c)). Local Mach numbers obtained with the cone probe and from the static and impact pressures agree for $M = 4$ and 6. The schlieren bow-shock Mach numbers appear to be consistent with the other results. Theory agrees with the wind-tunnel data at $M = 4$ but gives higher local Mach numbers at $M = 6$ and 8.

In figures 15(a) and 15(b) local Mach numbers are compared as a function of free-stream Mach number at $\alpha = 0°$ and 10°. The schlieren and cone data agree at $\alpha = 10°$ and show the same rate of change with Mach number at $\alpha = 0°$. The impact and static-pressure data near the model surface are lower than the other data, particularly at $M = 8$, for both angles of attack. Theoretical local Mach number data (ref. 28) across the flow field at $\alpha = 0°$ are shown for comparison. The theoretical results agree with the experimental results.

The variation in local Mach number gradient across the proposed ramjet inlet (see p. 10) may be determined from table IV and figure 15. This gradient varies from 0.2 at $M = 4$ and $\alpha = 0°$ to 0.6 at $M = 6$ and $\alpha = 10°$.

Total-Pressure Recovery

Total-pressure-recovery results are compared in figures 16(a) to 16(c) for $M = 4$, 6, and 8 at $\alpha = 0°$ and 10°. At $\alpha = 0°$ the results show that as Mach number increases from 4 to 8 the variation in total-pressure recovery with respect to z/D increases. Theory (ref. 28) and wind-tunnel (schlieren) bow-shock pressure recoveries agree at all Mach numbers. The high total-pressure recoveries near the bow shock suggest that the bow shock is weak at $x/D > 7.37$, as expected. Theoretical results agree with the wind-tunnel data at $M = 4$, predict a slightly higher recovery at $M = 6$, and indicate a much higher recovery at $M = 8$. This pronounced difference in total recovery is thought to result from internal shock effects resulting from the side fairings at $M = 8$, which theory (ref. 28) does not account for. This effect is also noted in figures 10(c) and 10(d) and 14(b) and 14(c) for Mach numbers of 6 and 8.

At $\alpha = 10°$ (figs. 16(a) to 16(c)) the wind-tunnel data show generally the same trends with increasing Mach number as do the zero angle-of-attack data. The bow shock lies much closer to the model surface and is stronger, particularly at $M = 8$, as shown by the lower bow-shock recoveries, than at $\alpha = 0°$ at $M = 4$, 6, and 8.

The total-pressure-recovery plots of figure 16 make it possible to estimate the local Mach number at $M = 8$ at the approximate inlet centerline location ($x/D \approx 7.77$ and $z/D = 0.4$) of the ramjet engine that is to be tested on the X-15 airplane. A line was faired through the data points at $M = 8$ in figure 16(c), the total-pressure recovery at $z/D = 0.4$ was determined, and the local Mach number was calculated for use in figure 15.

Mass-Flow Ratio

Inlets tend to be located aft on the undersides of proposed advanced hypersonic aircraft in order to take advantage of the vehicle compression effect and to reduce hot jet-exhaust impingement problems. Determining the actual three-dimensional real-gas mass flows through the inlet is a formidable and time-consuming task for these inlet locations.

One simple approach commonly used to estimate inlet mass flows quickly is to assume that the inlet is located beneath a flat wedge (see following sketch). An ideal gas and a typical aircraft trajectory are also assumed. The trajectory provides the aircraft velocity, ambient density (from the altitude), and angle of attack. From the

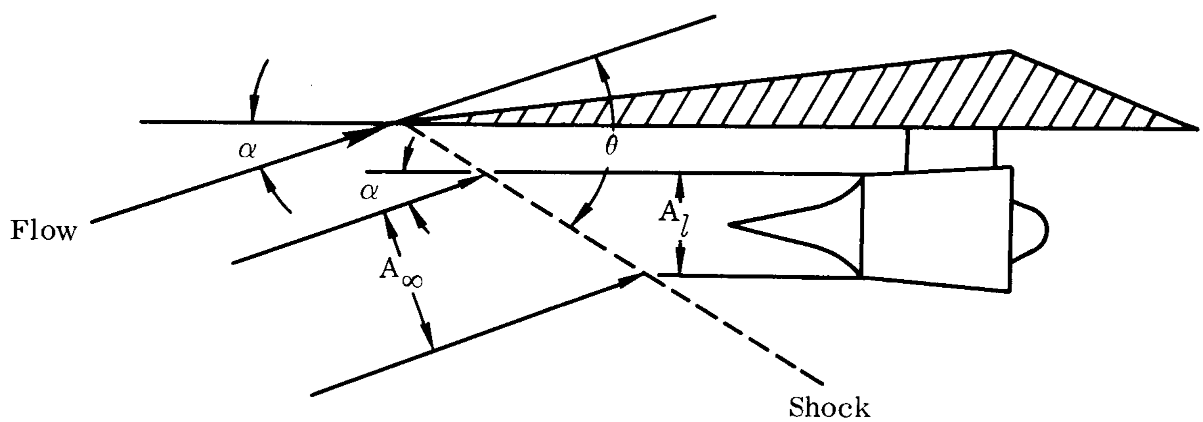

flow-field geometry that results from these assumptions and from the trajectory data, the inlet mass flows may be estimated quickly by using the following equation:

$$\frac{A_\infty}{A_l} = \frac{\sin \theta}{\sin(\theta - \alpha)} = \frac{m_l}{m_\infty}$$

where

m_l = mass flow through inlet in flow field of wedge

m_∞ = free-stream capture mass flow

It is of interest to compare the ideal mass flow based on this two-dimensional oblique-shock assumption with wind-tunnel results for the X-15 airplane. For the proposed ramjet inlet (see p. 10), the inlet mass-flow ratios for $M = 4$, 6, and 8 at $\alpha = 0°$ and $10°$ were calculated by using (1) the two-dimensional flow-field assumptions and (2) the X-15 wind-tunnel local Mach numbers and total-pressure recoveries (figs. 15 and 16). An ideal gas was assumed for both cases. A comparison of these results is shown in figure 17. At both angles of attack over the entire Mach number range, the two-dimensional oblique-shock assumption predicts a larger mass-flow ratio than the X-15 wind-tunnel data. At zero angle of attack this effect suggests that an expansion instead of a compression occurs for the experimental data when free-stream conditions are compared to local flow conditions. This result correlates with the $\alpha = 0°$ data shown in figure 8.

Another means of comparing the results is to plot the percentage difference between the two-dimensional oblique shock and the mass flow from the X-15 flow-field data. The vertical lines on figure 17 show the percentage mass flow overpredicted by the two-dimensional mass-flow assumption, as obtained by using the following expression:

$$\frac{\left(\frac{m_l}{m_\infty}\right)_{\text{two-dimensional}} - \left(\frac{m_l}{m_\infty}\right)_{\text{X-15 data}}}{\left(\frac{m_l}{m_\infty}\right)_{\text{two-dimensional}}} 100$$

At $\alpha = 10°$, the data indicate that the two-dimensional assumption overpredicts the X-15 data mass flow by 27 percent to 43 percent in the $M = 4$ to 8 range. At $\alpha = 0°$ there is a slight overprediction at $M = 4$ and a 17-percent overprediction at $M = 8$.

CONCLUSIONS

Analysis of the wind-tunnel, flight, and theoretical results used to investigate the flow field beneath the fuselage of the X-15 airplane led to the following conclusions:

1. Typical flow-field gradients across the proposed hypersonic ramjet engine inlet are local Mach number variations from 0.2 (Mach number of 4 and angle of attack of 0°) to 0.6 (Mach number of 6 and angle of attack of 10°); impact-pressure-ratio variations from 0.05 (Mach number of 4 and angle of attack of 0°) to 0.18 (Mach number of 8 and angle of attack of 10°); and local-flow-angle variations from 0.3° (Mach number of 4 and angle of attack of 0°) to 2.7° (Mach number of 8 and angle of attack of 10°).

2. The lower-centerline surface static-pressure ratio changed little beyond 3.5 diameters from the nose (end of nose curvature) for a fixed angle of attack at any

Mach number covered. At zero angle of attack, however, the local static pressure was less than the free-stream static pressure, which indicates that an overall expansion has occurred from free stream to the local condition.

3. At an angle of attack of 0°, the theoretical results agreed with the surface static-pressure ratio, impact-pressure ratio, bow-shock location, flow angularity, and local Mach number wind-tunnel results. Flight-test static-pressure and impact-pressure results also agreed with the wind-tunnel results.

4. Use of a two-dimensional oblique-shock-wave assumption for the X-15 airplane was found to overpredict the mass flow through the proposed inlet (by 27 to 43 percent at an angle of attack of 10° and by as much as 17 percent at an angle of attack of 0°) when compared with wind-tunnel results, particularly at high Mach number and angle of attack.

Flight Research Center
National Aeronautics and Space Administration
Edwards, Calif., July 28, 1967
729-00-00-01-24

REFERENCES

1. Petersen, Richard H.; Gregory, Thomas J.; and Smith, Cynthia L.: Some Comparisons of Turboramjet-Powered Hypersonic Aircraft for Cruise and Boost Missions. J. Aircraft, vol. 3, no. 5, Sept.-Oct. 1966, pp. 398-405.

2. Brewer, G. Daniel: Manned Hypersonic Vehicles. Lockheed Horizons, issue 4, 1966, pp. 16-23.

3. Wood, K. D.: Aerospace Vehicle Design. Vol. II - Spacecraft Design. Johnson Pub. Co. (Boulder, Colo.), 1964, pp. 123, 124.

4. Nichols, Mark R.: Aerodynamics of Airframe-Engine Integration of Supersonic Aircraft. NASA TN D-3390, 1966.

5. Swan, Walter C.: A Discussion of Selected Aerodynamic Problems On Integration of Propulsion Systems With Airframe on Transport Aircraft. Aerodynamics of Power Plant Installation, Part I. AGARDograph 103, Oct. 1965, pp. 23-68.

6. Fetterman, David E.; McLellan, Charles H.; Jackson L. Robert; Henry, Beverly Z., Jr.; and Henry, John R.: A Review of Hypersonic Cruise Vehicles. Conference on Aircraft Aerodynamics, NASA SP-124, 1966, pp. 523-564.

7. Rubert, Kennedy F.: Hypersonic Air-Breathing Propulsion-System Testing on the X-15. Progress of the X-15 Research Airplane Program, NASA SP-90, 1965, pp. 127-132.

8. Palitz, Murray: Measured and Calculated Flow Conditions on the Forward Fuselage of the X-15 Airplane and Model at Mach Numbers From 3.0 to 8.0. NASA TN D-3447, 1966.

9. Rippey, J.: Flow-Field Investigation of a 0.0667-Scale Model of the X-15 Research Vehicle at Mach 4, 6, and 8. Tech. Doc. Rep. No. AEDC-TDR-64-201, Arnold Eng. Dev. Center, Oct. 1964.

10. Mechtly, E. A.: The International System of Units - Physical Constants and Conversion Factors. NASA SP-7012, 1964.

11. Anon.: Wind Tunnel Tests and Model Information for 0.067-Scale Heat Transfer and Pressure Model of the X-15 Research Airplane at $M = 7.0$ at the AEDC 50-Inch Diameter B-Minor Wind Tunnel. Rep. No. NA57-1197, North American Aviation, Inc., Nov. 22, 1957.

12. Anon.: Wind-Tunnel Model Information for 0.067-Scale Heat Transfer and Pressure Model of the X-15 Research Airplane. Rep. No. NA-56-1226, North American Aviation, Inc., Nov. 29, 1956.

13. Patterson, James C., Jr.: Aerodynamic Characteristics of a 0.0667-Scale Model of the X-15A-2 Research Airplane at Transonic Speeds. NASA TM X-1198, 1966.

14. Franklin, Arthur E.; and Lust, Robert M.: Investigation of the Aerodynamic Characteristics of a 0.067-Scale Model of the X-15 Airplane (Configuration 3) at Mach Numbers of 2.29, 2.98 and 4.65. NASA TM X-38, 1959.

15. Anon.: Test and Model Information for Wind Tunnel Tests of an 0.02-Scale Model of the X-15 Research Vehicle in the JPL 20-Inch Supersonic Wind Tunnel. Rep. No. NA-63-636, North American Aviation, Inc., May 29, 1963 (rev. June 6, 1963).

16. Dunn, C. L.; and Powell, Al: Aerodynamic Dimensional Data for the X-15 Airplane. Rep. No. NA-56-810, North American Aviation, Inc., July 10, 1956 (rev. Feb. 10, 1959).

17. Bristol, M. A.: Aerodynamic Dimensional Data for the X-15A-2 Airplane. Rep. No. NA-56-810 Appendix B, North American Aviation, Inc., Dec. 16, 1963.

18. Anon.: Test Facilities Handbook. Fifth ed., vol. 4, Arnold Eng. Dev. Center, July 1963.

19. Schaefer, William T., Jr.: Characteristics of Major Active Wind Tunnels at the Langley Research Center. NASA TM X-1130, 1965.

20. Wind Tunnel Staff: Wind Tunnel Facilities at the Jet Propulsion Laboratory. Tech. Release No. 34-257 (Contract No. NAS 7-100), Jet Propulsion Lab., Calif. Inst. of Tech., Apr. 18, 1961 (rev. Jan. 1, 1962).

21. Anon.: Manual for Users of the Unitary Plan Wind Tunnel Facilities of the National Advisory Committee for Aeronautics. NACA, 1956.

22. Weaver, Robert W.: Tests of the X-15 Model in the JPL 20-Inch Supersonic and 21-Inch Hypersonic Wind Tunnels for NASA Flight Research Center. WT 21-160 (Contract No. NAS 7-100), Jet Propulsion Lab., Calif. Inst. of Tech., Dec. 15, 1964.

23. Weaver, Robert W.: Tests of the X-15 Model for NASA Flight Research Center in the JPL 20-Inch Supersonic and 21-Inch Hypersonic Wind Tunnels. WT 20-561, Jet Propulsion Lab., Calif. Inst. of Tech., June 15, 1964.

24. Norris, John D.: Calibration of Conical Pressure Probes for Determination of Local Flow Conditions at Mach Numbers From 3 to 6. NASA TN D-3076, 1965.

25. Kopal, Zdeněk: Tables of Supersonic Flow Around Cones. Tech. Rep. No. 1, Mass. Inst. of Tech., 1947.

26. Dennard, John S.; and Spencer, Patricia B.: Ideal-Gas Tables for Oblique-Shock Flow Parameters in Air at Mach Numbers From 1.05 to 12.0. NASA TN D-2221, 1964.

27. Ames Research Staff: Equations, Tables, and Charts for Compressible Flow. NACA Rept. 1135, 1953. (Supersedes NACA TN 1428.)

28. Gallo, William F.; and Rakich, John V.: Investigation of Methods for Predicting Flow in the Shock Layer Over Bodies at Small Angles of Attack. NASA TN D-3946, 1967.

29. Pyle, Jon S.: Comparison of Flight Pressure Measurements With Wind-Tunnel Data and Theory for the Forward Fuselage of the X-15 Airplane at Mach Numbers From 0.8 to 6.0. NASA TN D-2241, 1964.

TABLE I

COORDINATES FOR SHOCK SYSTEM FROM SCHLIEREN PHOTOGRAPHS

[See figure 7 for definition of axes]

(a) M = 3

Bow		Side fairing		Wing leading edge		Skid		Wing trailing edge	
x/D	z/D	x/D	z/D	x/D	z/D	x/D	z/D	x/D	z/D
$\alpha = 0°$									
0	-0.43	3.93	0	6.59	0	7.78	0	8.64	0
.36	-.25	4.28	.13	6.78	.05	7.85	.05	8.93	.16
.71	-.08	4.64	.25	7.14	.24	8.03	.14	9.28	.34
1.07	.07	5.00	.38	7.50	.38	8.21	.26	9.64	.52
1.43	.23	5.36	.51	7.85	.52	8.39	.36	10.00	.68
1.79	.39	6.25	.84	8.21	.67	8.57	.46	10.35	.84
2.68	.78	7.14	1.18	8.57	.95	8.75	.55	10.71	.97
3.57	1.16	8.03	1.48	8.93	.85	8.93	.65	11.07	1.11
4.46	1.54	8.93	1.80	9.28	1.09	9.28	.86	11.42	1.27
5.36	1.90	9.82	2.13	9.64	1.23	----	----	-----	----
7.14	2.62	10.35	2.33	10.00	1.39	----	----	-----	----
8.93	3.34	-----	----	10.35	1.54	----	----	-----	----
10.71	4.06	-----	----	10.71	1.68	----	----	-----	----
$\alpha = 10°$									
0	-0.43	3.82	0	6.83	0	7.78	0	9.70	0
.36	-.29	3.93	.02	7.14	.11	7.86	.07	10.00	.09
.71	-.16	4.28	.14	7.50	.22	8.22	.21	10.35	.21
1.07	-.04	4.64	.21	7.85	.34	8.58	.30	10.71	.32
1.43	.07	5.00	.36	8.21	.46	8.93	.71	11.07	.45
1.79	.20	5.36	.45	8.57	.57	9.82	1.29	11.25	.55
2.68	.46	6.25	.68	8.93	.69	10.72	1.79	-----	---
3.57	.73	7.14	.91	9.28	.80	-----	----	-----	---
4.46	.99	7.85	1.08	9.64	.91	-----	----	-----	---
5.36	1.21	----	----	10.00	1.04	-----	----	-----	---
7.14	1.63	----	----	10.35	1.13	-----	----	-----	---
8.93	1.98	----	----	10.71	1.25	-----	----	-----	---

TABLE I. – Continued

COORDINATES FOR SHOCK SYSTEM FROM SCHLIEREN PHOTOGRAPHS

[See figure 7 for definition of axes]

(b) M = 4

Bow		Side fairing		Wing leading edge		Skid		Wing trailing edge	
x/D	z/D	x/D	z/D	x/D	z/D	x/D	z/D	x/D	z/D
$\alpha = 0°$									
0	-0.43	4.16	0	6.83	0	7.75	0	9.46	0
.36	-.29	6.07	.53	7.14	.08	7.85	.09	9.64	.05
.71	-.14	6.43	.62	7.50	.20	8.03	.16	10.00	.16
1.07	0	6.78	.71	7.85	.30	8.21	.25	10.35	.27
1.43	.13	7.14	.82	8.21	.45	8.39	.32	10.71	.36
1.79	.25	8.03	1.06	8.57	.52	8.57	.38	11.07	.48
2.68	.55	8.93	1.30	8.93	.63	8.75	.46	11.42	.59
3.57	.84	9.28	1.39	9.28	.72	8.93	.51	11.78	.71
4.46	1.14	----	----	9.64	.84	9.10	.58	-----	----
5.36	1.42	----	----	10.00	.95	9.28	.64	-----	----
6.25	1.70	----	----	10.35	1.05	9.46	.71	-----	----
7.14	1.97	----	----	10.71	1.16	----	----	-----	----
8.03	2.25	----	----	11.07	1.27	----	----	-----	----
8.93	2.54	----	----	11.42	1.38	----	----	-----	----
$\alpha = 10°$									
0	-0.41	3.75	0	7.15	0	7.82	0	9.57	0
.36	-.29	4.11	.09	7.32	.05	7.86	.02	9.65	.02
.71	-.19	4.47	.18	7.68	.13	8.22	.20	9.82	.07
1.79	.13	5.36	.39	8.04	.22	8.58	.34	10.00	.13
2.68	.37	6.25	.56	8.93	.38	8.93	.48	10.17	.18
5.36	.95	7.15	.73	9.82	.64	9.82	.79	10.36	.21
7.14	1.24	8.04	.88	----	----	10.72	1.07	10.72	.32
8.93	1.53	8.93	1.04	----	----	-----	----	-----	----

TABLE I. – Continued

COORDINATES FOR SHOCK SYSTEM FROM SCHLIEREN PHOTOGRAPHS

[See figure 7 for definition of axes]

(c) M = 4.65

Bow		Side fairing		Wing leading edge		Skid		Wing trailing edge	
x/D	z/D	x/D	z/D	x/D	z/D	x/D	z/D	x/D	z/D
$\alpha = 0°$									
0	-0.43	4.26	0	7.00	0	7.80	0	9.51	0
.36	-.29	4.64	.09	7.14	.03	7.85	.05	9.64	.03
.71	-.15	5.00	.18	7.50	.13	8.03	.16	9.82	.07
1.07	-.03	5.36	.27	7.85	.22	8.21	.23	10.00	.13
1.43	.05	6.25	.48	8.21	.38	8.39	.30	10.18	.16
2.21	.37	7.14	.70	8.57	.44	8.57	.37	10.35	.21
2.68	.50	8.03	.91	8.93	.54	8.75	.43	10.53	.25
3.57	.75	8.93	1.13	9.28	.63	8.93	.47	10.71	.30
4.46	1.02	9.82	1.34	9.64	.71	9.10	.53	10.89	.34
5.36	1.25	10.35	1.46	10.00	.77	9.28	.58	11.07	.38
6.25	1.54	-----	----	10.35	.91	9.46	.64	11.25	.43
8.03	1.95	-----	----	10.71	1.00	----	----	11.42	.46
9.82	2.43	-----	----	11.07	1.09	----	----	11.60	.50
$\alpha = 10°$									
0	-0.43	4.44	0	6.98	0	7.82	0	9.82	0
.36	-.25	4.64	.04	7.14	.04	7.86	.02	10.00	.04
.71	-.14	5.00	.10	7.50	.11	8.22	.18	10.17	.09
1.07	-.03	5.36	.15	7.85	.19	8.58	.32	10.36	.14
1.43	.07	6.25	.30	8.21	.27	8.93	.43	10.72	.21
1.79	.16	7.14	.46	8.57	.35	9.82	.75	-----	----
2.68	.34	8.03	.61	8.93	.41	10.72	1.05	-----	----
4.46	.69	8.93	.76	9.28	.49	-----	----	-----	----
6.25	.89	9.28	.82	9.64	.57	-----	----	-----	----
8.03	1.11	----	----	10.00	.64	-----	----	-----	----
9.82	1.32	----	----	10.35	.72	-----	----	-----	----

TABLE I. – Continued

COORDINATES FOR SHOCK SYSTEM FROM SCHLIEREN PHOTOGRAPHS

[See figure 7 for definition of axes]

(d) M = 6.6

Bow		Side fairing		Wing leading edge		Wing trailing edge	
x/D	z/D	x/D	z/D	x/D	z/D	x/D	z/D
α = 0°							
0	-0.41	3.73	0	7.19	0	9.39	0
.36	-.25	3.93	.07	7.50	.07	9.64	.07
.71	-.13	4.28	.14	7.85	.14	10.00	.18
1.07	0	4.64	.22	8.21	.23	10.35	.29
1.43	.11	5.00	.30	8.53	.30	10.71	.38
1.79	.21	5.36	.37	8.93	.38	11.07	.48
2.68	.46	6.25	.55	9.28	.46	11.42	.58
3.57	.67	7.14	.73	9.64	.54	11.78	.71
4.46	.86	8.03	.91	10.00	.61	12.14	.79
5.36	1.06	8.57	1.02	10.35	.68	-----	----
6.25	1.24	----	----	10.71	.76	-----	----
7.14	1.43	----	----	11.07	.84	-----	----
8.93	1.79	----	----	11.53	.91	-----	----
10.39	2.07	----	----	11.78	.98	-----	----
α = 10°							
0	-0.41	4.29	0	7.70	0	-----	----
1.79	.13	4.47	.09	8.03	.04	-----	----
3.57	.43	5.36	.20	8.93	.18	-----	----
5.36	.61	6.25	.33	9.82	.32	-----	----
7.14	.75	7.14	.44	10.72	.44	-----	----
8.93	.86	8.03	.54	-----	----	-----	----

TABLE I. – Concluded

COORDINATES FOR SHOCK SYSTEM FROM SCHLIEREN PHOTOGRAPHS

[See figure 7 for definition of axes]

(e) M = 8

Bow		Side fairing		Wing leading edge		Wing trailing edge	
x/D	z/D	x/D	z/D	x/D	z/D	x/D	z/D
$\alpha = 0°$							
0	-0.41	4.84	0	7.32	0	9.10	0
.36	-.25	5.00	.02	7.50	.04	9.28	.04
.71	-.19	5.36	.07	7.85	.11	9.64	.13
1.07	0	5.71	.13	8.21	.18	10.00	.21
1.43	.11	6.07	.19	8.57	.26	10.35	.30
1.79	.21	6.43	.25	8.93	.34	10.71	.34
2.68	.42	6.78	.30	9.28	.41	11.07	.39
3.57	.63	7.14	.37	9.64	.48	11.42	.45
4.46	.80	8.03	.50	10.00	.55	11.78	.50
5.36	.96	8.93	.64	10.35	.63	-----	----
6.25	1.13	9.82	.78	10.71	.71	-----	----
7.14	1.29	10.71	.91	11.07	.79	-----	----
8.93	1.61	-----	----	11.42	.86	-----	----
$\alpha = 10°$							
0	-0.39	-----	----	-----	----	-----	----
1.79	.13	-----	----	-----	----	-----	----
3.57	.39	-----	----	-----	----	-----	----
5.36	.55	-----	----	-----	----	-----	----
7.14	.66	-----	----	-----	----	-----	----
8.95	.73	-----	----	-----	----	-----	----

TABLE II

AEDC RAKE SURVEY RESULTS

(a) M = 4; α = 0°

z/D	$p_{i1}/p_{i\infty}$	$p_{i2}/p_{i\infty}$	$p_{i3}/p_{i\infty}$	z/D (a)	$p_{i4}/p_{i\infty}$	$p_{i5}/p_{i\infty}$
x/D = 5.36						
0	0.164	0.648	0.483	-0.134	0.694	0.930
.022	.748	.915	.573	-.112	.815	.936
.055	.956	.958	.835	-.079	.729	.949
.112	.963	.956	.970	-.022	.868	.964
.167	.961	.948	.983	.033	.949	.975
.224	.958	.947	.980	.090	.963	.986
.280	.958	.946	.984	.146	.972	.994
.336	.950	.940	.963	.202	.972	.994
.392	.953	.943	.962	.258	.973	.997
.449	.957	.948	.952	.315	.978	.994
.504	.967	.958	.960	.370	.946	.994
.561	.979	.972	.970	.427	.942	.958
.616	.995	.986	.986	.482	.939	.971
.673	1.012	1.005	1.004	.539	.958	1.000
.729	1.037	1.026	1.019	.595	.982	1.025
.785	1.055	1.047	1.039	.651	1.007	1.039
.841	1.083	1.072	1.059	.707	1.016	1.045
.897	1.103	1.095	1.083	.763	1.030	.998
.982	1.135	1.123	1.115	.848	1.066	1.093
x/D = 6.43						
0	0.202	0.499	0.433	-0.134	0.465	1.003
.022	.494	.727	.607	-.112	.768	1.011
.065	.947	.952	.823	-.069	.863	1.034
.089	.971	.963	.928	-.045	.846	1.002
.110	.980	.969	.963	-.024	.858	.960
.166	.986	.975	.976	.032	.946	.965
.223	.992	.974	.983	.089	.957	.961
.335	.995	.981	.995	.201	.962	.967
.391	.985	.980	.994	.257	.966	.970
.449	.979	.977	1.000	.315	.975	.984
.504	.977	.961	1.001	.370	.982	.991
.559	.969	.962	1.001	.425	.990	.999
.616	.963	.951	.979	.482	.991	1.004
.672	.963	.950	.976	.538	.993	1.005
.740	.971	.959	.969	.606	.998	1.012
.785	.977	.965	.971	.651	.961	1.012
.840	.986	.974	.978	.706	.961	.966
.898	1.000	.986	.991	.764	.956	.972
.954	1.015	1.000	1.006	.820	.970	.988
.981	1.021	1.007	1.009	.847	.976	.995
x/D = 7.77						
0	0.281	0.426	0.382	-0.134	0.378	0.953
.047	.586	.726	.589	-.087	.797	.957
.092	.912	.951	.863	-.042	.893	.955
.114	.956	.965	.936	-.020	.898	.957
.170	.966	.970	.989	-.036	.962	.970
.261	.966	.969	.995	.127	.987	1.025
.283	.965	.970	.995	.149	.981	1.043
.339	.978	.970	.991	.205	.998	1.051
.381	.974	.971	.990	.247	1.017	1.029
.395	.973	.970	.982	.261	1.016	1.024
.443	.981	.974	.985	.309	1.004	1.056
.508	.985	.981	.986	.374	.975	.976
.563	.992	.985	.991	.429	.974	.983
.619	.996	.991	.995	.485	.975	.975
.732	1.005	.991	1.004	.598	.980	.985
.788	.992	.993	1.008	.654	.988	.988
.844	.979	.975	1.011	.710	.994	.996
.901	.977	.968	1.008	.767	1.000	1.002
.985	.962	.955	.982	.851	1.002	1.002

[a]Different z/D for $p_{i4}/p_{i\infty}$ and $p_{i5}/p_{i\infty}$ explained on page 8.

TABLE II. - Continued

AEDC RAKE SURVEY RESULTS

(b) M = 4; α = 5°

z/D	$p_{i1}/p_{i\infty}$	$p_{i2}/p_{i\infty}$	$p_{i3}/p_{i\infty}$	z/D (a)	$p_{i4}/p_{i\infty}$	$p_{i5}/p_{i\infty}$
x/D = 5.36						
0	1.084	1.075	1.091	-0.134	0.863	1.102
.056	1.089	1.079	1.099	-.078	1.091	1.118
.112	1.086	1.078	1.106	-.022	1.096	1.129
.170	1.082	1.073	1.095	.036	1.102	1.142
.225	1.056	1.051	1.092	.091	1.108	1.145
.281	1.056	1.054	1.084	.147	1.114	1.156
.337	1.059	1.048	1.079	.203	1.082	1.152
.393	1.072	1.063	1.062	.259	1.079	1.094
.449	1.095	1.089	1.067	.315	1.065	1.076
.506	1.125	1.117	1.091	.372	1.039	1.068
.561	1.158	1.152	1.123	.427	1.053	1.096
.618	1.189	1.183	1.156	.484	1.084	1.125
.674	1.213	1.207	1.186	.540	1.112	1.152
.731	1.248	1.241	1.211	.597	1.141	1.181
.787	1.279	1.269	1.252	.653	1.185	1.212
.843	1.304	1.291	1.279	.709	1.208	1.243
.898	1.333	1.321	1.304	.764	1.242	1.269
.956	1.357	1.346	1.328	.822	1.271	1.294
1.012	1.375	1.364	1.349	.878	1.289	1.315
1.039	1.395	1.361	1.366	.905	1.303	1.330
x/D = 6.43						
0	1.111	1.098	0.751	-0.134	0.642	1.099
.035	1.102	1.099	1.059	-.099	.593	1.093
.093	1.100	1.104	1.103	-.041	.980	1.089
.148	1.106	1.106	1.119	.014	1.079	1.107
.204	1.102	1.099	1.121	.070	1.088	1.099
.260	1.103	1.101	1.119	.126	1.089	1.102
.317	1.110	1.099	1.119	.183	1.099	1.114
.372	1.104	1.097	1.121	.238	1.097	1.117
.429	1.097	1.091	1.121	.295	1.105	1.125
.485	1.074	1.069	1.102	.351	1.109	1.128
.541	1.055	1.055	1.091	.407	1.112	1.139
.597	1.056	1.049	1.071	.463	1.109	1.139
.653	1.067	1.058	1.063	.519	1.079	1.099
.710	1.084	1.077	1.062	.576	1.069	1.091
.822	1.135	1.127	1.105	.688	1.046	1.077
.878	1.159	1.151	1.128	.744	1.067	1.100
.935	1.187	1.177	1.154	.801	1.089	1.122
.990	1.209	1.201	1.184	.856	1.115	1.148
1.018	1.225	1.215	1.190	.884	1.129	1.158
x/D = 7.77						
0	1.069	1.088	0.769	-0.134	0.539	1.184
.062	1.126	1.111	1.091	-.072	.672	1.209
.114	1.113	1.107	1.097	-.020	1.033	1.215
.175	1.120	1.111	1.102	.041	1.082	1.190
.232	1.131	1.112	1.126	.098	1.068	1.107
.288	1.126	1.116	1.121	.154	1.088	1.117
.344	1.120	1.116	1.123	.210	1.101	1.117
.401	1.114	1.112	1.127	.267	1.105	1.124
.457	1.108	1.103	1.131	.323	1.105	1.126
.513	1.099	1.101	1.121	.379	1.107	1.124
.568	1.099	1.097	1.121	.434	1.107	1.126
.624	1.096	1.089	1.128	.490	1.106	1.131
.680	1.091	1.078	1.113	.546	1.109	1.134
.738	1.054	1.051	1.098	.604	1.113	1.138
.792	1.054	1.049	1.082	.658	1.116	1.141
.850	1.057	1.052	1.069	.716	1.083	1.137
.906	1.171	1.067	1.062	.772	1.071	1.098
.936	1.080	1.076	1.066	.802	1.065	1.096

[a]Different z/D for $p_{i4}/p_{i\infty}$ and $p_{i5}/p_{i\infty}$ explained on page 8.

TABLE II. – Continued

AEDC RAKE SURVEY RESULTS

(c) M = 4; α = 10°

z/D	$p_{i1}/p_{i\infty}$	$p_{i2}/p_{i\infty}$	$p_{i3}/p_{i\infty}$	z/D (a)	$p_{i4}/p_{i\infty}$	$p_{i5}/p_{i\infty}$
			x/D = 5.36			
0	1.264	1.257	1.318	-0.134	0.654	1.264
.010	1.258	1.257	1.305	-.124	.788	1.266
.066	1.267	1.266	1.298	-.068	1.257	1.295
.122	1.259	1.255	1.296	-.012	1.286	1.322
.178	1.257	1.249	1.269	.044	1.309	1.339
.235	1.241	1.235	1.264	.101	1.314	1.352
.291	1.242	1.237	1.247	.157	1.313	1.351
.349	1.263	1.253	1.242	.215	1.245	1.254
.403	1.269	1.262	1.255	.269	1.212	1.207
.459	1.295	1.292	1.264	.325	1.228	1.212
.515	1.333	1.328	1.287	.381	1.224	1.231
.572	1.367	1.365	1.326	.438	1.236	1.269
.628	1.403	1.400	1.363	.494	1.269	1.305
.685	1.433	1.432	1.401	.551	1.307	1.343
.740	1.476	1.474	1.430	.606	1.349	1.379
.797	1.511	1.507	1.475	.663	1.391	1.416
.852	1.537	1.511	1.509	.718	1.419	1.452
.870	1.015	1.013	1.522	.736	1.434	1.465
			x/D = 6.43			
.099	1.314	1.319	1.314	-0.035	1.257	1.282
.111	1.314	1.319	1.316	-.023	1.259	1.282
.167	1.309	1.316	1.329	.035	1.280	1.289
.222	1.299	1.299	1.332	.088	1.293	1.298
.280	1.289	1.286	1.336	.146	1.298	1.299
.335	1.265	1.261	1.329	.201	1.307	1.326
.392	1.258	1.253	1.283	.258	1.325	1.340
.448	1.243	1.237	1.264	.314	1.328	1.344
.460	1.240	1.228	1.265	.326	1.329	1.341
.504	1.247	1.245	1.247	.370	1.316	1.338
.560	1.258	1.255	1.248	.426	1.253	1.257
.616	1.266	1.265	1.256	.482	1.218	1.233
.672	1.291	289	1.266	.538	1.227	1.234
.728	1.322	1.319	1.287	.594	1.231	1.240
.785	1.349	1.349	1.318	.651	1.243	1.268
.841	1.377	1.374	1.347	.707	1.267	1.297
.885	1.405	1.398	1.372	.751	1.292	1.322
.952	1.438	1.432	1.409	.818	1.327	1.357
1.009	1.472	1.461	1.432	.875	1.356	1.388
1.046	1.015	1.008	1.455	.912	1.379	1.401
			x/D = 7.77			
0	1.315	1.285	1.117	-0.134	0.496	1.361
.020	1.324	1.291	1.294	-.114	.667	1.428
.055	1.321	1.309	1.300	-.079	1.165	1.446
.093	1.319	1.314	1.309	-.041	1.355	1.469
.122	1.326	1.314	1.311	-.012	1.353	1.472
.167	1.328	1.317	1.314	.033	1.339	1.424
.213	1.335	1.325	1.219	.079	1.294	1.340
.246	1.343	1.332	1.326	.112	1.277	1.286
.256	1.356	1.344	1.329	.122	1.277	1.284
.262	1.339	1.355	1.328	.128	1.275	1.288
.279	1.368	1.339	1.329	.145	1.277	1.309
.293	1.349	1.332	1.337	.159	1.281	1.328
.312	1.343	1.332	1.351	.178	1.294	1.318
.353	1.345	1.336	1.341	.219	1.298	1.328
.414	1.341	1.331	1.341	.280	1.323	1.324
.482	1.318	1.321	1.341	.348	1.316	1.328
.526	1.289	1.299	1.338	.392	1.316	1.329
.549	1.281	1.279	1.337	.415	1.319	1.332
.593	1.255	1.254	1.336	.459	1.325	1.328
.639	1.235	1.234	1.308	.505	1.317	1.330
.683	1.223	1.221	1.265	.549	1.321	1.343
.752	1.226	1.226	1.234	.618	1.324	1.346
.798	1.234	1.230	1.228	.664	1.253	1.287

[a]Different z/D for $p_{i4}/p_{i\infty}$ and $p_{i5}/p_{i\infty}$ explained on page 8.

TABLE II. – Continued

AEDC RAKE SURVEY RESULTS

(d) M = 4; α = 14.5°

z/D	$p_{i1}/p_{i\infty}$	$p_{i2}/p_{i\infty}$	$p_{i3}/p_{i\infty}$	z/D (a)	$p_{i4}/p_{i\infty}$	$p_{i5}/p_{i\infty}$
			x/D = 5.36			
0	1.444	1.454	1.479	-0.134	0.876	1.439
.018	1.469	1.457	1.463	-.116	1.176	1.451
.055	1.479	1.467	1.506	-.079	1.432	1.473
.097	1.489	1.481	1.509	-.037	1.469	1.491
.123	1.487	1.477	1.499	-.011	1.483	1.503
.135	1.482	1.471	1.485	.001	1.488	1.511
.187	1.487	1.468	1.474	.053	1.511	1.543
.238	1.490	1.478	1.458	.104	1.535	1.561
.251	1.479	1.469	1.462	.117	1.539	1.562
.259	1.469	1.465	1.465	.125	1.536	1.561
.291	1.477	1.467	1.473	.157	1.527	1.560
.303	1.470	1.455	1.461	.169	1.513	1.557
.335	1.478	1.473	1.465	.201	1.422	1.504
.391	1.494	1.492	1.473	.257	1.415	1.396
.429	1.499	1.493	1.482	.295	1.413	1.420
.442	1.494	1.504	1.483	.308	1.405	1.427
.468	1.515	1.515	1.495	.334	1.419	1.419
.512	1.541	1.537	1.501	.378	1.435	1.432
.531	1.553	1.551	1.507	.397	1.435	1.437
.581	1.580	1.581	1.536	.447	1.445	1.459
.599	1.598	1.596	1.555	.465	1.455	1.475
.638	1.621	1.619	1.576	.504	1.469	1.502
.692	1.658	1.654	1.619	.558	1.510	1.541
.708	1.664	1.667	1.627	.574	1.523	1.552
			x/D = 6.43			
.009	1.523	1.515	1.434	-0.125	0.709	1.455
.017	1.525	1.519	1.471	-.117	.820	1.456
.074	1.554	1.546	1.509	-.060	1.444	1.473
.129	1.554	1.557	1.543	-.005	1.457	1.489
.185	1.548	1.555	1.566	.051	1.488	1.523
.241	1.513	1.521	1.570	.107	1.515	1.519
.297	1.502	1.502	1.576	.163	1.523	1.533
.354	1.485	1.483	1.529	.220	1.542	1.555
.410	1.486	1.477	1.495	.276	1.564	1.571
.466	1.465	1.465	1.477	.332	1.562	1.581
.522	1.467	1.469	1.467	.388	1.453	1.448
.578	1.479	1.480	1.465	.444	1.439	1.430
.635	1.496	1.495	1.480	.501	1.431	1.433
.691	1.519	1.517	1.489	.557	1.436	1.442
.747	1.549	1.549	1.512	.613	1.448	1.452
			x/D = 7.77			
0	1.572	1.552	1.532	-0.134	1.466	1.698
.019	1.575	1.567	1.536	-.115	1.621	1.705
.075	1.581	1.578	1.564	-.058	1.618	1.739
.131	1.589	1.586	1.579	-.003	1.599	1.686
.188	1.593	1.583	1.588	.054	1.529	1.541
.244	1.608	1.619	1.596	.110	1.533	1.529
.297	1.599	1.594	1.619	.163	1.568	1.562
.356	1.594	1.588	1.599	.222	1.570	1.571
.413	1.586	1.569	1.597	.279	1.575	1.571
.499	1.473	1.477	1.579	.365	1.568	1.570

[a]Different z/D for $p_{i4}/p_{i\infty}$ and $p_{i5}/p_{i\infty}$ explained on page 8.

TABLE II. – Continued

AEDC RAKE SURVEY RESULTS

(e) $M = 6$; $\alpha = 0°$

z/D	$p_{i1}/p_{i\infty}$	$p_{i2}/p_{i\infty}$	$p_{i3}/p_{i\infty}$	z/D (a)	$p_{i4}/p_{i\infty}$	$p_{i5}/p_{i\infty}$
			$x/D = 5.36$			
0	0.034	0.019	0.086	-0.134	0.357	0.905
.059	.200	.730	.824	-.075	.139	.914
.086	.776	.730	.934	-.048	.272	.917
.100	.902	.864	.931	-.034	.676	.920
.123	.923	.909	.913	-.011	.904	.925
.149	.902	.891	.894	.015	.911	.930
.178	.887	.874	.886	.044	.911	.938
.217	.891	.872	.886	.083	.904	.949
.258	.898	.881	.899	.124	.895	.943
.286	.907	.890	.909	.152	.901	.932
.352	.940	1.125	.941	.218	.924	.946
.418	.965	1.127	.970	.284	.946	.989
.486	1.000	1.129	1.014	.352	.984	1.043
.532	1.031	1.129	1.038	.398	1.015	1.077
.564	1.063	1.129	1.067	.430	1.043	1.095
.599	1.088	1.131	1.094	.465	1.062	1.107
.665	1.159	1.134	1.157	.531	1.095	1.148
.733	1.215	1.189	1.213	.599	1.157	1.200
.798	1.269	1.243	1.264	.664	1.211	1.246
.867	1.316	1.292	1.307	.733	1.261	1.296
.935	1.344	1.326	1.337	.801	1.312	1.335
.991	1.268	1.328	1.329	.857	1.344	1.356
1.017	.961	.947	.959	.883	1.351	1.357
			$x/D = 6.43$			
0	0.030	0.733	0.077	-0.134	0.643	0.891
.064	.062	.733	.685	-.070	.260	.916
.086	.609	.733	.901	-.048	.241	.954
.098	.831	.741	.903	-.036	.267	.968
.109	.889	.853	.896	-.025	.356	.984
.121	.898	.880	.895	-.013	.468	.991
.148	.887	.875	.892	.014	.850	.927
.170	.884	.872	.891	.036	.894	.904
.237	.884	.873	.888	.103	.914	.908
.282	.888	.878	.892	.148	.911	.921
.326	.893	.883	.898	.192	.919	.935
.374	.899	.885	.904	.240	.925	.950
.417	.910	.894	.907	.283	.925	.958
.463	.921	.904	.920	.329	.915	.951
.518	.940	.923	.941	.384	.924	.942
.575	.963	.946	.962	.441	.941	.960
.630	.977	.961	.979	.496	.958	.980
.687	.999	.982	1.006	.553	.980	1.007
.776	1.053	1.030	1.053	.642	1.026	1.063
.844	1.099	1.076	1.096	.710	1.057	1.088
.912	1.152	1.126	1.147	.778	1.094	1.127
.979	1.194	1.172	1.189	.845	1.141	1.171
1.033	1.227	1.205	1.220	.899	1.176	1.202

z/D	$p_{i1}/p_{i\infty}$	$p_{i2}/p_{i\infty}$	$p_{i3}/p_{i\infty}$	z/D (a)	$p_{i4}/p_{i\infty}$	$p_{i5}/p_{i\infty}$
			$x/D = 7.37$			
0	0.045	0.735	0.171	-0.134	0.700	0.886
.051	.117	.736	.407	-.083	.547	.916
.098	.782	.738	.882	-.036	.396	.919
.105	.854	.775	.881	-.029	.406	.919
.115	.885	.847	.881	-.019	.436	.920
.131	.884	.869	.881	-.003	.510	.919
.181	.881	.868	.888	.047	.869	.905
.193	.883	.873	.892	.059	.898	.904
.260	.886	.879	.901	.126	.914	.947
.328	.897	.884	.909	.194	.912	.928
.428	.907	.899	.911	.294	.934	.943
.509	.915	.905	.919	.375	.949	.960
.574	.926	.913	.925	.440	.950	.970
.597	.929	.918	.927	.463	.935	.966
.642	.939	.927	.939	.508	.937	.948
.710	.964	.949	.963	.575	.953	.962
.777	.981	.969	.982	.643	.968	.979
.845	1.003	.989	1.005	.711	.991	1.005
.910	1.031	1.016	1.032	.776	1.015	1.036
.979	1.070	1.055	1.069	.845	1.046	1.068
1.029	1.100	1.083	1.098	.895	1.062	1.081
			$x/D = 7.77$			
0	0.036	0.037	0.227	-0.134	0.714	0.910
.042	.033	.042	.314	-.092	.752	.919
.065	.046	.061	.516	-.069	.581	.911
.087	.337	.231	.835	-.047	.476	.886
.118	.915	.875	.896	-.016	.488	.891
.141	.906	.901	.891	.007	.572	.911
.164	.889	.888	.889	.030	.734	.907
.208	.885	.882	.890	.074	.900	.912
.253	.887	.884	.898	.119	.906	.908
.327	.892	.893	.909	.193	.925	.928
.384	.900	.897	.915	.250	.925	.955
.474	.913	.904	.922	.340	.944	.940
.564	.921	.918	.924	.430	.953	.954
.628	.926	.918	.933	.494	.966	.969
.656	.931	.924	.933	.522	.962	.974
.735	.949	.939	.951	.601	.949	.952
.786	.968	.956	.968	.652	.960	.959
.856	.986	.978	.988	.722	.977	.979
.939	1.008	.996	1.013	.805	.998	1.005
.998	1.031	1.017	1.032	.864	1.016	1.029
1.028	1.048	1.032	1.046	.894	1.028	1.044
1.033	1.051	1.036	1.049	.899	1.031	1.047

[a]Different z/D for $p_{i4}/p_{i\infty}$ and $p_{i5}/p_{i\infty}$ explained on page 8.

TABLE II. - Continued

AEDC RAKE SURVEY RESULTS

(f) M = 6; α = 5.0°

z/D	$p_{i1}/p_{i\infty}$	$p_{i2}/p_{i\infty}$	$p_{i3}/p_{i\infty}$	z/D (a)	$p_{i4}/p_{i\infty}$	$p_{i5}/p_{i\infty}$
x/D = 5.36						
0.008	0.180	0.126	1.156	-0.126	0.102	1.183
.043	1.159	1.186	1.150	-.091	.435	1.198
.109	1.085	1.094	1.084	-.025	1.178	1.150
.177	1.086	1.079	1.075	.043	1.112	1.134
.245	1.086	1.071	1.080	.111	1.127	1.112
.312	1.114	1.091	1.071	.178	1.128	1.098
.379	1.172	1.139	1.139	.245	1.198	1.107
.447	1.256	1.226	1.228	.313	1.141	1.181
.511	1.343	1.314	1.309	.377	1.222	1.255
.581	1.432	1.397	1.396	.447	1.311	1.338
.649	1.505	1.482	1.471	.515	1.389	1.419
.718	1.535	1.522	1.501	.584	1.486	1.485
.750	1.510	1.515	1.489	.616	1.508	1.496
.822	.962	.950	.936	.688	.962	.942
x/D = 7.37						
0.098	0.634	0.308	1.197	-0.036	0.116	1.117
.105	1.241	1.069	1.167	-.029	.115	1.167
.112	1.216	1.244	1.164	-.022	.262	1.169
.133	1.097	1.129	1.136	-.001	.695	1.158
.163	1.079	1.082	1.104	.029	1.165	1.153
.220	1.109	1.093	1.122	.086	1.108	1.154
.276	1.118	1.105	1.126	.142	1.133	1.151
.332	1.126	1.109	1.126	.198	1.147	1.157
.383	1.130	1.113	1.127	.249	1.152	1.165
.445	1.136	1.120	1.135	.311	1.157	1.177
.500	1.126	1.119	1.132	.366	1.154	1.199
.557	1.104	1.109	1.124	.423	1.155	1.166
.612	1.104	1.087	1.108	.478	1.152	1.166
.669	1.119	1.101	1.108	.535	1.148	1.162
.726	1.150	1.125	1.142	.592	1.144	1.132
.782	1.194	1.165	1.185	.648	1.125	1.156
.837	1.238	1.209	1.229	.703	1.162	1.201
.894	1.281	1.254	1.271	.760	1.208	1.243
.949	1.322	1.294	1.312	.815	1.251	1.285
1.006	1.348	1.321	1.339	.872	1.292	1.326
1.038	1.360	1.337	1.349	.904	1.314	1.341
x/D = 7.77						
0	0.048	0.034	1.135	-0.134	0.131	1.142
.022	.957	.442	1.195	-.112	.159	1.158
.039	1.239	1.254	1.170	-.095	.240	1.161
.056	1.126	1.149	1.136	-.078	.589	1.158
.079	1.101	1.111	1.121	-.055	1.099	1.157
.113	1.098	1.095	1.113	-.021	1.145	1.159
.158	1.109	1.099	1.122	.024	1.120	1.167
.203	1.139	1.113	1.148	.069	1.124	1.170
.228	1.144	1.133	1.145	.094	1.131	1.172
.270	1.135	1.121	1.145	.136	1.149	1.169
.316	1.139	1.124	1.145	.182	1.158	1.169
.358	1.148	1.131	1.141	.224	1.162	1.175
.427	1.148	1.131	1.145	.293	1.173	1.188
.495	1.137	1.126	1.142	.361	1.169	1.206
.527	1.131	1.117	1.136	.393	1.164	1.208
.562	1.099	1.101	1.124	.428	1.166	1.176
.630	1.116	1.098	1.113	.496	1.159	1.174
.679	1.135	1.109	1.126	.545	1.142	1.169
.721	1.162	1.133	1.153	.587	1.133	1.137
.764	1.195	1.169	1.185	.630	1.128	1.155
.809	1.226	1.201	1.217	.675	1.156	1.186
.878	1.272	1.249	1.266	.744	1.205	1.233
.944	1.314	1.291	1.306	.810	1.253	1.281
.999	1.335	1.315	1.327	.865	1.290	1.317

[a]Different z/D for $p_{i4}/p_{i\infty}$ and $p_{i5}/p_{i\infty}$ explained on page 8.

TABLE II.– Continued

AEDC RAKE SURVEY RESULTS

(g) $M = 6$; $\alpha = 10.0°$

z/D	$p_{i1}/p_{i\infty}$	$p_{i2}/p_{i\infty}$	$p_{i3}/p_{i\infty}$	z/D (a)	$p_{i4}/p_{i\infty}$	$p_{i5}/p_{i\infty}$
x/D = 5.36						
0	0.517	0.299	1.409	-0.134	0.289	1.422
.011	1.564	1.550	1.371	-.123	.799	1.422
.023	1.405	1.407	1.368	-.111	1.346	1.421
.032	1.392	1.358	1.373	-.102	1.346	1.424
.043	1.406	1.375	1.381	-.091	1.360	1.429
.066	1.434	1.403	1.402	-.068	1.366	1.442
.109	1.449	1.426	1.408	-.025	1.401	1.462
.135	1.459	1.431	1.415	.001	1.413	1.447
.157	1.472	1.430	1.431	.023	1.429	1.447
.191	1.468	1.457	1.436	.057	1.444	1.459
.203	1.476	1.451	1.435	.069	1.449	1.462
.234	1.476	1.456	1.440	.100	1.463	1.464
.246	1.496	1.454	1.452	.112	1.466	1.465
.278	1.527	1.499	1.465	.144	1.468	1.415
.324	1.556	1.522	1.489	.190	1.458	1.396
.368	1.605	1.558	1.552	.234	1.452	1.445
.413	1.679	1.632	1.632	.279	1.485	1.525
.458	1.752	1.708	1.709	.324	1.557	1.600
.504	1.826	1.782	1.780	.370	1.642	1.677
.550	1.855	1.837	1.818	.416	1.718	1.747
.581	1.589	1.820	1.796	.447	1.773	1.799
.594	.995	1.576	1.044	.460	1.792	1.805
.607	.995	.979	.962	.473	1.819	1.814
x/D = 6.43						
0	0.627	0.380	1.552	-0.134	0.837	1.399
.017	1.547	1.549	1.376	-.117	1.329	1.405
.060	1.466	1.422	1.412	-.074	1.385	1.422
.105	1.497	1.459	1.451	-.029	1.408	1.432
.151	1.527	1.491	1.476	.017	1.444	1.459
.172	1.532	1.501	1.488	.038	1.456	1.474
.187	1.534	1.506	1.493	.053	1.461	1.495
.240	1.541	1.519	1.513	.106	1.495	1.521
.297	1.526	1.506	1.490	.163	1.534	1.525
.323	1.533	1.502	1.495	.189	1.541	1.524
.338	1.516	1.508	1.484	.204	1.546	1.526
.358	1.512	1.487	1.472	.224	1.553	1.525
.395	1.521	1.486	1.481	.261	1.535	1.513
.419	1.543	1.512	1.499	.285	1.538	1.483
.487	1.582	1.539	1.530	.353	1.504	1.465
.554	1.657	1.614	1.641	.420	1.519	1.521
.622	1.699	1.677	1.668	.488	1.586	1.609
.677	1.292	1.663	1.646	.543	1.659	1.667
.691	.986	1.267	1.080	.557	1.674	1.681
.768	.985	.966	.952	.634	1.698	1.559
.796	.986	.968	.954	.662	1.646	.970
.803	.987	.966	.954	.669	1.000	.971
.817	.984	.966	.952	.683	.979	.969
x/D = 7.77						
0	0.419	0.079	1.628	-0.134	0.672	1.534
.013	1.573	1.507	1.467	-.121	.966	1.545
.030	1.464	1.502	1.420	-.104	1.357	1.547
.046	1.466	1.425	1.428	-.088	1.469	1.546
.074	1.488	1.452	1.447	-.060	1.450	1.517
.119	1.532	1.494	1.484	-.015	1.452	1.475
.142	1.545	1.507	1.496	.008	1.454	1.482
.187	1.564	1.534	1.528	.053	1.499	1.544
.215	1.605	1.556	1.556	.081	1.524	1.555
.232	1.589	1.587	1.543	.098	1.538	1.562
.321	1.591	1.566	1.553	.187	1.572	1.563
.367	1.585	1.560	1.547	.233	1.579	1.573
.389	1.574	1.555	1.546	.255	1.582	1.570
.412	1.567	1.550	1.548	.278	1.583	1.572
.457	1.543	1.529	1.524	.323	1.573	1.569
.502	1.516	1.513	1.505	.368	1.581	1.569
.545	1.519	1.481	1.473	.411	1.584	1.551
.575	1.536	1.506	1.498	.441	1.561	1.546
.612	1.547	1.517	1.506	.478	1.528	1.489
.626	1.545	1.519	1.507	.492	1.521	1.498
.637	1.556	1.517	1.509	.503	1.505	1.504
.717	1.578	1.551	1.543	.583	1.532	1.518
.769	1.353	1.532	1.527	.635	1.552	1.551
.785	.982	1.285	1.357	.651	1.563	1.557
.866	.980	.961	.950	.732	1.577	1.549
.884	.982	.961	.950	.750	1.566	1.004
.901	.982	.961	.950	.767	1.279	.975

[a]Different z/D for $p_{i4}/p_{i\infty}$ and $p_{i5}/p_{i\infty}$ explained on page 8.

TABLE II. – Continued

AEDC RAKE SURVEY RESULTS

(h) M = 6; α = 14.5°

z/D	$p_{i1}/p_{i\infty}$	$p_{i2}/p_{i\infty}$	$p_{i3}/p_{i\infty}$	z/D	$p_{i4}/p_{i\infty}$	$p_{i5}/p_{i\infty}$
x/D = 6.43						
0	0.741	0.250	1.756	-0.134	0.925	1.711
.009	1.966	1.706	1.702	-.125	1.359	1.713
.023	1.788	1.772	1.710	-.111	1.679	1.727
.049	1.836	1.763	1.778	-.085	1.695	1.769
.072	1.887	1.826	1.823	-.062	1.711	1.799
.094	1.923	1.869	1.850	-.040	1.743	1.829
.117	1.943	1.898	1.878	-.017	1.791	1.841
.139	1.982	1.929	1.879	.005	1.824	1.859
.173	1.977	1.937	1.907	.039	1.865	1.894
.211	1.985	1.939	1.923	.077	1.878	1.926
.218	1.988	1.948	1.926	.084	1.887	1.937
.249	1.999	1.962	1.942	.115	1.905	1.924
.289	1.979	1.948	1.918	.155	1.936	1.908
.308	1.982	1.950	1.906	.174	1.932	1.918
.347	1.959	1.960	1.908	.213	1.942	1.882
.398	1.971	1.923	1.914	.264	1.905	1.856
.420	1.989	1.949	1.943	.286	1.915	1.830
.444	1.998	1.961	1.946	.310	1.905	1.855
.484	1.962	1.944	1.932	.350	1.898	1.871
.496	1.916	1.931	1.909	.362	1.921	1.885
.506	1.228	1.904	1.884	.372	1.932	1.888
.517	.982	1.553	1.324	.383	1.943	1.888
.533	.979	.966	.944	.399	1.938	1.897
.578	.978	.963	.943	.444	1.945	1.893
.599	.979	.963	.941	.465	1.935	1.471
.627	.979	.960	.941	.493	1.365	.958
x/D = 7.77						
0	1.154	0.640	1.912	-0.134	1.085	1.937
.012	1.958	1.992	1.826	-.122	1.565	1.962
.053	1.953	1.888	1.896	-.081	1.819	1.973
.109	2.043	1.995	1.972	-.025	1.871	1.895
.142	2.061	2.021	2.001	.008	1.899	1.918
.187	2.092	2.061	2.053	.053	1.963	2.006
.232	2.108	2.082	2.053	.098	2.012	2.049
.277	2.100	2.069	2.053	.143	2.093	2.060
.314	2.088	2.062	2.049	.180	2.081	2.072
.346	2.061	2.041	2.023	.212	2.082	2.073
.412	2.018	1.997	1.988	.278	2.068	2.019
.436	1.989	1.974	1.948	.302	2.042	2.019
.479	1.919	1.942	1.922	.345	2.029	1.988
.530	1.449	1.803	1.792	.396	2.002	1.920
.543	.973	1.713	1.652	.409	1.965	1.915
.554	.974	.955	.936	.420	1.943	1.889
.636	.977	.956	.939	.502	1.837	1.206
.658	.976	.958	.939	.524	1.526	.955
.669	.977	.958	.939	.535	.965	.955

[a]Different z/D for $p_{i4}/p_{i\infty}$ and $p_{i5}/p_{i\infty}$ explained on page 8.

TABLE II. - Continued

AEDC RAKE SURVEY RESULTS

(i) M = 8; α = -3.0°

z/D	$p_{i1}/p_{i\infty}$	$p_{i2}/p_{i\infty}$	$p_{i3}/p_{i\infty}$	$p_{i4}/p_{i\infty}$
x/D = 6.16				
0	0.013	0.016	0.017	0.727
.022	.044	.046	.027	.686
.045	.064	.057	.046	.680
.067	.085	.063	.068	.687
.090	.094	.067	.089	.701
.135	.077	.074	.138	.738
.153	.067	.075	.157	.750
.198	.062	.082	.202	.774
.234	.099	.101	.293	.775
.293	.278	.262	.599	.778
.338	.570	.564	.706	.799
.382	.689	.695	.756	.828
.428	.742	.757	.793	.864
.483	.798	.811	.823	.893
.505	.815	.826	.823	.912
.521	.823	.833	.816	.920
.540	.829	.836	.849	.938
.554	.813	.815	.880	.949
.608	.901	.912	.947	.993
.627	.943	.955	.931	1.008
.645	.979	.984	.947	1.024
.665	.933	.940	.960	1.031
.689	.949	.956	.977	1.044
.719	.969	.975	.994	1.061
.764	1.001	1.003	1.017	1.104
.810	1.034	1.036	1.054	1.153
.860	1.077	1.080	1.104	1.200
.921	1.149	1.154	1.175	1.255
.968	1.200	1.203	1.221	1.306
1.006	1.241	1.244	1.264	1.346
x/D = 6.96				
0	0.017	0.016	0.052	0.664
.045	.076	.054	.109	.694
.090	.082	.068	.112	.685
.137	.081	.081	.107	.707
.180	.075	.090	.139	.720
.270	.105	.102	.312	.774
.315	.223	.186	.537	.794
.337	.357	.314	.636	.800
.360	.518	.487	.694	.800
.382	.642	.623	.725	.789
.406	.705	.694	.741	.777
.427	.728	.725	.747	.778
.483	.741	.742	.763	.796
.540	.756	.765	.788	.845
.597	.784	.795	.813	.879
.662	.831	.837	.829	.916
.709	.831	.835	.878	.950
.764	.912	.918	.966	.988
.787	.953	.960	.956	1.008
.809	.984	.991	.959	1.023
.831	.954	.960	.974	1.033
.853	.966	.972	.987	1.037
.877	.982	.987	1.001	1.048
.900	.998	1.002	1.013	1.061
.944	1.020	1.022	1.033	1.094
1.006	1.053	1.055	1.073	1.141
1.054	1.101	1.105	1.122	1.183
1.109	1.149	1.153	1.170	1.233
1.158	1.201	1.203	1.218	1.284
1.203	1.289	1.290	1.305	1.370
1.282	1.326	1.327	1.341	1.406
1.345	1.392	1.393	1.406	1.280
1.396	1.441	1.442	1.427	.980
1.411	1.451	1.417	.998	.981
1.430	.980	.978	.978	.980

z/D	$p_{i1}/p_{i\infty}$	$p_{i2}/p_{i\infty}$	$p_{i3}/p_{i\infty}$	$p_{i4}/p_{i\infty}$
x/D = 7.77				
0	0.017	0.016	0.110	0.642
.057	.075	.062	.177	.656
.180	.080	.095	.136	.694
.271	.088	.110	.254	.748
.315	.128	.125	.411	.744
.360	.283	.261	.616	.761
.383	.436	.409	.673	.772
.405	.587	.572	.707	.783
.428	.670	.665	.727	.794
.473	.739	.735	.750	.812
.517	.767	.762	.766	.816
.558	.776	.772	.764	.790
.596	.767	.764	.764	.799
.631	.764	.761	.776	.814
.675	.776	.779	.801	.831
.720	.798	.805	.823	.874
.764	.828	.835	.847	.923
.821	.857	.864	.851	.930
.877	.874	.881	.914	.959
.933	.944	.952	.981	.986
.957	.978	.985	.963	1.001
1.006	.968	.973	.984	1.021
1.039	.987	.993	1.003	1.035
1.130	1.027	1.031	1.040	1.092
1.175	1.054	1.058	1.071	1.128
1.220	1.094	1.097	1.111	1.164
1.310	1.169	1.172	1.187	1.236
1.362	1.211	1.214	1.228	1.281
1.400	1.243	1.245	1.259	1.309
1.444	1.287	1.288	1.302	1.352
1.524	1.359	1.382	1.371	1.409
1.556	1.387	1.387	1.399	.978
1.588	1.413	1.407	1.096	.977
1.603	1.133	1.038	.977	.978
1.614	.982	.977	.977	.978

TABLE II. – Continued

AEDC RAKE SURVEY RESULTS

(j) M = 8; $\alpha = 0°$

z/D	$p_{i1}/p_{i\infty}$	$p_{i2}/p_{i\infty}$	$p_{i3}/p_{i\infty}$	$p_{i4}/p_{i\infty}$
x/D = 6.16				
0	0.014	0.014	0.016	0.968
.011	.014	.014	.017	.961
.025	.014	.016	.025	.933
.046	.018	.027	.065	.886
.073	.046	.065	.256	.864
.101	.157	.259	.773	.862
.128	.577	.735	.872	.865
.158	.824	.851	.862	.873
.186	.843	.858	.862	.887
.242	.855	.869	.874	.919
.298	.872	.888	.899	.954
.355	.901	.921	.934	.992
.417	.943	.966	.982	1.044
.468	.985	1.003	1.015	1.093
.528	1.020	1.034	1.055	1.141
.579	1.057	1.073	1.099	1.199
.634	1.117	1.138	1.165	1.272
.690	1.189	1.212	1.242	1.347
.747	1.277	1.298	1.324	1.422
.802	1.357	1.375	1.399	1.499
.858	1.437	1.456	1.480	1.571
.916	1.521	1.539	1.561	.992
.971	1.597	1.616	1.281	.984
.991	1.613	1.024	.987	.985
.997	1.338	.982	.983	.982
1.018	.978	.981	.983	.980
x/D = 6.96				
0	0.013	0.014	0.032	0.790
.045	.018	.027	.041	.880
.102	.113	.171	.575	.897
.158	.772	.821	.865	.882
.214	.857	.869	.873	.872
.273	.851	.862	.864	.887
.327	.855	.868	.875	.910
.382	.876	.890	.896	.937
.439	.899	.915	.924	.969
.499	.930	.946	.955	1.012
.552	.963	.985	.999	1.051
.611	1.012	1.025	1.036	1.108
.664	1.041	1.055	1.071	1.148
.721	1.085	1.101	1.119	1.201
.776	1.142	1.160	1.178	1.259
.834	1.201	1.221	1.242	1.318
.888	1.269	1.288	1.306	1.373
.944	1.334	1.348	1.369	1.436
1.000	1.398	1.414	1.433	1.504
1.060	1.469	1.486	1.503	1.431
1.118	1.544	1.562	1.390	.987
1.146	1.215	.983	.981	.981
1.173	.975	.981	.980	.980
x/D = 7.77				
0	0.014	0.015	0.046	0.675
.052	.025	.031	.057	.848
.106	.105	.137	.434	.860
.162	.679	.749	.837	.876
.214	.844	.856	.861	.904
.268	.864	.872	.872	.917
.322	.872	.879	.879	.884
.376	.869	.879	.877	.898
.482	.884	.895	.905	.945
.535	.914	.920	.930	.971
.588	.941	.948	.957	1.001
.641	.970	.979	.990	1.032
.694	1.005	1.016	1.024	1.063
.745	1.029	1.039	1.046	1.096
.797	1.051	1.061	1.074	1.127
.851	1.108	1.096	1.110	1.169
.903	1.125	1.139	1.154	1.214
.956	1.171	1.187	1.202	1.271
1.009	1.231	1.247	1.263	1.326
1.011	1.229	1.245	1.259	1.321
1.067	1.292	1.303	1.319	1.374
1.121	1.346	1.357	1.373	1.427
1.174	1.402	1.413	1.429	1.484
1.232	1.463	1.473	1.489	.981
1.289	1.317	.984	.979	.979
1.344	.971	.976	.979	.980

TABLE II. – Continued

AEDC RAKE SURVEY RESULTS

(k) M = 8; α = 5.0°

z/D	$p_{i1}/p_{i\infty}$	$p_{i2}/p_{i\infty}$	$p_{i3}/p_{i\infty}$	$p_{i4}/p_{i\infty}$
		x/D = 6.16		
0	0.116	0.738	1.078	1.182
.012	.376	.848	1.047	1.186
.022	.551	.947	1.048	1.192
.034	.766	1.002	1.061	1.197
.045	.918	1.026	1.074	1.203
.056	.992	1.044	1.097	1.237
.067	1.024	1.060	1.122	1.245
.090	1.065	1.111	1.149	1.226
.112	1.118	1.147	1.178	1.239
.135	1.147	1.171	1.196	1.251
.172	1.169	1.196	1.218	1.267
.203	1.186	1.210	1.226	1.281
.247	1.199	1.229	1.166	1.226
.315	1.161	1.219	1.327	1.329
.360	1.287	1.350	1.277	1.368
.427	1.321	1.359	1.369	1.520
.494	1.415	1.467	1.523	1.647
.539	1.537	1.588	1.651	1.734
.607	1.669	1.708	1.744	1.874
.675	1.815	1.857	1.888	.989
.715	1.892	1.045	.982	.987
.731	.978	.987	.981	.987
		x/D = 6.96		
0	0.124	0.569	0.979	1.181
.009	.418	.663	.995	1.185
.016	.515	.736	1.014	1.187
.023	.554	.790	1.028	1.189
.040	.724	.927	1.076	1.200
.047	.789	.969	1.087	1.198
.064	.950	1.054	1.128	1.205
.087	1.065	1.110	1.157	1.209
.111	1.117	1.148	1.179	1.214
.124	1.129	1.159	1.185	1.216
.197	1.189	1.214	1.219	1.235
.257	1.214	1.238	1.247	1.273
.331	1.225	1.239	1.246	1.287
.344	1.226	1.245	1.194	1.247
.383	1.199	1.178	1.231	1.247
.481	1.349	1.318	1.322	1.438
.553	1.380	1.424	1.428	1.565
.629	1.504	1.549	1.585	1.663
.713	1.677	1.689	1.704	1.486
.773	1.749	1.777	1.804	.979
.792	1.785	1.812	1.112	.980
.819	1.009	.979	.974	.983
		x/D = 7.77		
0.009	0.441	0.498	0.926	1.172
.037	.704	.708	1.029	1.198
.056	.870	.851	1.079	1.209
.078	1.013	1.008	1.119	1.221
.112	1.121	1.132	1.162	1.229
.135	1.146	1.157	1.178	1.229
.157	1.167	1.179	1.210	1.235
.179	1.188	1.206	1.213	1.232
.224	1.189	1.209	1.216	1.228
.270	1.208	1.225	1.231	1.259
.315	1.222	1.234	1.237	1.270
.359	1.236	1.249	1.257	1.259
.404	1.239	1.254	1.254	1.296
.445	1.236	1.252	1.219	1.271
.457	1.233	1.246	1.199	1.249
.468	1.222	1.225	1.217	1.258
.478	1.195	1.202	1.234	1.266
.540	1.282	1.304	1.331	1.335
.586	1.296	1.310	1.323	1.393
.630	1.344	1.364	1.379	1.450
.674	1.404	1.424	1.438	1.311
.720	1.466	1.487	1.504	1.579
.764	1.528	1.547	1.565	1.629
.809	1.595	1.607	1.624	1.694
.844	1.641	1.657	1.675	1.101
.893	1.714	1.728	1.257	.984
.912	1.021	.989	.979	.984

TABLE II. – Continued

AEDC RAKE SURVEY RESULTS

(l) M = 8; α = 10.0°

z/D	$p_{i1}/p_{i\infty}$	$p_{i2}/p_{i\infty}$	$p_{i3}/p_{i\infty}$	$p_{i4}/p_{i\infty}$
		x/D = 6.16		
0	0.401	1.451	1.492	1.611
.021	1.431	1.508	1.487	1.649
.044	1.482	1.512	1.518	1.673
.066	1.477	1.524	1.558	1.692
.100	1.528	1.594	1.628	1.722
.112	1.555	1.618	1.648	1.729
.123	1.581	1.636	1.666	1.732
.145	1.643	1.690	1.720	1.736
.168	1.660	1.707	1.707	1.714
.213	1.712	1.747	1.755	1.712
.269	1.739	1.774	1.772	1.796
.324	1.784	1.834	1.831	1.968
.359	1.836	1.876	1.896	2.061
.381	1.863	1.921	1.954	2.124
.436	1.973	2.056	2.099	.989
.494	2.156	2.229	1.449	.988
.519	1.987	.982	.973	.989
.549	.933	.983	.975	.987
		x/D = 6.96		
0	0.087	1.602	1.493	1.622
.021	1.451	1.486	1.516	1.648
.044	1.477	1.508	1.549	1.669
.071	1.487	1.562	1.618	1.704
.100	1.566	1.647	1.672	1.740
.128	1.650	1.704	1.719	1.768
.156	1.708	1.747	1.741	1.787
.184	1.744	1.774	1.771	1.782
.212	1.765	1.797	1.792	1.791
.240	1.776	1.808	1.803	1.782
.268	1.782	1.818	1.800	1.767
.295	1.782	1.811	1.801	1.779
.325	1.791	1.845	1.799	1.799
.384	1.784	1.850	1.858	1.921
.437	1.866	1.914	1.917	2.035
.494	1.947	2.008	2.032	.982
.550	2.071	2.130	1.044	.979
.606	.934	.977	.967	.980
		x/D = 7.77		
0	0.083	1.197	1.483	1.679
.044	1.484	1.501	1.568	1.749
.100	1.599	1.658	1.688	1.771
.156	1.739	1.789	1.814	1.815
.213	1.822	1.859	1.839	1.836
.269	1.841	1.874	1.855	1.859
.326	1.837	1.883	1.856	1.818
.381	1.821	1.869	1.839	1.809
.437	1.800	1.847	1.821	1.845
.494	1.830	1.889	1.889	1.958
.550	1.902	1.957	1.970	.980
.605	1.921	1.002	.969	.983
.640	.938	.981	.971	.983

TABLE II. – Continued

AEDC RAKE SURVEY RESULTS

(m) M = 8; α = 20.0°

z/D	$p_{i1}/p_{i\infty}$	$p_{i2}/p_{i\infty}$	$p_{i3}/p_{i\infty}$	$p_{i4}/p_{i\infty}$
x/D = 6.16				
0	0.890	2.671	2.229	2.886
.012	2.709	2.595	2.703	2.931
.023	2.556	2.724	2.729	2.967
.034	2.691	2.862	2.766	3.076
.045	2.815	2.916	2.837	3.057
.057	2.873	2.930	2.879	3.086
.068	2.895	3.011	2.952	3.109
.079	2.946	3.052	3.038	3.124
.090	3.007	3.108	3.100	3.117
.101	3.054	3.165	3.145	3.053
.112	3.101	3.217	3.183	3.059
.124	3.156	3.268	3.236	3.051
.146	3.227	3.339	3.263	3.069
.169	3.255	3.333	3.243	3.067
.191	3.222	3.314	3.207	.958
.214	3.186	3.267	3.209	.934
.236	3.178	3.265	3.171	.936
.259	3.132	3.219	.959	.938
.256	2.799	.962	.903	.938
.286	.915	.942	.904	.938
x/D = 6.96				
0	0.858	2.971	2.768	3.225
.023	2.705	2.918	2.954	3.250
.034	2.854	2.982	3.093	3.239
.045	2.976	3.093	3.174	3.273
.057	3.018	3.128	3.201	3.249
.068	3.079	3.289	3.251	3.257
.079	3.238	3.345	3.352	3.251
.090	3.287	3.389	3.392	3.242
.102	3.335	3.440	3.393	3.227
.113	3.372	3.495	3.387	3.222
.124	3.412	3.497	3.397	3.198
.135	3.417	3.488	3.395	3.185
.157	3.409	3.492	3.426	3.216
.180	3.417	3.488	3.356	3.313
.203	3.368	3.411	3.301	.934
.225	3.281	3.339	3.239	.935
.247	3.224	3.267	3.172	.936
.290	.893	.944	.904	.937
x/D = 7.77				
0	1.125	3.161	2.966	3.272
.023	2.975	3.071	3.183	3.314
.034	3.062	3.153	3.277	3.326
.045	3.138	3.262	3.369	3.322
.056	3.243	3.367	3.406	3.332
.079	3.425	3.505	3.411	3.363
.090	3.429	3.516	3.412	3.318
.101	3.425	3.531	3.442	3.283
.113	3.450	3.526	3.441	3.279
.124	3.455	3.548	3.437	3.271
.136	3.464	3.544	3.411	3.252
.146	3.452	3.493	3.411	3.243
.158	3.415	3.488	3.409	3.244
.180	3.384	3.469	3.439	3.223
.203	3.411	3.473	3.319	3.308
.225	3.335	3.356	3.294	3.308
.248	3.255	3.309	3.236	3.143
.258	3.225	3.278	3.219	.936
.281	3.176	2.497	.907	.935
.298	.968	.946	.904	.934

TABLE III

LRC RAKE SURVEY RESULTS

(a) M = 4.65

z/D	$p_{i1}/p_{i\infty}$, y/D = 0	z/D	$p_{i2}/p_{i\infty}$, y/D = 0.401	z/D	$p_{i3}/p_{i\infty}$, y/D = 0.804
α = 0°, x/D = 6.16					
0.003	0.085	-0.202	0.361	-0.426	0.180
.009	.095	-.196	.566	-.420	.348
.023	.112	-.182	.749	-.406	.624
.043	.154	-.225	.810	-.386	.798
.083	.722	-.122	.754	-.346	.928
.137	.935	-.068	.806	-.292	1.069
.143	.938	-.062	.828	-.286	1.101
.157	.941	-.048	.868	-.272	1.125
.177	.945	-.028	.910	-.252	1.062
.217	.948	-.012	.932	-.214	.906
.271	1.002	.066	.932	-.158	.906
.405	.950	.200	.952	-.024	.942
.672	.967	.467	.934	.243	.964
.806	1.010	.601	.968	.377	1.024
1.074	1.118	.889	1.045	.645	1.044
1.208	1.186	1.003	1.128	.779	1.106
1.361	1.252	------	-----	------	-----
1.445	1.002	------	-----	------	-----
α = 0°, x/D = 7.77					
0.003	0.093	-0.202	0.248	-0.426	0.131
.009	.158	-.196	.316	-.420	.177
.023	.231	-.182	.385	-.406	.226
.043	.301	-.225	.512	-.381	.336
.083	.422	-.122	.804	-.346	.666
.137	.905	-.068	.902	-.292	.760
.143	.924	-.062	.905	-.286	.764
.157	.942	-.048	.907	-.272	.785
.177	.941	-.028	.916	-.252	.806
.217	.956	-.012	.949	-.214	.838
.271	.947	.066	.942	-.158	.849
.405	.964	.200	.955	-.024	.990
.672	.959	.467	.944	.243	.912
.806	.956	.601	.978	.377	.951
1.074	.975	.869	.946	.645	.967
1.208	1.009	1.003	.992	.779	1.007
1.476	1.086	------	-----	------	-----
1.610	1.368	------	-----	------	-----
1.824	1.194	------	-----	------	-----
1.958	.997	------	-----	------	-----
α = 5°, x/D = 6.16					
0.003	0.098	No data available			
.009	.142				
.043	1.073				
.083	1.063				
.137	1.083				
.137	1.083				
.143	1.084				
.177	1.088				
.217	1.094				
.271	1.090				
.405	1.080				
.672	1.125				
.806	1.211				
1.061	1.351				
1.195	1.000				
α = 5°, x/D = 7.77					
0.003	0.138	No data available			
.009	.409				
.023	.829				
.043	1.048				
.083	1.084				
.137	1.104				
.143	1.104				
.157	1.108				
.177	1.110				
.217	1.111				
.271	1.111				
.405	1.122				
.672	1.109				
.806	1.081				
1.024	1.156				
1.208	1.226				
1.382	1.298				
1.516	1.002				

TABLE III. – Concluded

LRC RAKE SURVEY RESULTS

(b) M = 4.65

z/D	$p_{i1}/p_{i\infty}$, y/D = 0	z/D	$p_{i2}/p_{i\infty}$, y/D = 0.401	z/D	$p_{i3}/p_{i\infty}$, y/D = 0.804
$\alpha = 10°$, x/D = 6.16					
0.003	0.127	-0.202	0.391	-0.426	0.306
.009	.129	-.196	.490	-.420	1.022
.023	1.309	-.182	.602	-.406	.540
.043	1.226	-.225	.815	-.386	.741
.083	1.254	-.122	1.242	-.346	1.536
.137	1.274	-.068	1.331	-.292	1.240
.143	1.273	-.062	1.334	-.286	1.246
.157	1.275	-.048	1.339	-.272	1.255
.177	1.278	-.028	1.339	-.252	1.266
.217	1.277	-.012	1.357	-.214	1.280
.271	1.270	.066	1.347	-.158	1.282
.405	1.249	.200	1.360	-.024	1.347
.672	1.320	.467	1.292	.243	1.325
.806	1.419	.601	1.390	.377	1.286
.812	1.412	------	-----	------	-----
.946	.996	------	-----	------	-----
$\alpha = 10°$, x/D = 7.77					
0.003	0.129	-0.202	0.331	-0.426	0.239
.009	.416	-.196	.401	-.420	.541
.023	1.270	-.182	.505	-.406	1.041
.043	1.270	-.225	.707	-.386	1.026
.083	1.290	-.122	1.191	-.346	1.158
.137	1.307	-.068	1.350	-.292	1.392
.143	1.309	-.062	1.346	-.286	1.390
.157	1.316	-.048	1.337	-.272	1.400
.177	1.322	-.028	1.331	-.252	1.440
.217	1.325	-.012	1.325	-.212	1.484
.271	1.329	.066	1.326	-.158	1.525
.405	1.336	.200	1.384	-.024	1.693
.672	1.252	.467	1.370	.243	1.352
.806	1.269	.601	1.305	.377	1.394
.812	1.348	------	-----	------	-----
.946	1.999	------	-----	------	-----
$\alpha = 20°$, x/D = 6.16					
0.003	0.283				
.009	1.838				
.023	1.976				
.043	2.023				
.083	2.076				
.137	2.127				
.143	2.136		No data available		
.157	2.150				
.177	2.160				
.217	2.167				
.271	2.158				
.407	2.115				
.485	2.053				
.619	1.000				
$\alpha = 20°$, x/D = 7.77					
0.003	0.283				
.009	1.805				
.023	1.813				
.043	1.864				
.083	1.943				
.137	1.999				
.143	2.000		No data available		
.157	2.004				
.177	2.011				
.217	2.026				
.271	2.013				
.405	2.000				
.445	1.982				
.579	1.000				

TABLE IV

AEDC CONE SURVEY RESULTS

(a) M = 4; α = -3.0°; y/D = 0

z/D	$p_{il}/p_{i\infty}$	M_l	σ, deg	ϵ, deg
x/D = 5.36				
0.181	0.782	3.93	-0.39	6.06
.238	.921	4.02	.30	2.63
.294	.930	4.01	.36	2.29
.349	.929	4.03	.34	2.27
.463	.919	4.12	.72	2.52
.575	.943	4.18	.37	2.27
.687	.956	4.11	.36	1.84
.800	.977	4.13	.44	1.53
.913	1.011	4.15	.54	1.06
1.024	1.052	3.96	.39	.23
1.056	1.063	3.97	.44	.07
x/D = 6.43				
0.235	0.829	3.95	0.27	5.24
.291	.944	4.11	.64	2.74
.346	.960	4.11	.64	2.37
.459	.977	4.06	.66	1.93
.571	.959	3.93	.68	1.56
.684	.929	3.98	.92	1.95
.796	.938	4.20	.98	2.22
.909	.957	4.11	1.25	1.80
1.020	.974	4.09	1.44	1.49
1.052	.977	4.08	.75	1.38
x/D = 7.37				
0.285	0.862	4.16	0.06	4.58
.341	.927	4.16	.26	3.01
.396	.934	4.11	.29	2.67
.454	.942	4.15	.31	2.58
.509	.951	4.15	.33	2.42
.621	.963	4.12	.38	2.15
.734	.983	4.10	.41	1.81
.846	.990	4.00	.48	1.38
.960	.938	4.00	.58	1.85
1.071	.940	4.19	.49	2.18
1.102	.946	4.20	.61	2.02

TABLE IV. – Continued

AEDC CONE SURVEY RESULTS

(b) $M = 4$; $\alpha = 0°$; $y/D = 0$

z/D	$p_{il}/p_{i\infty}$	M_l	σ, deg	ϵ, deg
$x/D = 5.36$				
0.181	0.982	3.95	0.29	0.59
.294	.978	4.05	.33	.92
.406	.967	4.05	.37	1.15
.518	.977	4.13	.39	1.31
.631	1.002	4.21	.40	1.16
.743	1.039	4.22	.42	.69
.856	1.085	4.19	.48	.17
.968	1.129	4.10	.46	-.45
1.079	1.174	4.09	.47	-.96
1.110	1.186	4.06	.39	-1.19
$x/D = 6.43$				
0.181	1.000	4.09	0.57	1.15
.293	1.005	4.07	.68	1.00
.405	1.002	4.05	.74	.87
.518	.989	4.08	.75	.99
.630	.978	4.07	.78	1.10
.743	.978	4.12	.84	1.28
.855	.991	4.13	.96	1.18
.967	1.016	4.13	1.22	.89
1.079	1.052	4.16	1.48	.57
$x/D = 7.37$				
0.182	0.976	4.06	0.17	1.25
.237	.989	4.13	.19	1.20
.294	.989	4.06	.26	1.16
.350	.990	4.04	.29	.94
.406	.993	4.07	.27	.98
.464	.996	4.00	.05	.92
.519	.999	4.00	.22	.86
.574	1.006	4.02	.30	.82
.631	1.007	4.02	.32	.79
.687	1.010	4.01	.37	.69
.743	.988	3.75	.40	.29
.799	.990	3.96	.35	.61
.855	.982	3.94	.45	.85
.912	.977	4.00	.47	1.01
.968	.978	4.06	.55	1.16
1.024	.983	4.09	.72	1.19
1.080	.990	4.12	.68	1.16
1.112	.994	4.13	.69	1.06

TABLE IV. – Continued

AEDC CONE SURVEY RESULTS

(c) M = 4; α = 5.0°; y/D = 0

z/D	$p_{il}/p_{i\infty}$	M_l	σ, deg	ϵ, deg
x/D = 5.36				
0.114	1.104	3.78	0.63	1.70
.170	1.104	3.82	.42	2.04
.228	1.099	3.81	.40	2.35
.283	1.084	3.77	.41	2.70
.339	1.066	3.79	.45	3.11
.395	1.074	3.93	.45	3.56
.452	1.077	3.93	.48	3.63
.507	1.095	3.98	.51	3.71
.620	1.160	4.04	.46	3.34
.732	1.222	3.98	.48	2.66
.844	1.288	3.97	.56	2.08
.957	1.336	3.85	.66	1.46
1.069	1.388	3.79	1.05	.94
1.102	1.406	3.85	1.16	.47
x/D = 6.43				
0.122	1.125	3.78	0.61	1.74
.177	1.126	3.81	.63	2.01
.232	1.118	3.81	.72	2.26
.290	1.122	3.88	.77	2.56
.347	1.125	3.90	.81	2.79
.402	1.123	3.88	.84	2.88
.458	1.112	3.86	.82	2.97
.572	1.073	3.86	.83	3.57
.680	1.075	3.95	.87	3.99
.909	1.169	4.01	1.23	3.21
1.020	1.219	3.95	1.38	2.68
1.053	1.235	3.97	1.17	2.57
x/D = 7.37				
0.094	1.126	3.89	0.28	1.86
.152	1.132	3.82	.27	1.82
.207	1.146	3.95	.24	2.11
.263	1.140	3.80	.29	2.01
.319	1.142	3.86	.31	2.20
.375	1.138	3.83	.27	2.38
.431	1.129	3.83	.65	2.58
.488	1.124	3.84	.36	2.72
.600	1.113	3.90	.42	3.20
.713	1.088	3.82	.80	3.43
.825	1.069	4.00	.50	4.19
.937	1.091	4.09	.59	4.21
1.049	1.131	4.02	.80	3.79
1.082	1.144	4.03	1.01	3.64

TABLE IV. – Continued

AEDC CONE SURVEY RESULTS

(d) M = 4; y/D = 0

z/D	$p_{il}/p_{i\infty}$	M_l	σ, deg	ϵ, deg
α = 10.0°, x/D = 6.43				
0.124	1.345	3.52	0.74	2.66
.236	1.323	3.52	.71	3.43
.349	1.281	3.60	.92	4.49
.405	1.273	3.69	.85	4.93
.461	1.258	3.70	.59	5.33
.517	1.260	3.77	.86	5.67
.630	1.278	3.74	.91	5.70
.742	1.330	3.80	.66	5.46
.854	1.388	3.76	1.05	4.98
.968	1.445	3.73	1.33	4.46
1.112	1.029	3.66	1.25	8.48
α = 10.5°, x/D = 7.37				
0.114	1.343	3.56	0.62	2.05
.169	1.347	3.58	.55	2.49
.229	1.386	3.72	.54	2.80
.269	1.360	3.53	.54	2.83
.327	1.363	3.59	.54	3.29
.394	1.360	3.59	.52	3.56
.450	1.339	3.54	.60	3.77
.498	1.308	3.56	.47	4.08
.563	1.278	3.62	.58	4.76
.619	1.256	3.66	.65	5.28
.735	1.249	3.77	.93	6.07
.844	1.267	3.78	.95	6.05
.876	1.279	3.78	1.27	5.99

(e) M = 4; y/D = 0.536

z/D	$p_{il}/p_{i\infty}$	M_l	σ, deg	ϵ, deg
α = -3.0°, x/D = 7.37				
0.124	0.758	4.21	3.78	5.90
.236	.886	4.11	2.09	3.63
.349	.943	3.92	2.08	2.26
.460	.899	4.00	1.41	2.78
.573	.912	4.06	1.41	2.78
.685	.918	4.04	1.34	2.42
.797	.931	4.05	1.33	2.23
.909	.937	4.03	.97	2.01
α = 0°, x/D = 7.37				
0.248	0.982	3.62	1.16	0.31
.364	.961	3.67	0	.38
.472	.954	3.91	.18	1.18
.587	.959	3.95	.26	1.20
.698	.968	3.97	.30	1.13
.812	.980	4.00	.32	.98
.922	.986	3.96	.18	.79
α = 5.0°, x/D = 7.37				
0.242	1.089	3.89	-1.68	2.93
.354	1.091	3.79	-1.33	2.97
.466	1.098	3.80	-.93	3.05
.579	1.110	3.80	-.56	3.01
.690	1.109	3.81	-.32	3.08
.804	1.109	3.81	-.26	3.14
.889	1.075	3.64	-.77	3.20
α = 10.0°, x/D = 7.37				
0.110	1.319	3.40	-1.95	2.41
.223	1.270	3.24	-3.35	3.01
.334	1.285	3.63	-2.97	4.56
.450	1.295	3.57	-2.55	4.48
.558	1.318	3.61	-2.17	4.49
.677	1.320	3.59	-1.88	4.58
.784	1.319	3.61	-1.70	7.74
.905	1.224	3.62	-1.68	6.03
.968	1.237	3.71	-1.39	6.29

TABLE IV. – Continued

AEDC CONE SURVEY RESULTS

(f) $M = 6$; $\alpha = -3.0°$; $y/D = 0$

z/D	$p_{il}/p_{i\infty}$	M_l	σ, deg	ε, deg
x/D = 6.43				
0.328	0.751	6.00	0.02	1.78
.443	.761	5.98	.09	1.52
.555	.795	6.00	.17	1.40
.662	.838	6.00	.19	.84
.779	.885	6.00	.32	.29
.892	.927	6.06	.19	-.14
1.004	.978	6.00	.87	-.53
x/D = 7.37				
0.420	0.753	5.73	-0.30	1.61
.533	.774	6.00	-.17	1.70
.645	.776	5.85	-.18	1.35
.758	.802	6.00	-.09	1.37
.870	.847	6.06	.04	.81
.983	.883	6.06	.03	.38
1.069	.916	6.13	.20	.03

(g) $M = 6$; $\alpha = 0°$; $y/D = 0$

z/D	$p_{il}/p_{i\infty}$	M_l	σ, deg	ε, deg
x/D = 5.36				
0.162	0.905	5.54	-0.23	-0.81
.219	.893	5.76	-.25	-.26
.274	.905	5.91	-.19	-.06
.331	.927	6.00	-.16	-.08
.387	.959	6.06	-.15	-.20
.444	.977	5.96	-.11	-.46
.499	1.005	6.00	-.05	-.53
.769	1.231	6.06	.17	-2.13
.859	1.302	5.89	.22	-2.93
.949	1.342	5.72	.47	-3.31
x/D = 6.43				
0.148	0.892	5.78	-0.29	-0.17
.217	.871	5.76	-.34	-.14
.276	.874	5.76	-.32	-.04
.331	.880	5.79	-.26	-.01
.387	.887	5.81	-.21	0
.442	.898	5.86	-.15	.01
.499	.913	5.93	-.14	0
.589	.950	6.00	-.13	-.18
.679	.976	5.95	-.09	-.46
.768	1.021	6.00	.07	-.65
.859	1.083	6.00	.13	-1.12
.949	1.149	6.06	.50	-1.77
1.071	1.221	5.76	.53	-2.68
1.092	1.230	5.74	.41	-2.79
x/D = 7.37				
0.175	0.875	5.25	-0.19	-0.77
.228	.878	5.69	-.21	.02
.283	.878	5.64	-.16	-.01
.336	.885	5.67	-.11	.02
.390	.893	5.75	-.07	.05
.444	.900	5.72	-.07	.01
.498	.905	5.71	-.07	0
.588	.915	5.75	-.01	.01
.678	.935	5.82	.04	-.03
.768	.966	5.87	.10	-.22
.858	.992	5.83	.17	-.43
.947	1.031	5.96	.75	-.61
1.037	1.081	5.97	.51	-1.03
1.095	1.119	5.98	.32	-1.34

TABLE IV. – Continued

AEDC CONE SURVEY RESULTS

(h) M = 6; α = 5.0°; y/D = 0

z/D	$p_{il}/p_{i\infty}$	M_l	σ, deg	ϵ, deg
x/D = 5.36				
0.143	1.080	5.33	-0.12	0.90
.198	1.073	5.27	-.12	1.22
.255	1.082	5.48	-.12	1.68
.311	1.103	5.61	-.05	1.93
.367	1.138	5.78	-.03	2.02
.423	1.209	5.87	-.07	1.84
.479	1.280	5.88	.02	1.48
.536	1.357	5.89	.09	.99
.592	1.425	5.75	.07	.49
.648	1.493	5.70	.06	.07
.704	1.524	5.48	.22	-.49
.762	1.496	5.43	.17	-1.70
x/D = 6.43				
0.108	1.087	5.37	-0.41	0.62
.164	1.104	5.51	-.40	.99
.221	1.113	5.53	-.33	1.20
.277	1.118	5.57	-.33	1.38
.333	1.111	5.49	-.33	1.54
.389	1.091	5.45	-.25	1.94
.446	1.104	5.79	-.27	2.25
.501	1.129	5.91	-.22	2.30
.558	1.174	6.00	-.17	2.31
.614	1.228	5.96	-.11	1.97
.670	1.284	5.95	-.09	1.54
.726	1.338	5.95	-.09	1.22
.783	1.379	5.84	.02	.84
.829	1.411	5.83	.03	.56
.902	1.416	5.79	.46	-1.16
x/D = 7.37				
0.129	1.096	5.45	-0.01	0.77
.164	1.129	5.73	.01	.88
.255	1.127	5.56	.04	1.14
.345	1.134	5.57	.13	1.42
.400	1.136	5.62	.12	1.58
.457	1.122	5.56	.15	1.69
.515	1.096	5.56	.12	2.05
.569	1.109	5.84	.23	2.46
.625	1.121	5.85	.23	2.44
.681	1.166	5.99	.23	2.35
.738	1.211	6.00	.34	2.12
.793	1.253	5.90	.49	1.78
.850	1.295	5.87	.67	1.45
.906	1.323	5.79	.74	1.18
.962	1.352	5.78	.88	.87

TABLE IV. - Continued

AEDC CONE SURVEY RESULTS

(i) M = 6; α = 10.0°; y/D = 0

z/D	$p_{il}/p_{i\infty}$	M_l	σ, deg	ϵ, deg
x/D = 5.36				
0.200	1.394	4.95	0.31	2.33
.265	1.424	5.20	.28	2.85
.313	1.469	5.31	.29	3.00
.367	1.508	5.31	.33	3.12
.425	1.599	5.50	.23	3.04
.481	1.689	5.48	.29	2.66
.539	1.773	5.52	.31	2.11
.569	1.757	6.06	.33	.13
.584	1.743	5.77	.30	.16
x/D = 6.43				
0.096	1.408	4.90	-0.05	1.00
.152	1.448	5.04	-.05	1.56
.208	1.467	5.10	-.05	1.96
.265	1.467	5.19	-.07	2.47
.323	1.455	5.21	-.05	2.86
.377	1.438	5.20	-.07	3.38
.434	1.467	5.47	-.04	3.79
.479	1.485	5.39	-.01	3.82
.559	1.576	5.67	-.02	3.75
.602	1.613	5.64	-.01	3.44
x/D = 7.37				
0.150	1.452	4.99	-0.07	1.58
.204	1.490	5.05	-.02	1.59
.259	1.497	5.21	-.02	2.14
.315	1.495	5.22	-.01	2.51
.372	1.482	5.23	-.01	2.85
.428	1.453	5.22	-.04	3.29
.484	1.435	5.25	-.05	3.79
.541	1.459	5.60	.05	4.10
.597	1.475	5.59	.06	4.11
.653	1.509	5.68	.03	4.02
.709	1.519	5.56	.12	3.79

TABLE IV. - Continued

AEDC CONE SURVEY RESULTS

(j) M = 6; α = 14.5°; y/D = 0

z/D	$p_{il}/p_{i\infty}$	M_l	σ, deg	ϵ, deg
x/D = 5.36				
0.127	1.752	4.48	0.18	2.81
.182	1.791	4.63	.19	3.53
.220	1.791	4.55	.15	3.93
.240	1.803	4.68	.13	4.11
.293	1.845	4.84	.10	4.74
.342	1.885	4.90	.14	4.97
.385	1.926	4.93	.13	5.11
.430	1.997	5.71	.11	3.59
.463	1.959	6.06	.12	2.22
x/D = 6.43				
0.123	1.864	4.54	0.47	2.59
.179	1.876	4.53	.49	3.27
.235	1.893	4.67	.44	3.90
.292	1.879	4.73	.47	4.42
.348	1.859	4.70	.45	4.89
.404	1.882	4.98	.46	5.51
x/D = 7.37				
0.111	1.898	4.58	0.11	2.37
.167	1.982	4.86	.14	2.98
.223	1.975	4.63	.12	3.28
.282	1.972	4.74	.12	3.97
.335	1.946	4.81	.11	4.48
.392	1.920	4.91	.11	4.97
.448	1.893	5.04	.11	5.27

(k) M = 6; α = 0°; y/D = 0.268

z/D	$p_{il}/p_{i\infty}$	M_l	σ, deg	ϵ, deg
x/D = 6.43				
0.226	0.894	5.81	-0.23	1.09
.288	.898	5.82	-.24	1.17
.339	.906	5.82	-.18	1.20
.394	.931	5.89	-.10	1.20
.450	.932	5.91	-.13	1.23
.507	.947	5.95	-.09	1.20
.563	.969	6.06	-.10	1.12
.675	1.009	6.00	-.12	.74
.792	1.074	6.00	-.14	.40
.843	1.107	6.06	-.20	.17
.899	1.152	6.06	-.25	-.13
.956	1.193	6.00	-.31	-.54
1.012	1.228	6.00	-.46	-.86
1.039	1.246	5.98	-.34	-1.05
x/D = 7.37				
0.225	0.909	5.81	0.11	1.26
.281	.910	5.75	.14	1.24
.337	.919	5.77	.24	1.25
.393	.923	5.75	.21	1.18
.449	.927	5.80	.18	1.21
.506	.934	5.84	.23	1.22
.562	.935	5.78	.26	1.20
.619	.946	5.85	.25	1.20
.674	.960	5.87	.24	1.15
.731	.981	5.90	.23	1.03
.787	.996	5.88	.22	.83
.842	1.013	5.90	.17	.70
.898	1.037	5.91	.23	.58
.955	1.065	5.88	.20	.41
1.011	1.096	5.86	.25	.15
1.039	1.110	5.91	-.23	.03

TABLE IV. - Continued

AEDC CONE SURVEY RESULTS

(l) M = 6; α = 5.0°; y/D = 0.268

z/D	$p_{il}/p_{i\infty}$	M_l	σ, deg	ϵ, deg
x/D = 6.43				
0.147	1.068	5.61	-0.84	2.10
.205	1.086	5.66	-.68	2.24
.255	1.091	5.71	-.74	2.34
.317	1.088	5.64	-.36	2.56
.365	1.088	5.72	-.28	2.71
.428	1.073	5.62	-.26	3.08
.485	1.089	5.81	-.20	3.29
.540	1.114	5.85	-.16	3.34
.597	1.164	6.00	-.11	3.19
.653	1.218	6.00	-.15	2.89
.709	1.272	6.06	-.28	2.43
.765	1.322	5.98	-.24	2.04
.821	1.364	5.83	-.19	1.67
.877	1.401	5.79	-.24	1.29
.933	1.398	6.06	-.04	.03
x/D = 7.37				
0.186	1.106	5.69	-0.78	2.05
.241	1.103	5.45	-.78	2.04
.299	1.108	5.54	-.71	2.36
.354	1.114	5.56	-.63	2.52
.410	1.118	5.57	-.54	2.63
.467	1.118	5.60	-.48	2.74
.523	1.094	5.45	-.40	2.93
.579	1.087	5.56	-.34	3.27
.635	1.104	5.77	-.29	3.50
.691	1.134	5.91	-.24	3.48
.747	1.179	6.00	-.27	3.28
.804	1.222	6.00	-.35	2.98
.859	1.261	5.98	-.41	2.69
.901	1.296	5.96	-.14	2.41

(m) M = 6; α = 10.0°; y/D = 0.268

z/D	$p_{il}/p_{i\infty}$	M_l	σ, deg	ϵ, deg
x/D = 6.43				
0.131	1.524	5.44	-1.17	4.19
.197	1.527	5.36	-.92	4.39
.253	1.521	5.36	-.71	4.54
.309	1.502	5.20	-.57	4.81
.365	1.540	5.33	-.48	4.99
.422	1.571	5.28	-.35	4.95
.477	1.641	5.42	-.34	4.83
.533	1.696	5.45	-.35	4.46
x/D = 7.37				
0.170	1.585	5.69	-1.29	3.55
.226	1.555	4.99	-1.56	3.15
.282	1.568	5.11	-1.34	3.60
.344	1.572	5.14	-1.18	3.88
.394	1.560	5.21	-1.06	4.11
.450	1.530	5.14	-.95	4.50
.506	1.512	5.18	-.85	5.00
.562	1.537	5.44	-.66	5.30
.618	1.556	5.43	-.60	5.28
.674	1.595	5.43	-.30	5.20
.731	1.612	5.43	-.41	4.87

TABLE IV. - Continued

AEDC CONE SURVEY RESULTS

(n) M = 6; α = 14.5°; y/D = 0.268

z/D	$p_{il}/p_{i\infty}$	M_l	σ, deg	ϵ, deg
y/D = 0.268, α = 14.5°, x/D = 6.43				
0.140	1.831	4.53	-2.44	4.11
.195	1.867	4.57	-2.13	4.52
.251	1.876	4.63	-1.76	5.03
.307	1.878	4.71	-1.58	5.48
.365	1.883	4.83	-1.33	5.92
.420	1.864	4.77	-1.19	6.36
.475	1.903	5.00	-1.03	6.48
y/D = 0.268, α = 14.5°, x/D = 7.37				
0.122	1.886	4.58	-2.61	4.14
.177	1.969	4.76	-2.21	4.37
.234	1.986	4.68	-1.98	4.58
.290	1.989	4.73	-1.75	5.00
.347	1.971	4.73	-1.55	5.43
.402	1.935	4.75	-1.30	5.87
.459	1.898	4.78	-1.12	6.38
.515	1.858	4.84	-.99	6.63

(o) M = 6; α = -3.0°; y/D = 0.536

z/D	p_{il} $p_{i\infty}$	M_l	σ, deg	ϵ, deg
x/D = 7.37				
0.138	0.636	5.29	4.40	5.13
.250	.759	5.37	2.20	2.76
.361	.746	5.39	1.83	3.04
.473	.759	5.56	1.63	3.16
.584	.779	5.64	1.55	2.98
.698	.825	5.85	1.29	2.60
.810	.868	5.87	1.25	2.18
.924	.852	5.43	.79	1.68
1.034	.895	5.82	.75	1.95
1.109	.923	5.91	.66	1.69

(p) M = 6; α = 0°; y/D = 0.536

z/D	$p_{il}/p_{i\infty}$	M_l	σ, deg	ϵ, deg
x/D = 6.43				
0.225	0.888	5.75	0.26	1.67
.282	.897	5.67	.06	1.46
.339	.905	5.66	.14	1.32
.394	.923	5.74	.22	1.23
.450	.940	5.75	.15	1.11
.507	.953	5.71	.15	.96
.567	.938	5.44	.10	.75
.618	.939	5.56	0	.93
.678	.962	5.91	-.02	1.13
.731	.982	5.91	-.03	.98
.787	1.009	5.93	-.07	.83
.843	1.044	6.00	-.22	.64
.899	1.079	5.93	-.34	.38
.956	1.104	5.84	-.52	.07
1.014	1.134	5.86	-.68	-.08
x/D = 7.37				
0.290	0.911	5.62	0.22	1.09
.346	.898	5.50	.19	1.16
.402	.904	5.61	.31	1.30
.455	.911	5.63	.38	1.28
.514	.920	5.64	.40	1.27
.568	.936	5.69	.40	1.17
.627	.951	5.69	.33	1.05
.682	.964	5.71	.37	.92
.739	.944	5.47	.40	.81
.796	.947	5.67	.24	1.14
.851	.970	5.78	.21	1.14
.908	.988	5.75	.18	.98
.964	1.008	5.75	.16	.84
1.019	1.036	5.85	.20	.70
1.036	1.042	5.83	.16	.65

TABLE IV. – Continued

AEDC CONE SURVEY RESULTS

(q) $M = 6$; $\alpha = 5.0°$; $y/D = 0.536$

z/D	$p_{il}/p_{i\infty}$	M_l	σ, deg	ϵ, deg
x/D = 6.43				
0.245	1.142	5.32	-1.58	2.93
.302	1.172	5.43	-1.41	2.83
.357	1.188	5.46	-1.25	2.78
.413	1.182	5.36	-1.10	2.74
.468	1.175	5.40	-1.37	2.95
.525	1.175	5.43	-1.06	3.20
.581	1.174	5.48	-.87	3.36
.638	1.172	5.43	-.80	3.49
.694	1.213	5.66	-.69	3.59
.749	1.265	5.77	-.73	3.35
.806	1.319	5.74	-.82	2.98
.918	1.413	5.65	-1.03	2.28
.975	1.464	5.70	-.99	2.00
1.031	1.491	5.49	-1.08	1.58
1.086	1.483	5.88	-1.31	2.64
x/D = 7.37				
0.171	1.144	5.12	-2.76	2.73
.274	1.151	5.33	-1.74	2.62
.350	1.154	5.31	-1.58	2.77
.396	1.165	5.38	-1.38	2.88
.452	1.182	5.47	-1.20	2.97
.507	1.196	5.43	-1.03	3.03
.565	1.192	5.35	-1.02	2.94
.620	1.183	5.36	-1.07	3.09
.679	1.178	5.40	-.97	3.29
.733	1.176	5.47	-.81	3.45
.788	1.171	5.42	-.81	3.61
.844	1.205	5.70	-.70	3.74
.901	1.251	5.79	-.71	3.52
.957	1.295	5.78	-.84	3.18
1.016	1.339	5.79	-1.01	2.90

TABLE IV. - Continued

AEDC CONE SURVEY RESULTS

(r) M = 6; α = 10.0°; y/D = 0.536

z/D	$p_{il}/p_{i\infty}$	M_l	σ, deg	ϵ, deg
x/D = 6.43				
0.154	1.371	4.70	-3.55	4.35
.210	1.408	4.85	-3.28	4.54
.267	1.466	5.04	-3.02	4.57
.323	1.492	5.04	-2.94	4.44
.379	1.500	5.00	-2.82	4.48
.435	1.515	5.06	-2.66	4.62
.492	1.504	5.02	-2.50	4.74
.548	1.473	4.98	-2.22	5.16
.604	1.496	5.22	-1.95	5.48
.661	1.542	5.33	-1.75	5.48
.716	1.607	5.43	-1.71	5.31
.773	1.671	5.43	-1.77	4.86
.830	1.694	5.23	-1.51	4.39
x/D = 7.37				
0.158	1.410	4.62	-3.21	3.75
.213	1.439	4.77	-3.00	4.19
.270	1.479	4.91	-2.90	4.15
.325	1.489	4.93	-2.70	4.25
.382	1.518	5.03	-2.41	4.45
.431	1.538	5.09	-2.20	4.47
.494	1.541	5.09	-2.10	4.55
.548	1.543	5.13	-1.91	4.74
.607	1.528	5.12	-1.75	4.84
.649	1.495	5.01	-1.67	5.14
.720	1.507	5.23	-1.31	5.61
.785	1.539	5.29	-1.51	5.57

(s) M = 6; α = 14.5°; y/D = 0.536

z/D	$p_{il}/p_{i\infty}$	M_l	σ, deg	ϵ, deg
x/D = 7.37				
0.164	1.784	3.98	-4.17	5.24
.220	1.844	4.25	-3.98	6.06
.275	1.944	4.56	-3.68	6.05
.332	1.976	4.43	-3.77	6.04
.404	2.028	4.58	-3.35	6.28
.444	2.029	4.58	-3.18	6.33
.501	1.996	4.52	-2.99	6.63
.556	1.956	4.58	-2.77	7.08
.614	1.913	4.95	-2.38	7.52
.669	1.886	5.09	-2.10	7.81

TABLE IV. – Continued

AEDC CONE SURVEY RESULTS

(t) M = 8; α = -3.0°; y/D = 0

z/D	$p_{il}/p_{i\infty}$	σ, deg	ϵ, deg
x/D = 7.37			
0.403	0.549	0.99	5.91
.472	.747	-.37	1.04
.562	.753	-.22	.51
.606	.758	-.20	.69
.719	.834	-.26	.62
.808	.859	-.13	.06
.944	.969	-.07	-1.06
1.072	1.034	.34	-1.24

(u) M = 8; α = 0°; y/D = 0

z/D	$p_{il}/p_{i\infty}$	σ, deg	ϵ, deg
x/D = 6.16			
0.202	0.850	-0.57	-0.43
.248	.860	-.47	-.41
.292	.867	-.48	-.44
.337	.885	-.41	-.42
.382	.918	-.40	-.59
.439	.923	-.31	-.74
.494	1.052	-.31	-.49
.551	1.014	-.38	-1.90
.606	1.061	-.31	-1.18
.674	1.136	-.22	-1.45
.742	1.234	-.20	-1.80
.809	1.328	-.24	-2.31
.877	1.417	-.24	-2.81
.945	1.504	-.08	-3.32
1.011	1.592	-.14	-4.36
1.017	1.605	-.05	-4.49
x/D = 6.96			
0.247	0.864	-0.64	-0.52
.293	.853	-.50	-.69
.336	.861	-.35	-.37
.382	.876	-.31	-.32
.438	.905	-.31	-.44
.494	.929	-.30	-.63
.551	.922	-.28	-.77
.606	1.018	-.18	-.28
.675	1.025	-.20	-1.50
.742	1.079	-.09	-1.13
.808	1.143	-.13	-1.44
.877	1.216	-.18	-1.87
.944	1.296	-.05	-2.28
1.011	1.368	-.07	-2.73
1.072	1.444	.26	-3.06
x/D = 7.37			
0.236	0.843	-0.34	0.20
.287	.893	-.45	-.25
.325	.864	-.61	-.78
.408	.873	-.38	-.36
.442	.884	-.38	-.34
.495	.906	-.30	-.41
.551	.934	-.30	-.54
.607	.932	-.26	-.72
.664	1.019	-.20	-.31
.720	1.021	-.43	-1.19
.776	1.056	-.19	-1.15
.834	1.101	-.16	-1.30
.889	1.151	-.21	-1.59
.945	1.208	-.15	-1.89
1.006	1.280	-.09	-2.24
1.056	1.336	-.11	-2.55
1.072	1.354	.14	-2.62

TABLE IV. – Continued

AEDC CONE SURVEY RESULTS

(v) M = 8; α = 5.0°; y/D = 0

z/D	$p_{il}/p_{i\infty}$	σ, deg	ϵ, deg
x/D = 6.16			
0.112	1.089	-0.54	0.96
.157	1.139	-.55	1.14
.202	1.169	-.49	1.13
.247	1.184	-.48	1.19
.292	1.186	-.48	1.25
.337	1.195	-.34	1.64
.382	1.325	-.29	1.88
.427	1.301	-.48	1.18
.472	1.371	-.36	1.50
.539	1.489	-.38	1.02
.606	1.625	-.73	.52
.674	1.761	-.67	.04
x/D = 6.96			
0.157	1.147	-0.64	0.77
.213	1.187	-.49	1.14
.270	1.209	-.38	1.25
.326	1.226	-.38	1.33
.382	1.218	-.29	1.35
.415	1.184	-.34	1.65
.438	1.230	-.23	1.85
.496	1.303	-.29	1.85
.551	1.361	-.28	1.59
.607	1.445	-.30	1.39
.662	1.526	-.66	1.02
.720	1.617	-.67	.57
.794	1.729	-.61	.11
.794	1.734	-.61	.11
x/D = 7.37			
0.157	1.197	-0.49	1.13
.224	1.188	-.48	.73
.291	1.216	-.33	1.32
.359	1.242	-.29	1.45
.426	1.239	-.28	1.47
.497	1.275	-.14	2.09
.562	1.314	-.31	1.68
.629	1.398	-.22	1.57
.697	1.490	-.25	1.15
.773	1.604	-.50	.69
.831	1.685	-.45	.29
.871	1.752	-.54	-1.40

(w) M = 8; α = 10.0°; y/D = 0

z/D	$p_{il}/p_{i\infty}$	σ, deg	ϵ, deg
x/D = 6.16			
0.102	1.557	-1.28	1.38
.156	1.653	-1.12	1.93
.202	1.699	-1.01	2.19
.248	1.733	-.94	2.45
.292	1.753	-.99	2.61
.337	1.789	-.75	3.11
.381	1.846	-.85	3.31
.427	1.871	-.83	2.88
.472	2.033	-.70	3.15
.517	2.157	-.73	-.05
x/D = 6.96			
0.112	1.627	-1.09	1.61
.134	1.681	-1.02	1.56
.158	1.726	-.87	1.61
.179	1.751	-1.07	1.84
.202	1.782	-1.02	1.92
.224	1.784	-1.01	2.04
.247	1.795	-.94	2.16
.269	1.799	-.86	2.24
.292	1.803	-.89	2.41
.314	1.791	-.81	2.63
.337	1.795	-.77	2.79
.359	1.805	-.82	2.93
.383	1.795	-.79	3.12
.427	1.841	-.65	3.53
.471	1.888	-.72	3.52
.516	1.974	-.66	3.14

TABLE IV. – Continued

AEDC CONE SURVEY RESULTS

(x) $M = 8$; $\alpha = 20.0°$; $y/D = 0$

z/D	$p_{il}/p_{i\infty}$	σ, deg	ε, deg
x/D = 6.16			
0.083	2.994	-2.03	2.24
.104	3.043	-1.96	2.35
.126	3.119	-1.97	2.45
.150	3.203	-2.46	2.68
.172	3.236	-1.68	2.82
.195	3.262	-1.63	3.21
.216	3.236	-1.56	3.40
.261	3.221	-1.45	-.72
x/D = 6.96			
0.089	3.340	-1.83	2.40
.112	3.340	-1.89	2.39
.135	3.410	-1.86	2.35
.157	3.410	-1.70	1.96
.180	3.460	-1.52	2.56
.203	3.400	-1.58	2.88
.225	3.340	-1.46	3.06
.253	3.260	-1.53	.21
x/D = 7.37			
0.067	3.116	-1.64	0.05
.089	3.276	-1.81	2.19
.111	3.385	-1.64	2.21
.135	3.443	-1.50	2.29
.181	3.453	-1.64	2.56
.225	3.342	-1.43	2.54

(y) $M = 8$; $\alpha = -3.0°$; $y/D = 0.268$

z/D	$p_{il}/p_{i\infty}$	σ, deg	ε, deg
x/D = 5.36			
0.405	0.829	-0.48	2.19
.472	.891	-.54	2.64
.539	.949	-.55	3.08
.607	1.004	-.57	3.52
.674	1.072	-.56	2.82
.741	1.157	-.52	4.25
.812	1.251	-.57	4.46
.876	1.345	-.48	5.12
.944	1.449	-.54	5.55
1.011	1.546	-.51	6.01
1.039	1.567	-.60	6.63
x/D = 6.96			
0.452	0.744	-0.71	1.61
.517	.755	-.79	1.96
.554	.843	-.71	1.07
.584	.788	-.44	2.00
.652	.827	-.66	2.21
.696	.850	-.66	2.46
.743	.882	-.72	2.68
.809	.934	-.73	2.94
.854	.970	-.76	3.16
.899	1.003	-.62	3.43
.966	1.043	-.61	3.82
1.034	1.096	-.55	4.17
1.057	1.115	-.56	4.20
1.081	1.141	-.63	4.28
1.081	1.138	-.68	4.26

TABLE IV. – Continued

AEDC CONE SURVEY RESULTS

(z) $M = 8$; $\alpha = 0°$; $y/D = 0.268$

z/D	$p_{i l}/p_{i\infty}$	σ, deg	ϵ, deg
x/D = 5.36			
0.202	0.886	-0.31	2.62
.270	.915	-.51	.63
.337	.974	-.54	.76
.405	1.015	-.57	1.23
.472	1.085	-.57	1.31
.539	1.182	-.49	1.61
.605	1.310	-.48	2.23
.741	1.532	-.48	3.42
.809	1.639	-.55	3.84
.849	1.639	-.76	5.04
x/D = 6.16			
0.247	0.817	-0.58	0.31
.315	.893	-.26	.40
.382	.925	-.58	.69
.449	.971	-.62	.82
.517	1.017	-.64	1.13
.584	1.063	-.66	1.32
.675	1.162	-.62	1.70
.742	1.270	-.62	2.19
.809	1.369	-.63	2.70
.876	1.478	-.56	3.04
.966	1.605	-.40	3.73
1.004	1.379	-.73	5.58
x/D = 6.96			
0.269	0.861	-0.44	0.59
.334	.823	-.64	.63
.353	.812	-.58	.50
.404	.954	-.65	.50
.420	.995	-.88	.03
.447	.916	-.40	.61
.471	.924	-.52	1.56
.504	.941	-.60	.79
.539	.955	-.60	.78
.606	1.001	-.59	.92
.674	1.038	-.69	1.23
.742	1.095	-.73	1.34
.876	1.261	-.63	2.17
.943	1.342	-.64	2.62
1.011	1.428	-.67	3.01
1.079	1.511	-.73	3.34
1.092	1.527	-1.35	3.43
x/D = 7.37			
0.269	0.864	-0.44	0.54
.359	.875	-.51	.67
.427	.886	-.76	.21
.493	.924	-.57	.56
.563	.946	-.60	.69
.629	.991	-.67	.75
.696	1.030	-.71	1.01
.764	1.073	-.71	1.22
.831	1.134	-.61	1.45
.899	1.205	-.55	.92
.966	1.294	-.49	2.30
1.034	1.366	-.48	2.95
1.092	1.437	-.69	3.02

TABLE IV. – Concluded

AEDC CONE SURVEY RESULTS

(aa) M = 8; α = 5.0°; y/D = 0.268

z/D	$p_{il}/p_{i\infty}$	σ, deg	ϵ, deg
x/D = 5.36			
0.202	1.176	-0.44	-1.17
.269	1.239	-.47	-1.56
.337	1.359	-.43	-1.57
.404	1.509	-.41	-1.08
.472	1.669	-.41	-.47
.539	1.846	-.41	-.15
.607	2.009	-.41	2.40
.620	2.025	-.49	2.43
x/D = 6.16			
0.300	1.213	-0.47	-1.29
.337	1.235	-.47	-1.60
.382	1.282	-.49	-1.76
.449	1.392	-.53	-1.65
.517	1.516	-.54	-1.17
.588	1.643	-.51	-.55
.651	1.782	-.62	-.21
.708	1.919	-.60	1.84
.722	1.914	-.50	1.81
.725	1.692	-.62	2.08
.731	1.047	-.91	3.44
x/D = 6.96			
0.146	1.162	-0.33	-1.17
.202	1.212	-.38	-1.35
.270	1.171	-.32	-1.31
.315	1.339	-.57	-1.72
.382	1.247	-.49	-.41
.449	1.272	-.56	-1.89
.516	1.348	-.58	-2.02
.586	1.465	-.68	-1.74
.629	1.538	-.63	-1.44
.697	1.642	-.56	-.94
.764	1.753	-.56	-.41
.815	1.657	-.49	1.58
x/D = 7.37			
0.134	1.165	-0.40	-1.53
.202	1.212	-.34	-1.17
.269	1.250	-.43	-1.29
.316	1.191	-.40	-1.46
.382	1.375	-.56	-1.70
.450	1.255	-.56	-1.67
.517	1.303	-.60	-2.13
.585	1.397	-.65	-2.00
.652	1.498	-.68	-1.55
.719	1.591	-.68	-1.07
.786	1.702	-.70	-.62
.854	1.705	-.74	1.32
.846	1.801	-.99	1.28

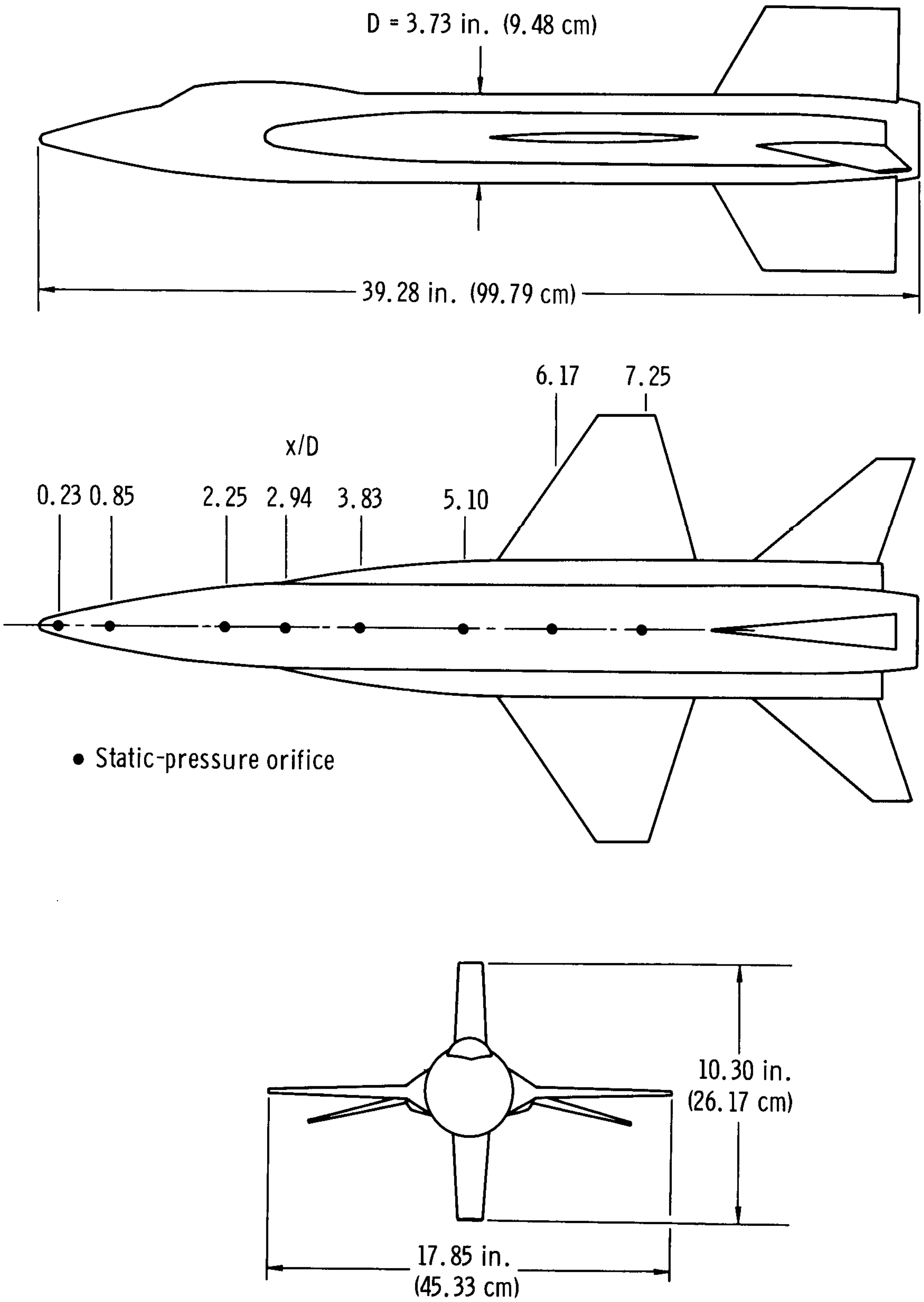

Figure 1. – Three-view drawing of the one-fifteenth-scale X-15 model.

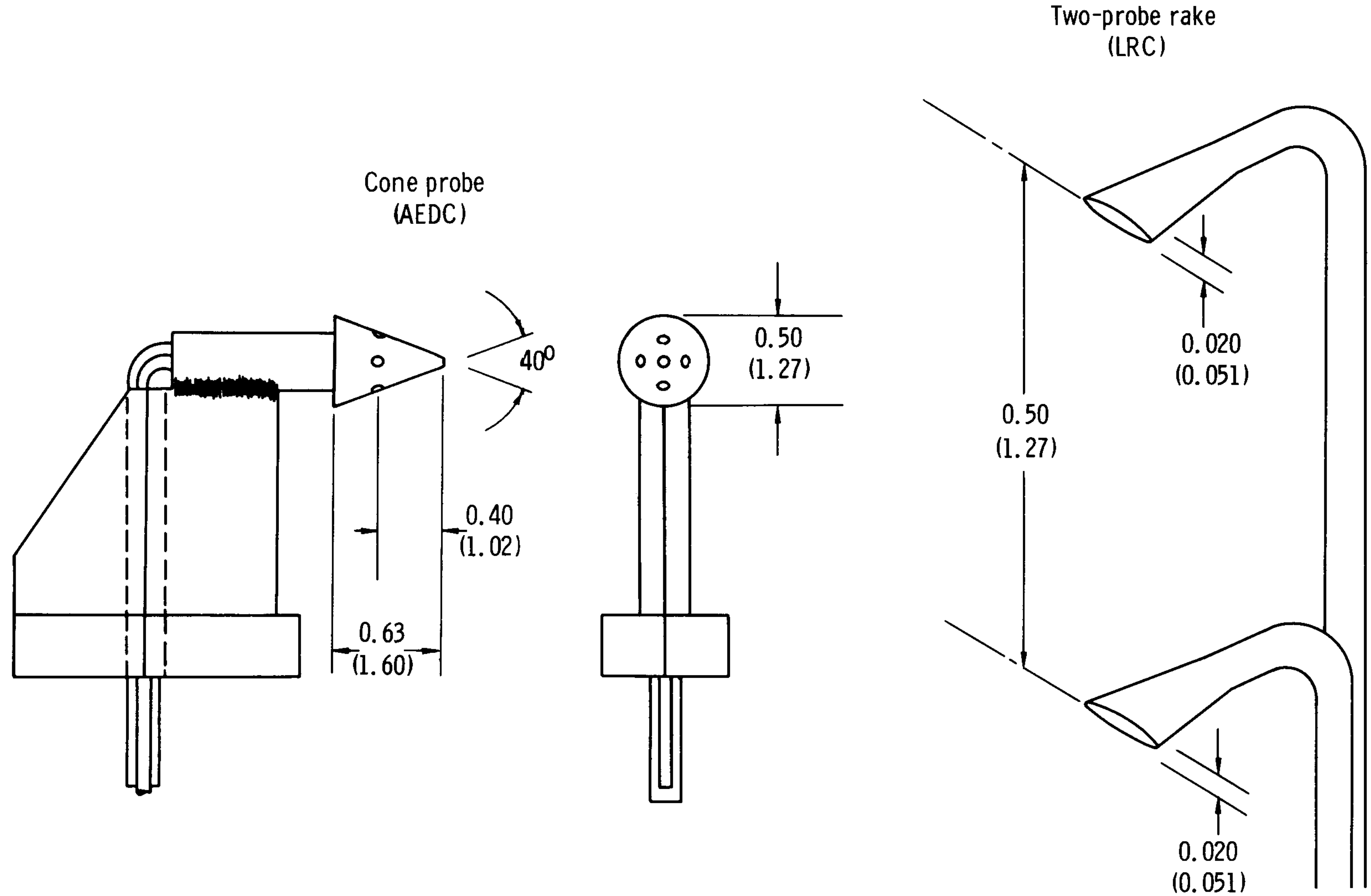

(a) Impact-pressure probes. Dimensions in inches (centimeters). Not drawn to scale. Cone-orifice inside diameter = 0.024 in. (0.061 cm); AEDC rake inside tube diameter = 0.040 in. (0.102 cm).

Figure 2. – Instrumentation and model details.

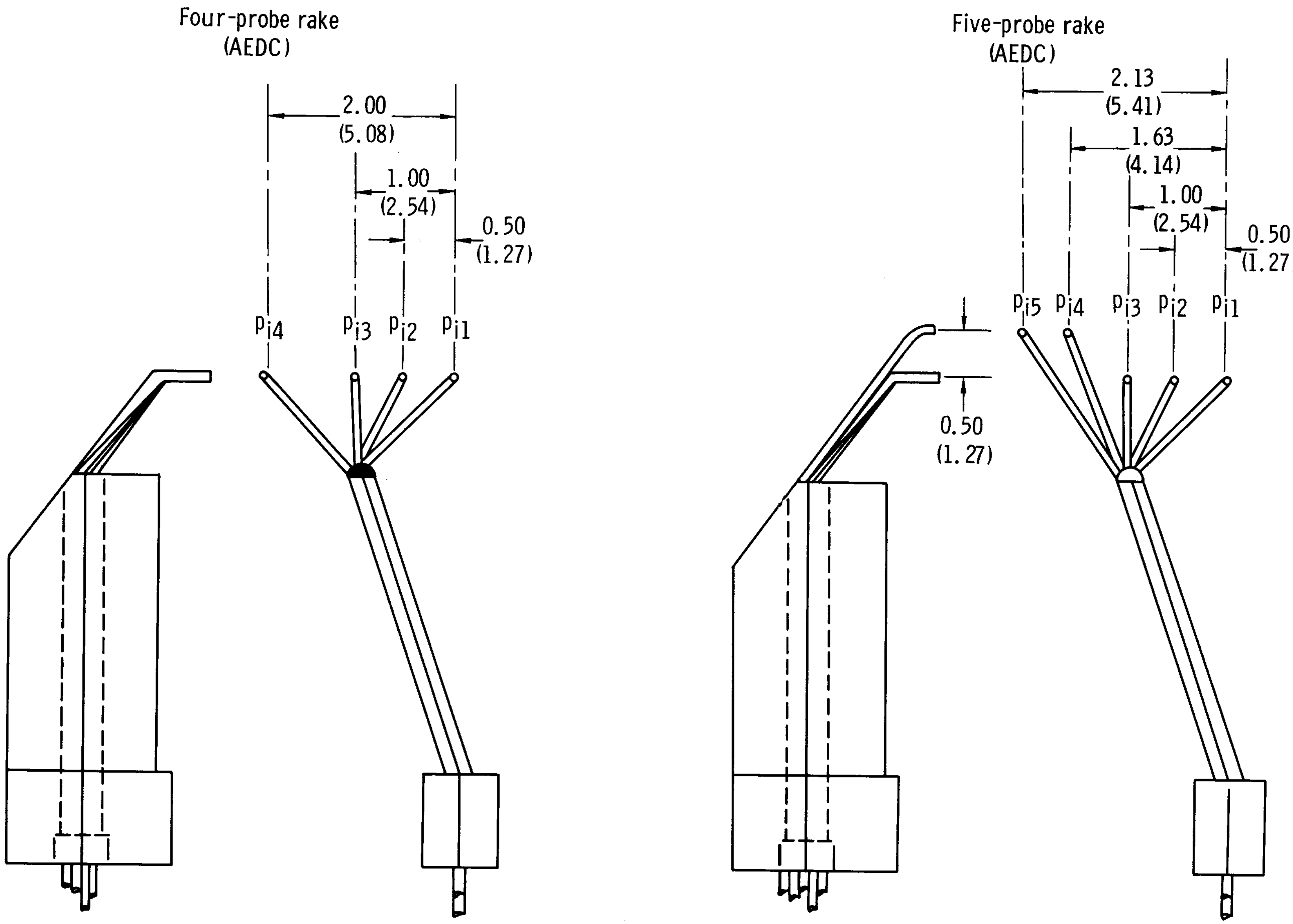

(a) Continued.

Figure 2. – Continued.

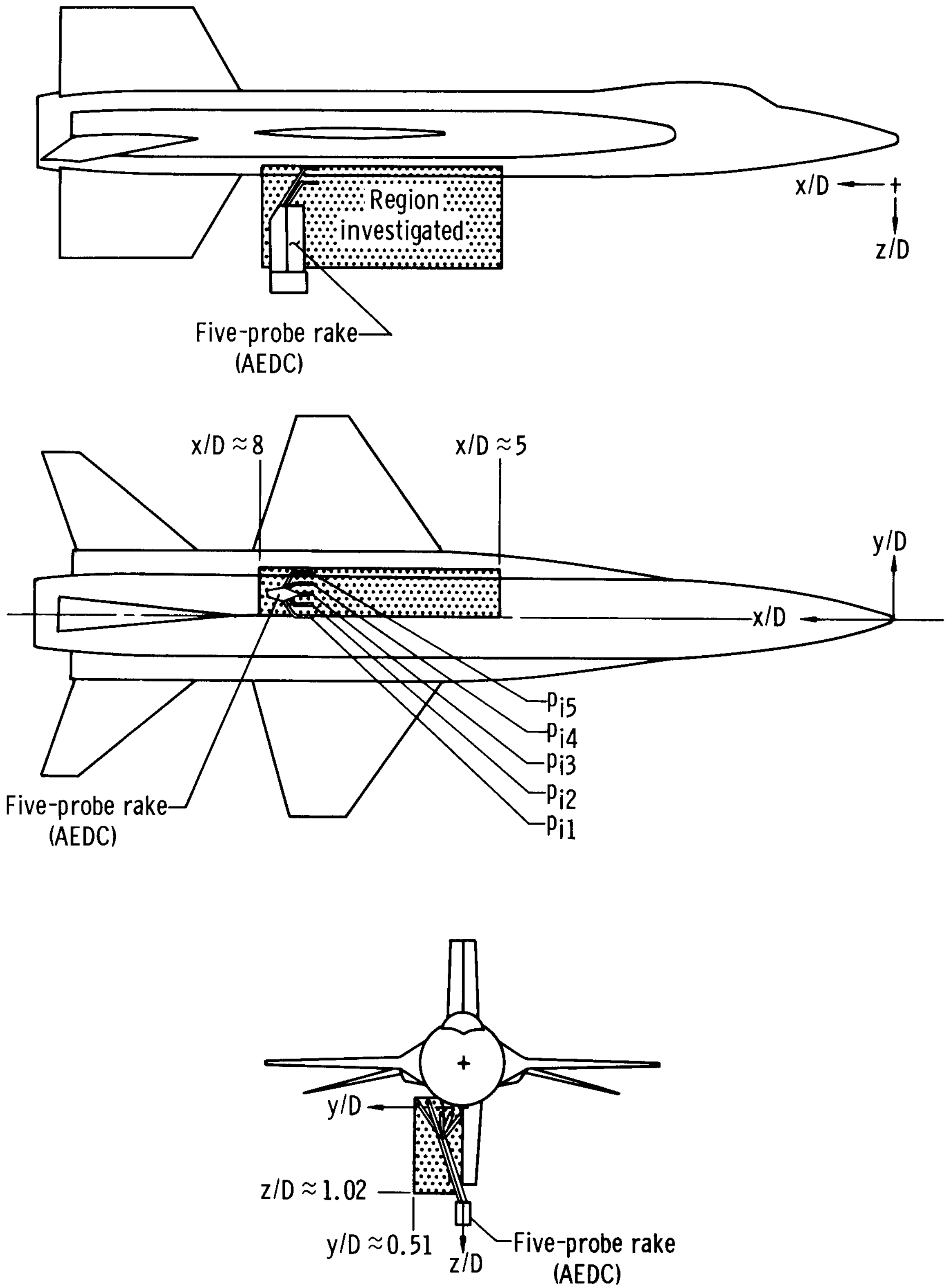

(b) Typical model-probe (rake) relationship, coordinate system, and region investigated.

Figure 2. – Concluded.

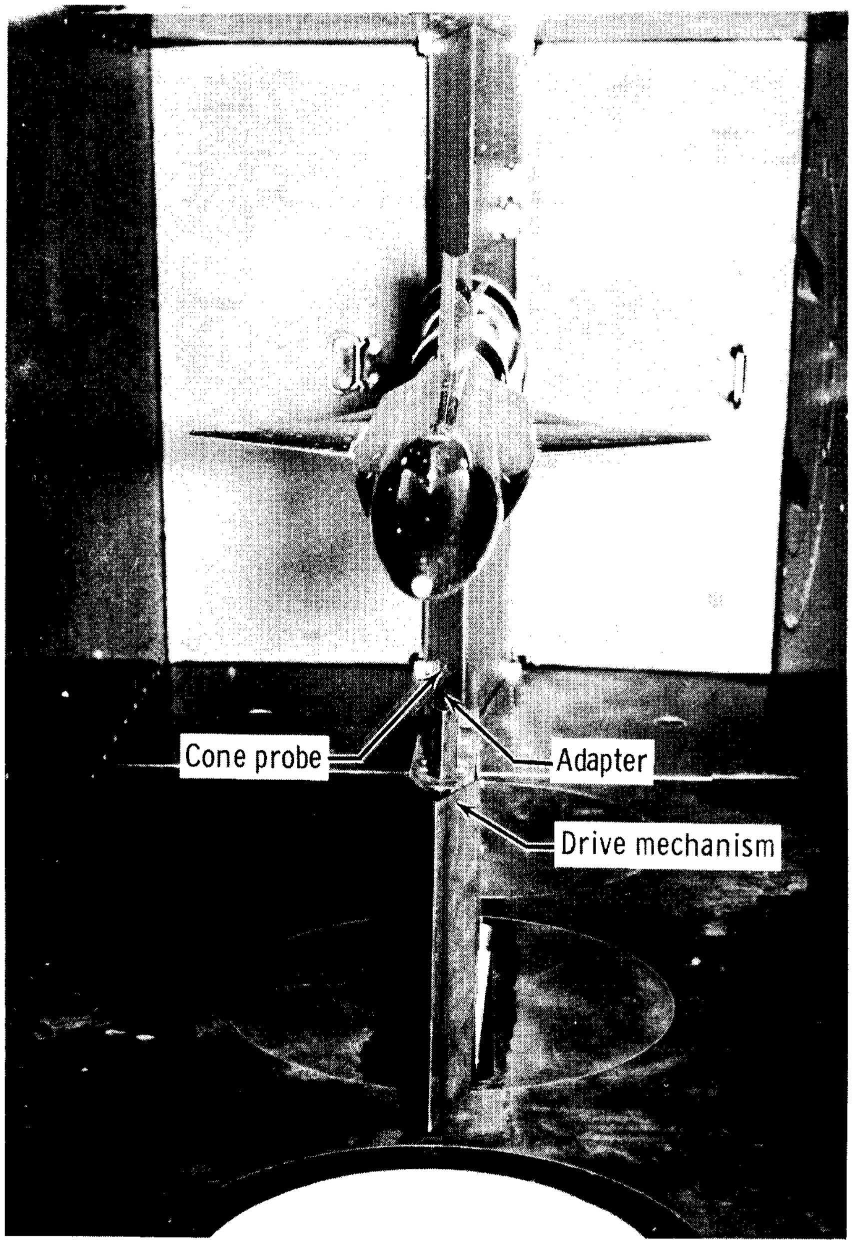

Figure 3. – Model installation in the AEDC von Kármán Gas Dynamics Facility Tunnel A.

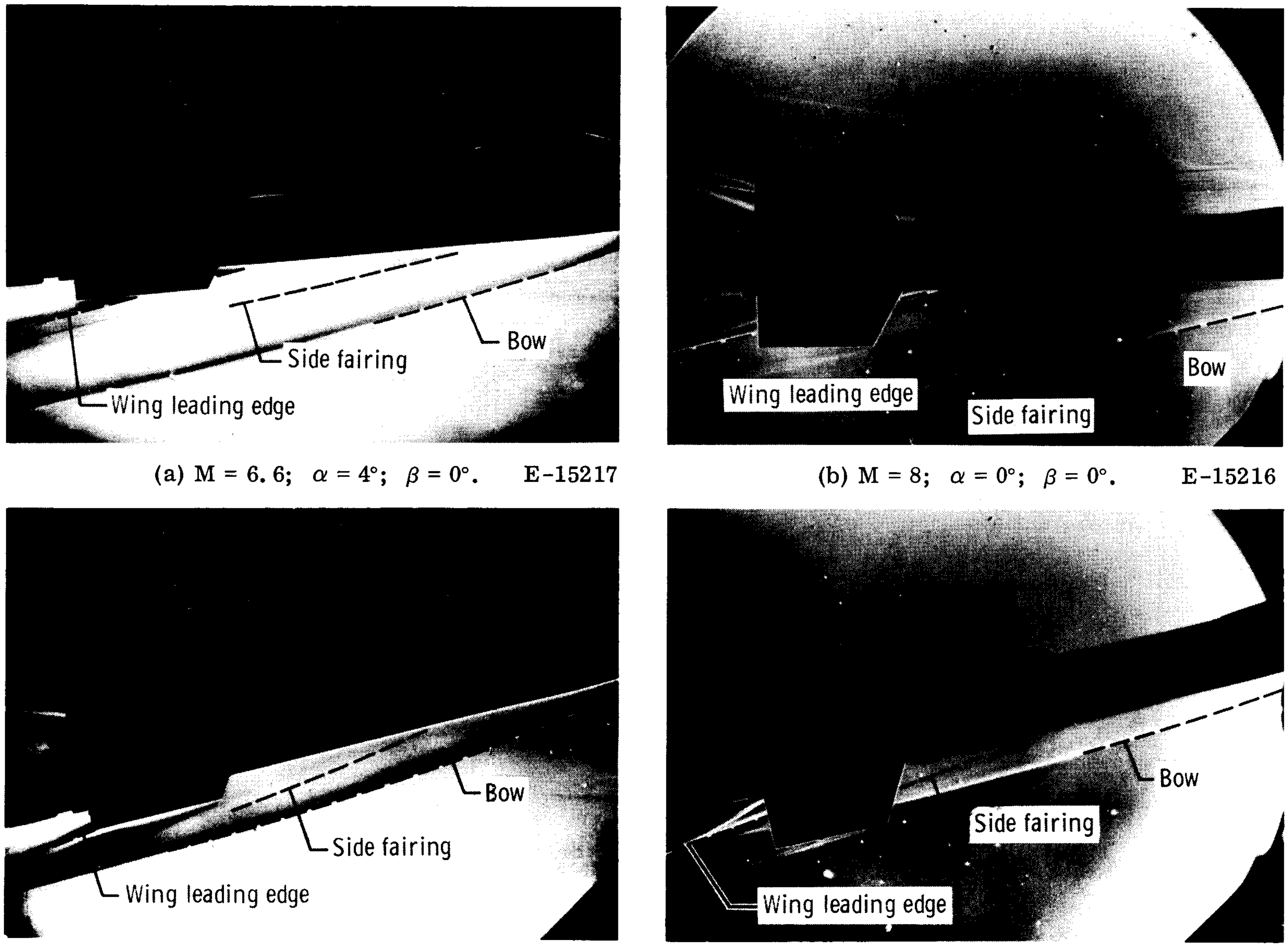

(a) M = 6.6; $\alpha = 4°$; $\beta = 0°$. E-15217

(b) M = 8; $\alpha = 0°$; $\beta = 0°$. E-15216

(c) M = 6.6; $\alpha = 12°$; $\beta = 0°$. E-15218

(d) M = 8; $\alpha = 12°$; $\beta = 0°$. E-15219

Figure 4. – Typical JPL schlieren photographs (one-fiftieth-scale model).

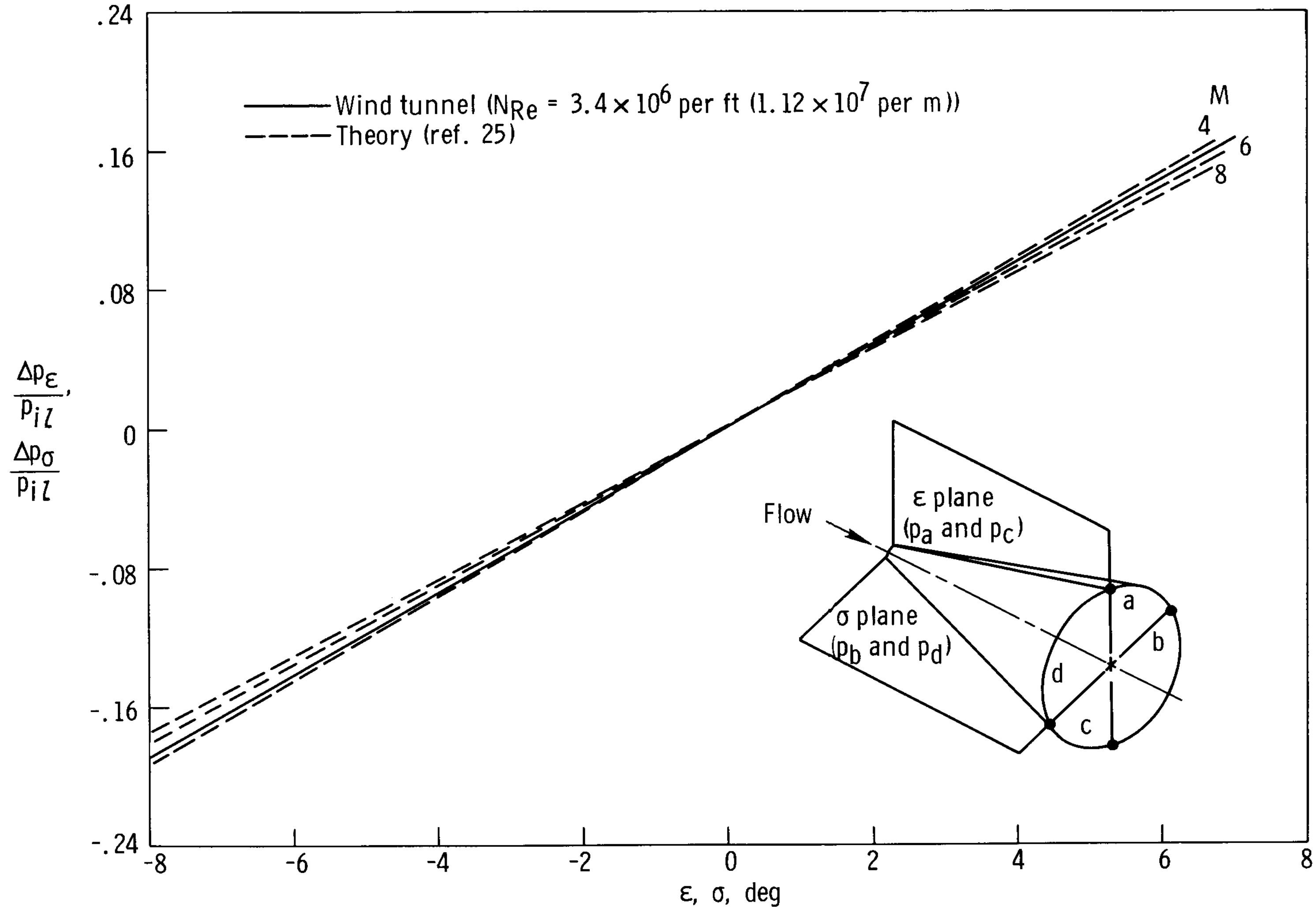

Figure 5. – Calibration curve of cone pressure ratio as a function of local flow angles.

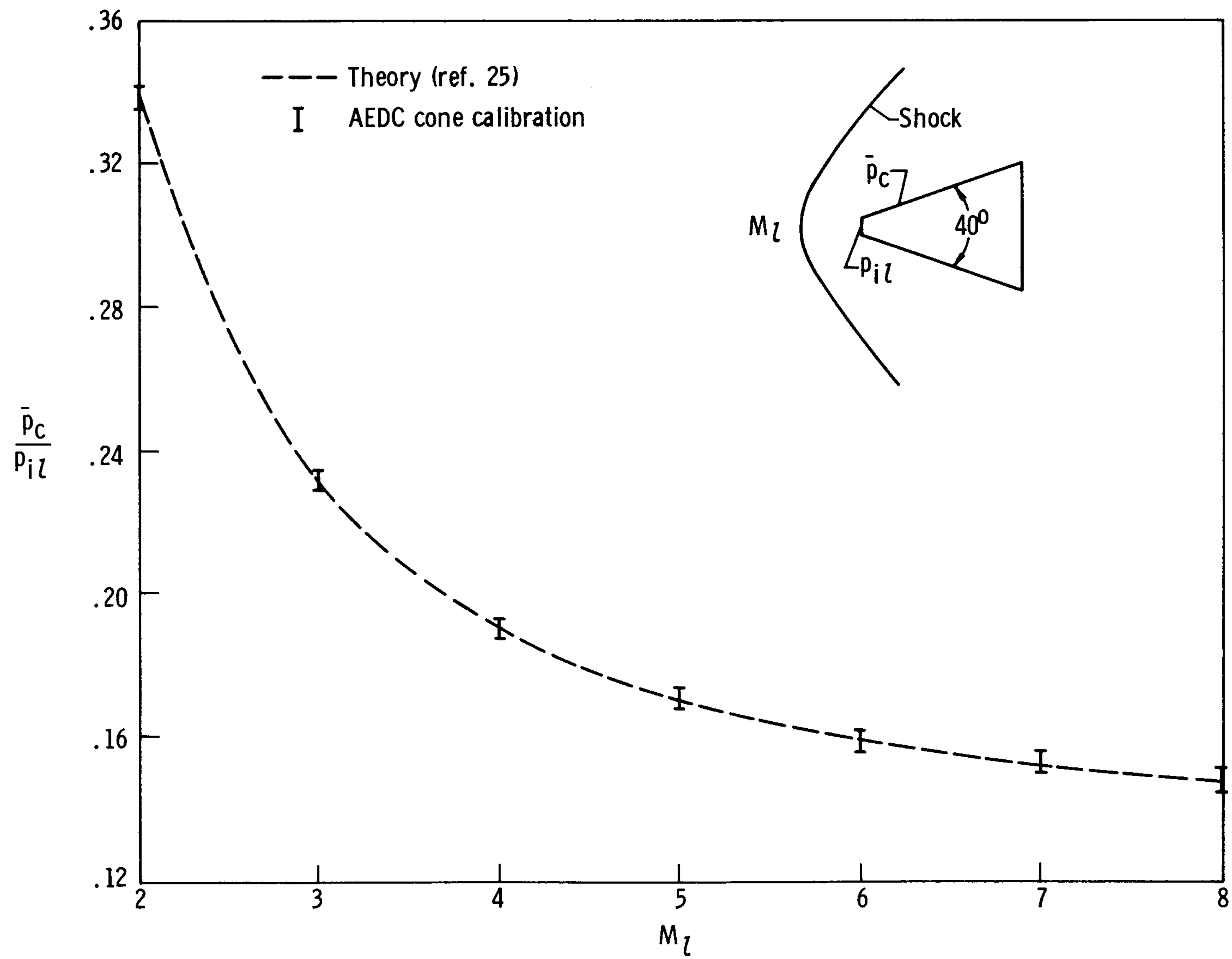

Figure 6. – Mach number calibration curve for the 40° cone probe. $N_{Re} = 3.4 \times 10^6$ per foot (1.12×10^7 per meter).

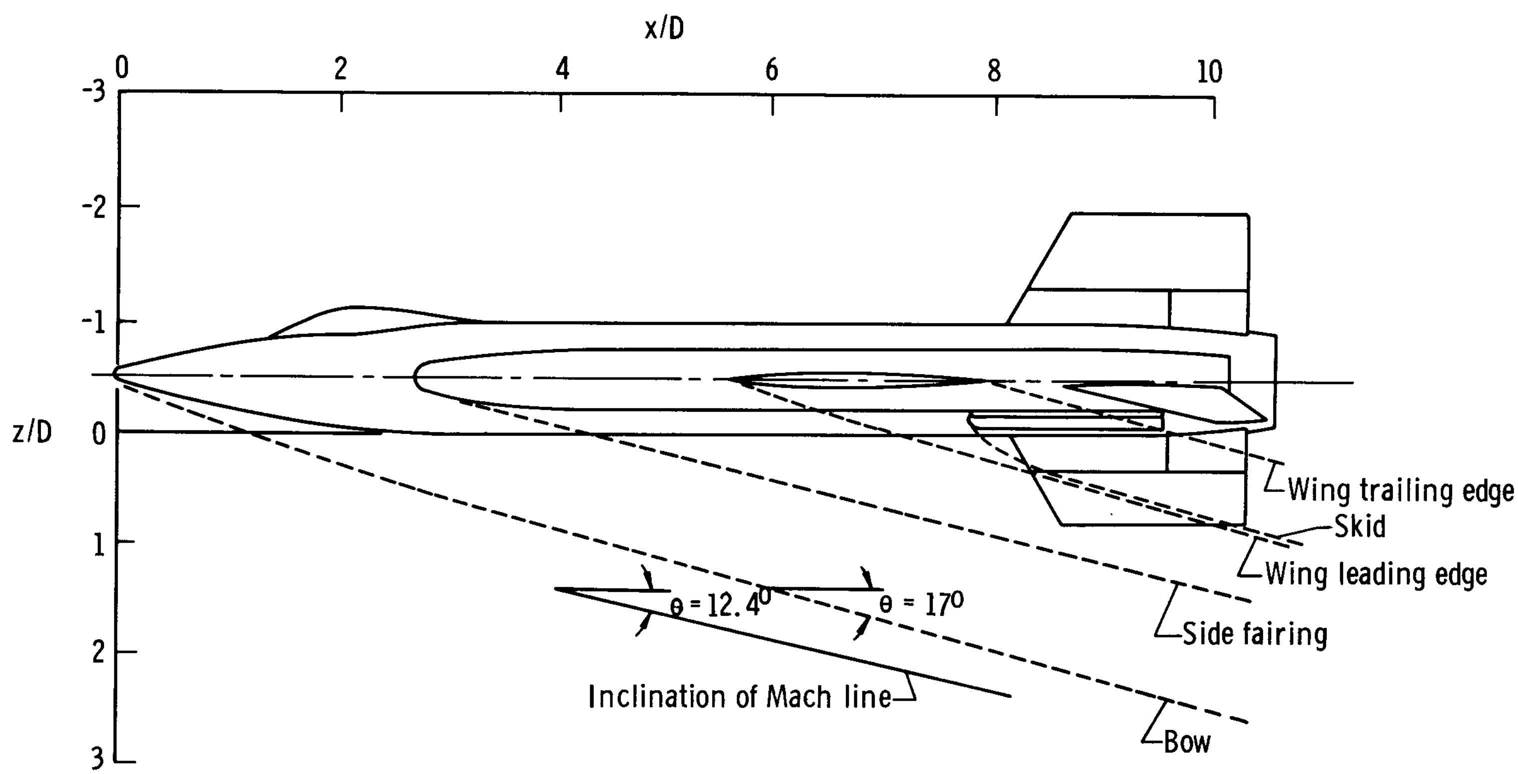

Figure 7. – Shock structure as determined from schlieren photographs of one-fiftieth- and one-fifteenth-scale X-15 models. $M = 4.65$; $\alpha = 0°$; $\beta = 0°$; $y/D = 0$.

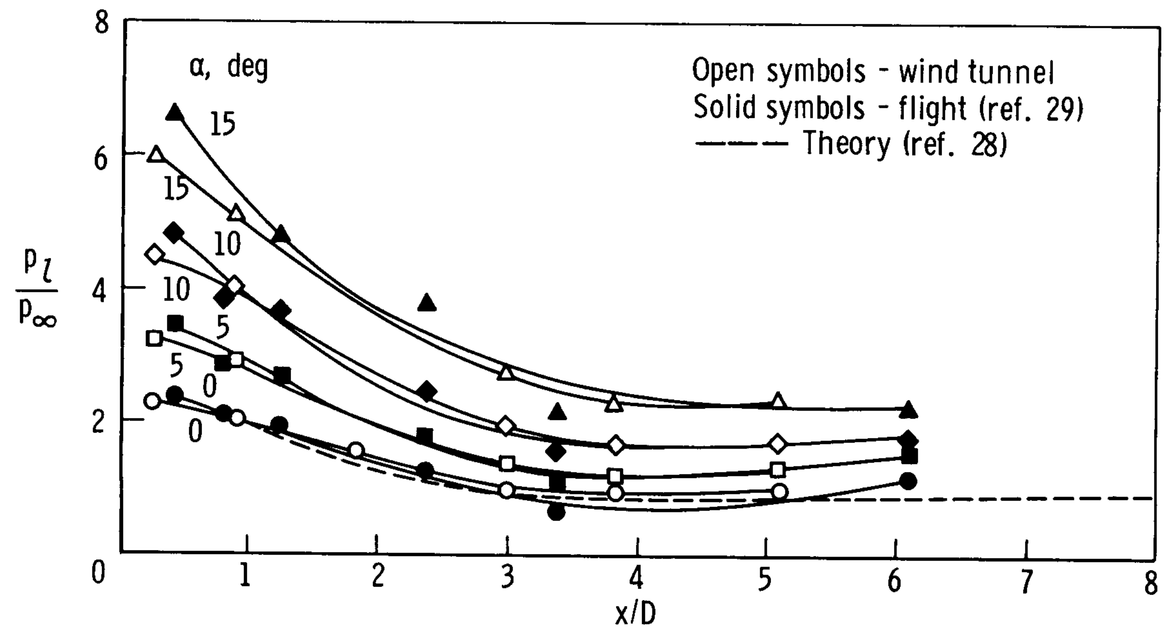

(a) M = 4.

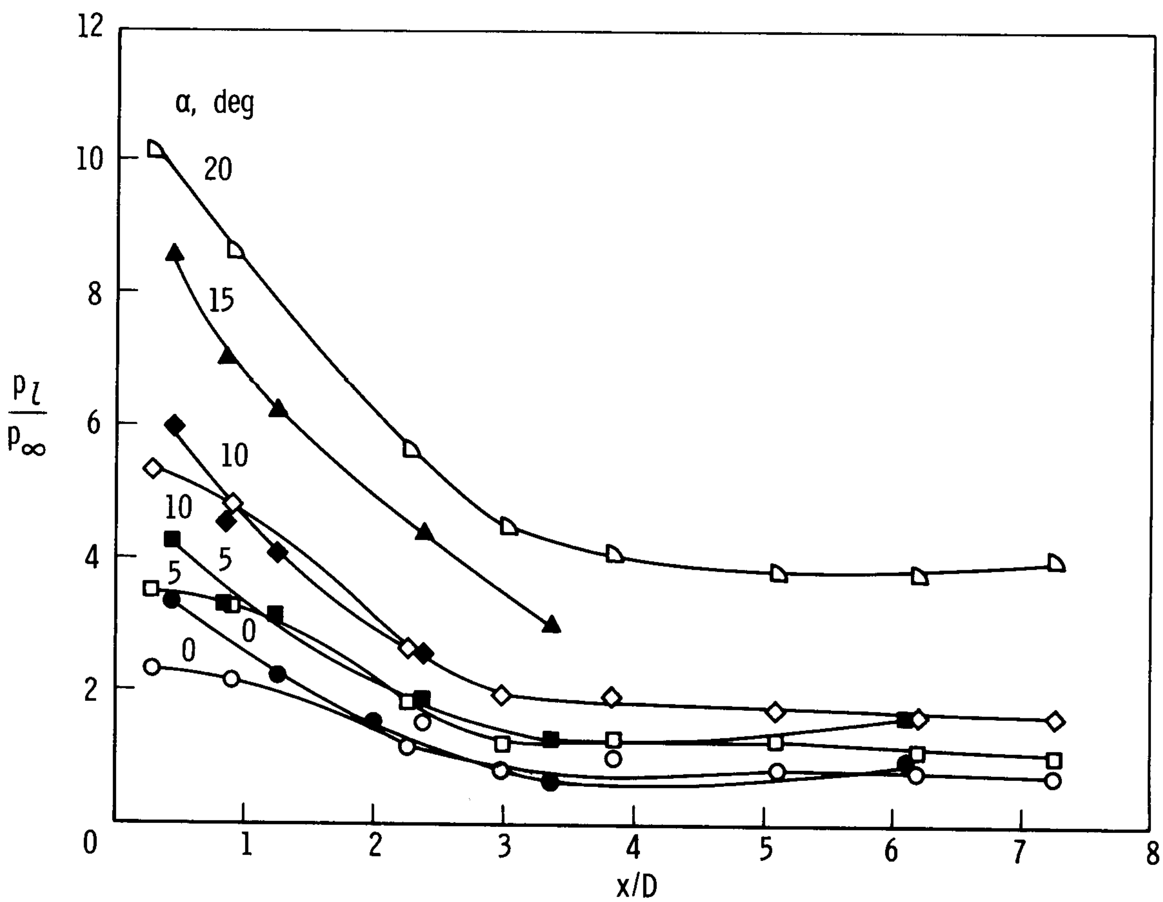

(b) M = 4.65.

Figure 8. – Variation of static-pressure ratio at fuselage bottom centerline.

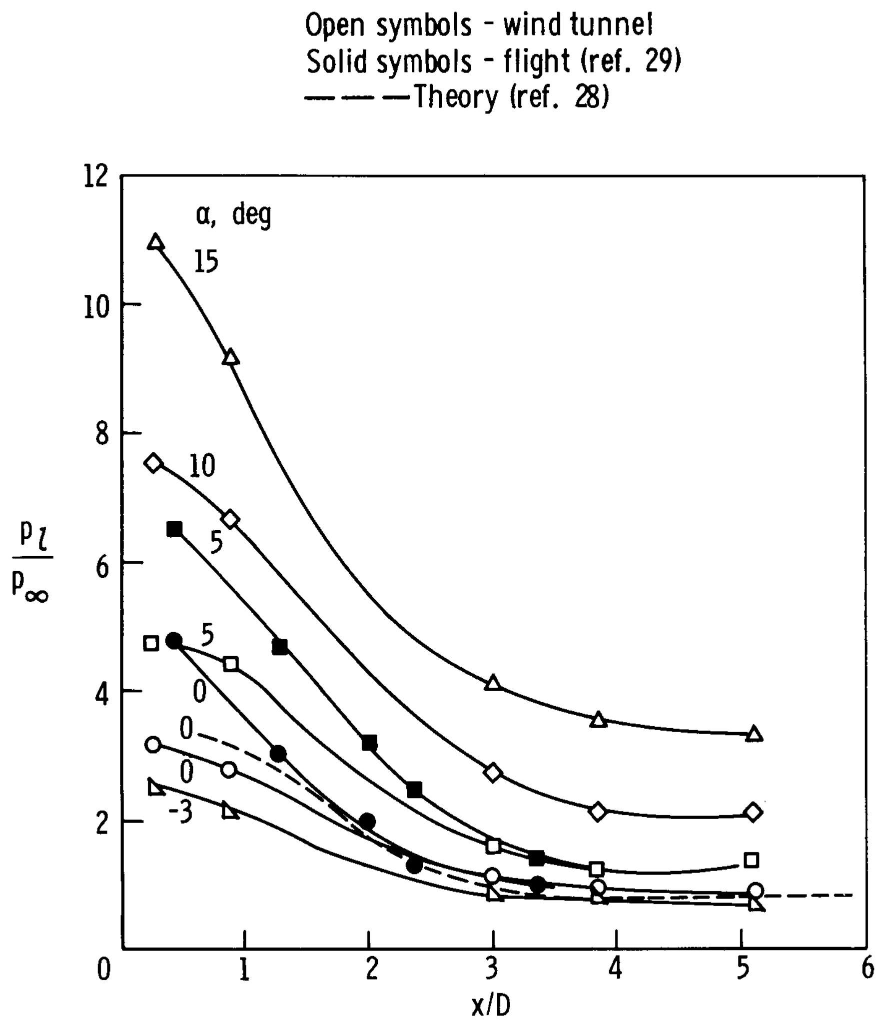

(c) M = 6.

Figure 8. – Continued.

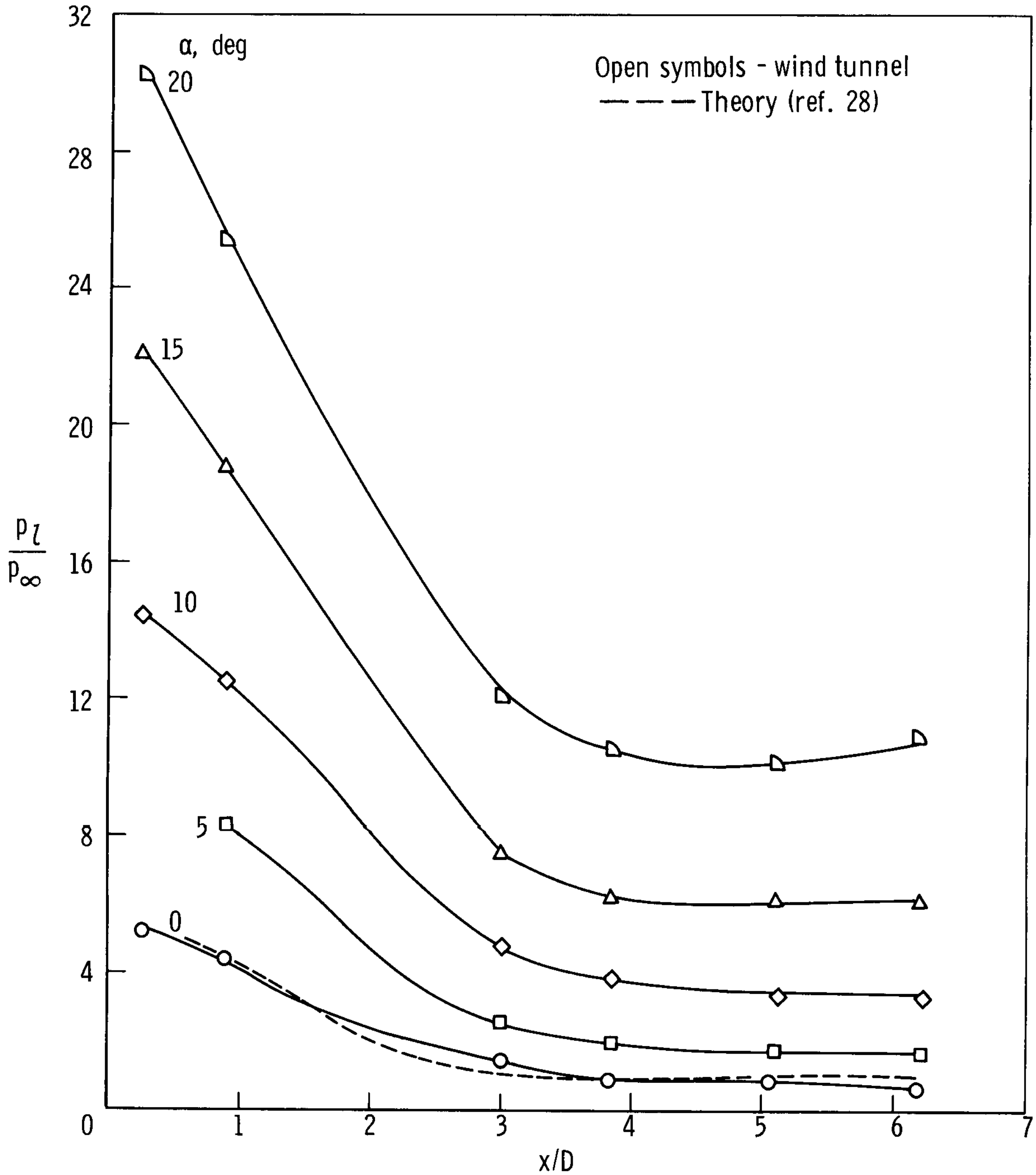

(d) M = 8.

Figure 8. – Concluded.

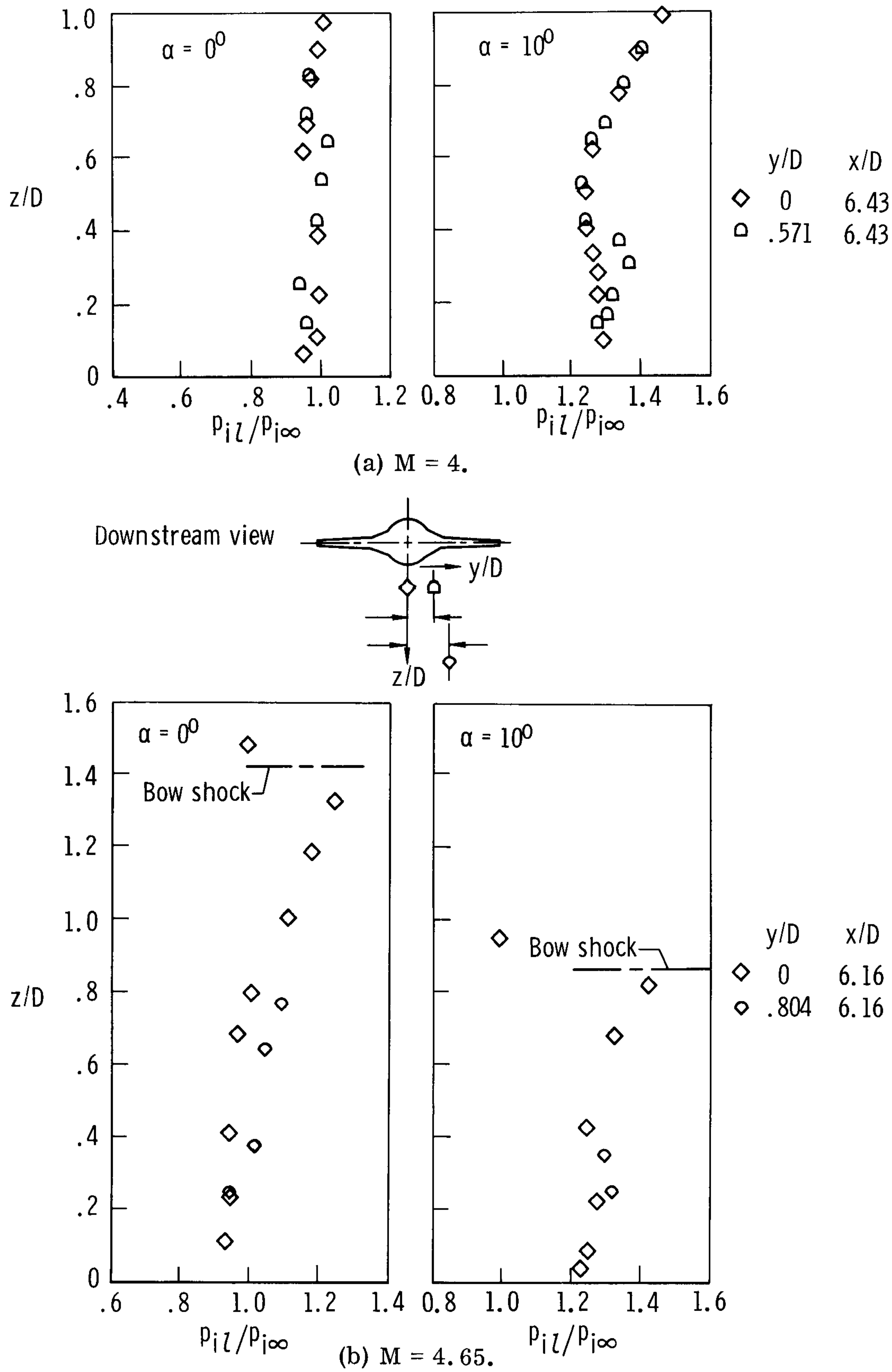

Figure 9. – Variation of the impact-pressure ratio at the intermediate survey stations.

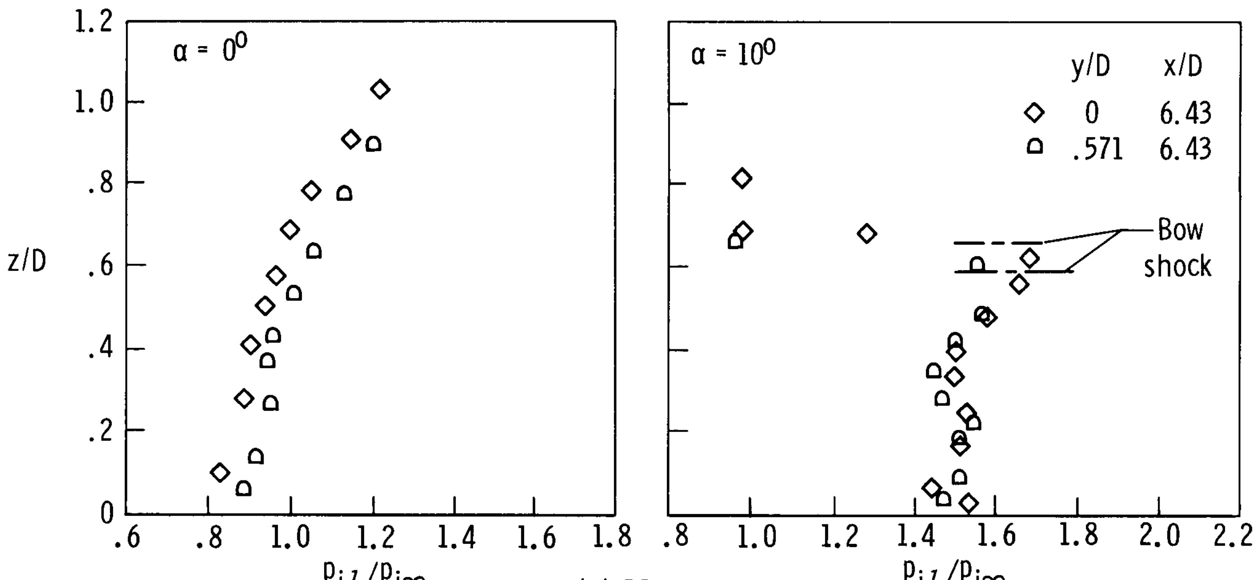

(c) M = 6.

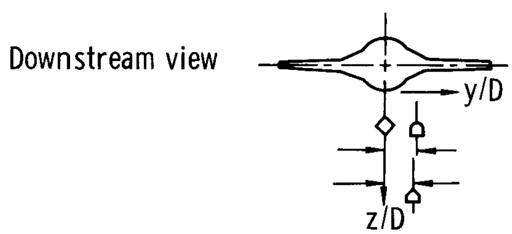

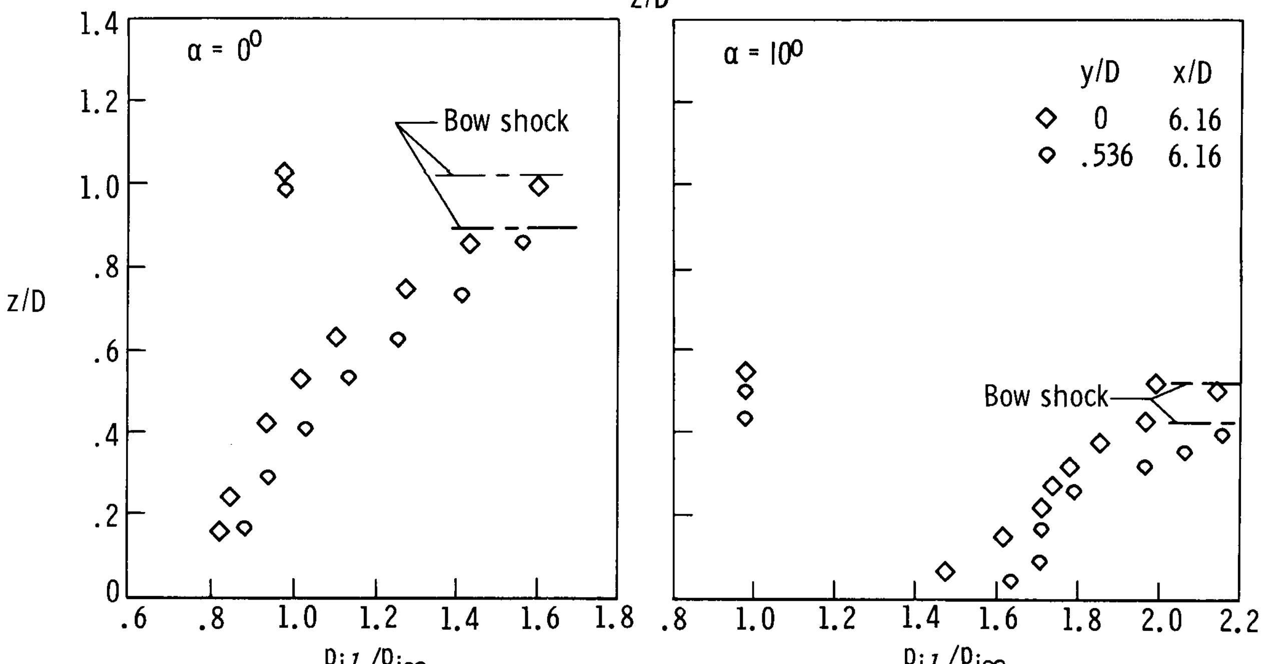

(d) M = 8.

Figure 9. – Concluded.

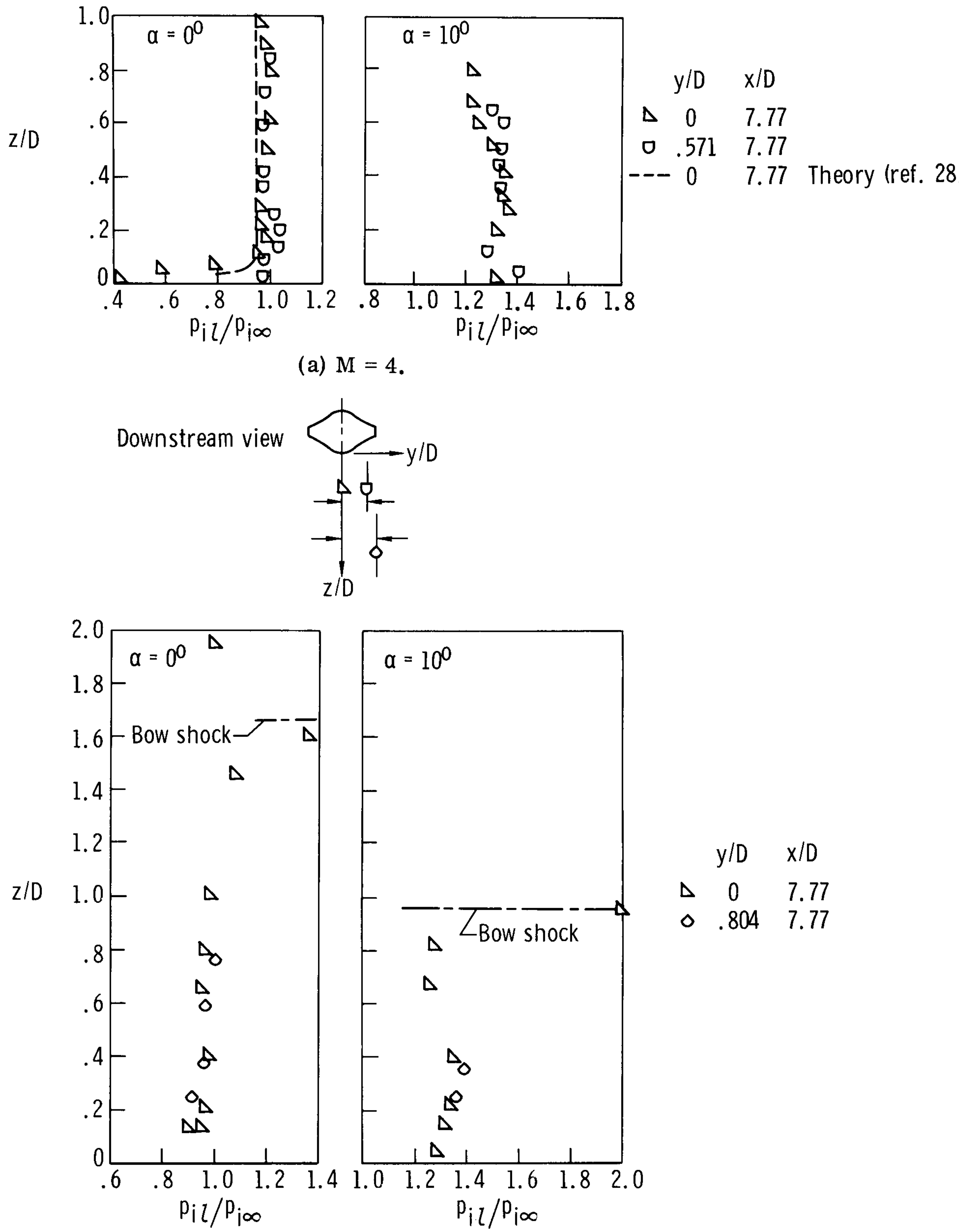

(b) M = 4.65

Figure 10. – Variation of the impact-pressure ratio at the downstream survey station.

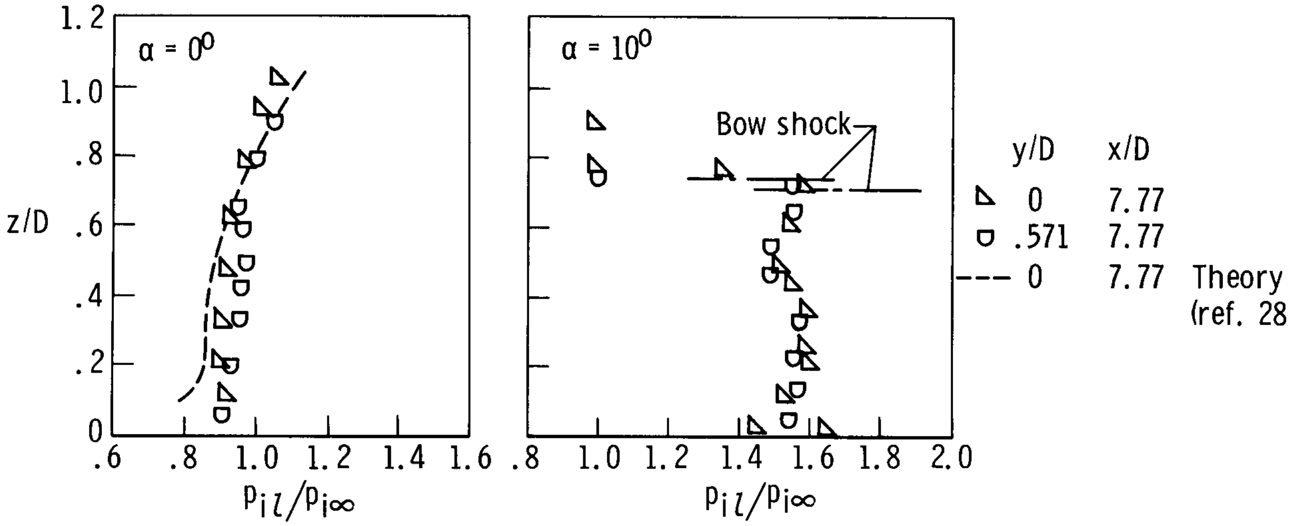

(c) M = 6.

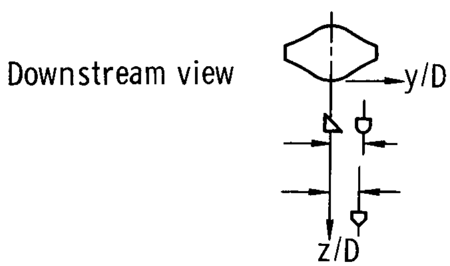

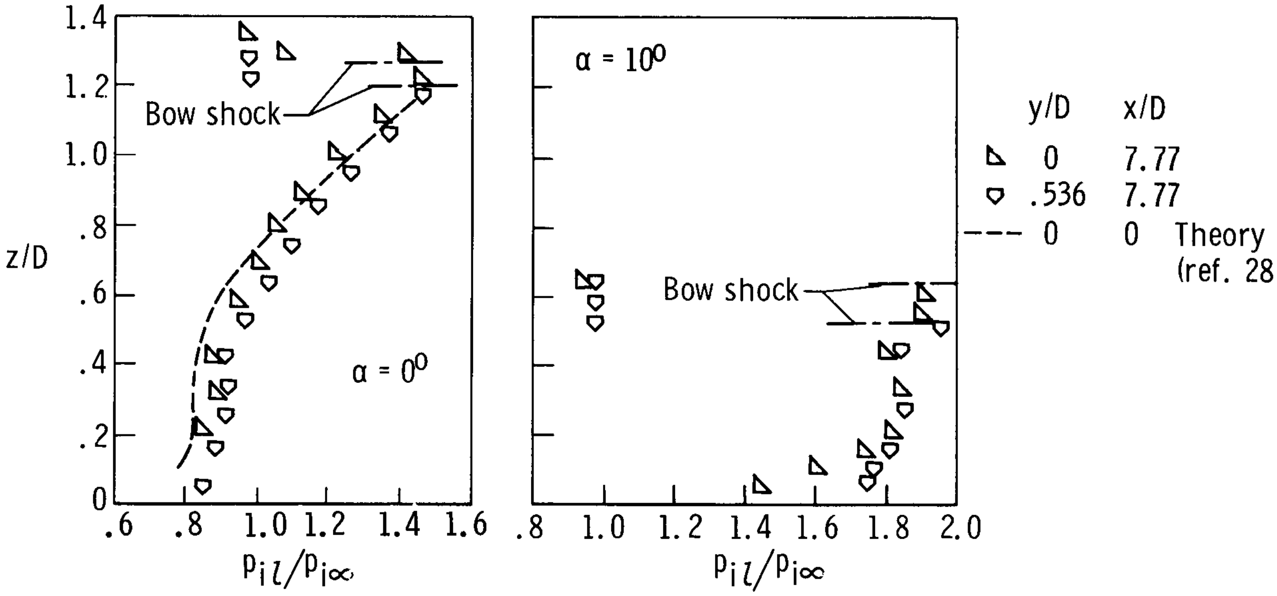

(d) M = 8.

Figure 10. — Concluded.

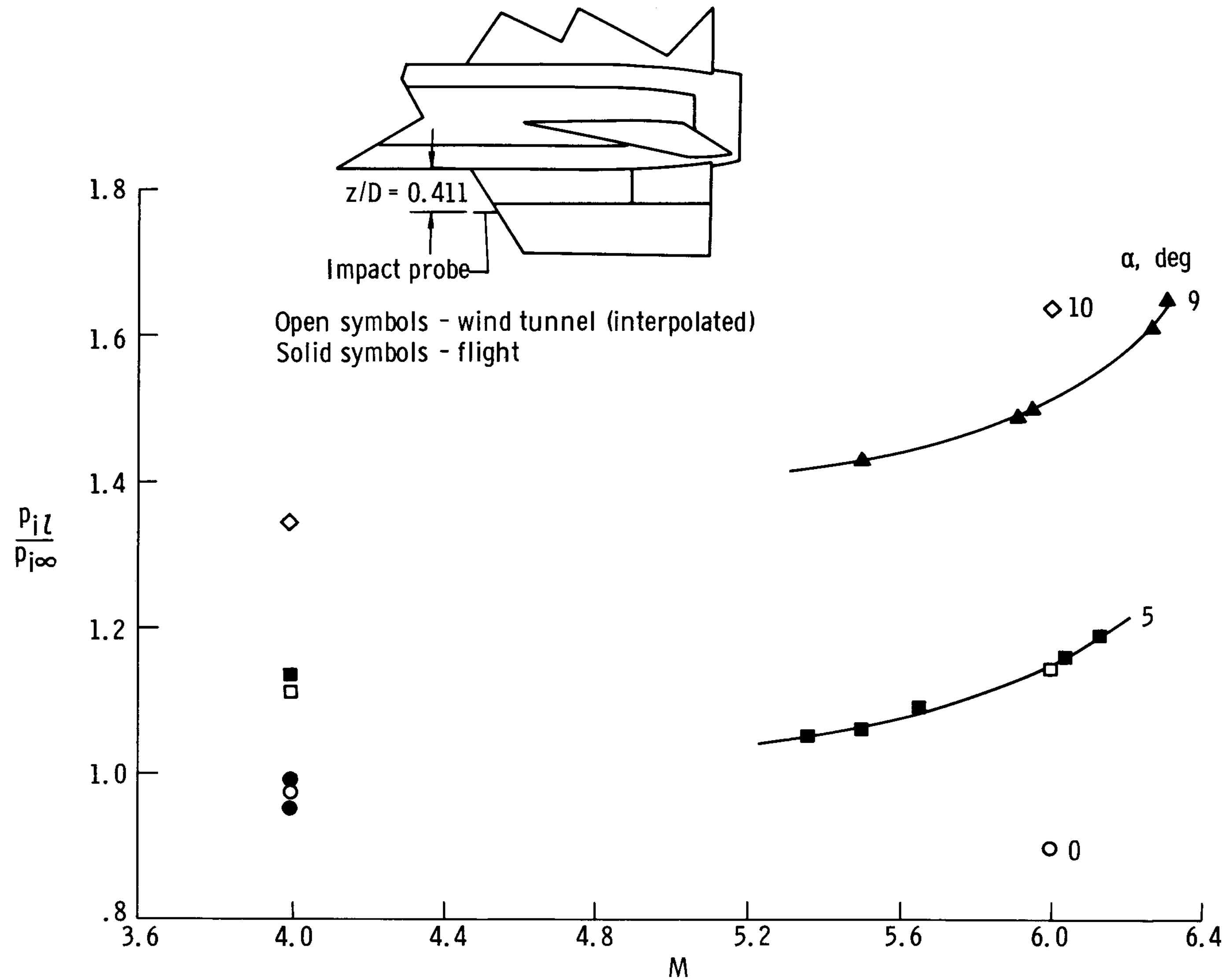

Figure 11.— Comparison between quasi-steady-state flight and wind-tunnel impact-pressure ratio results. $x/D = 8.20$; $z/D = 0.411$.

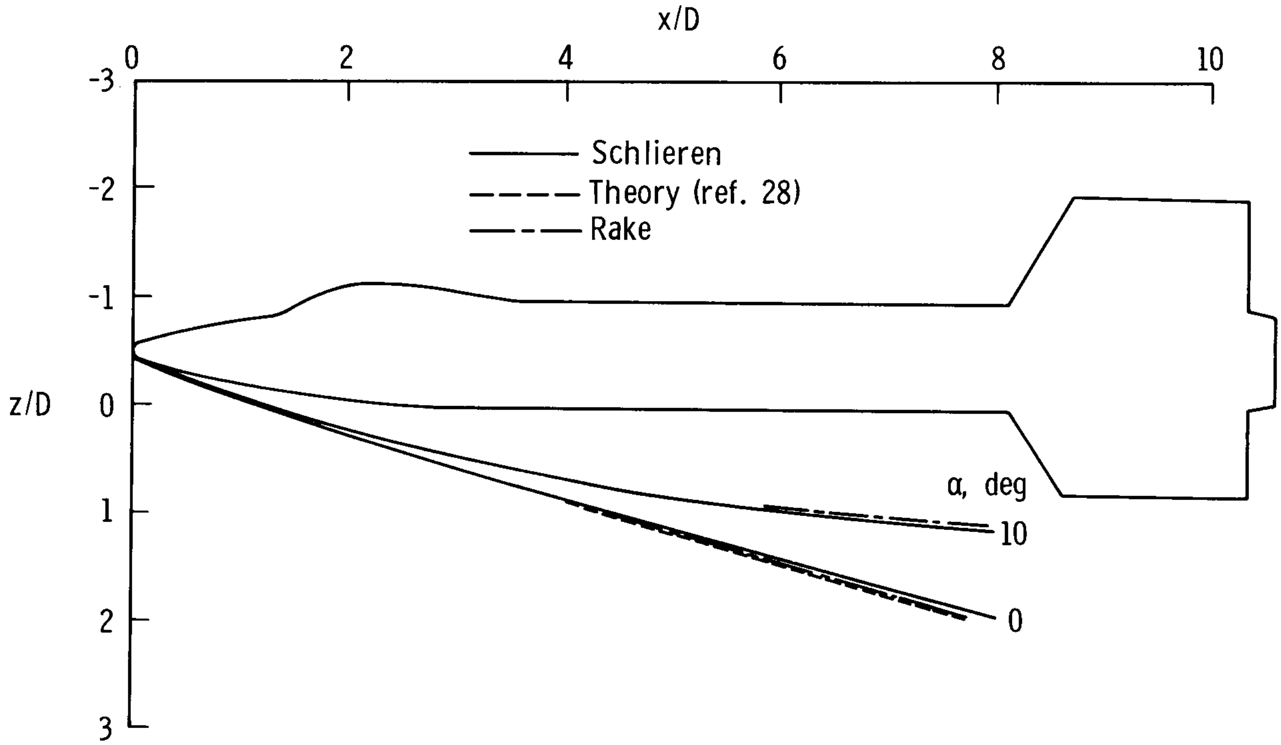

(a) M = 4.65.

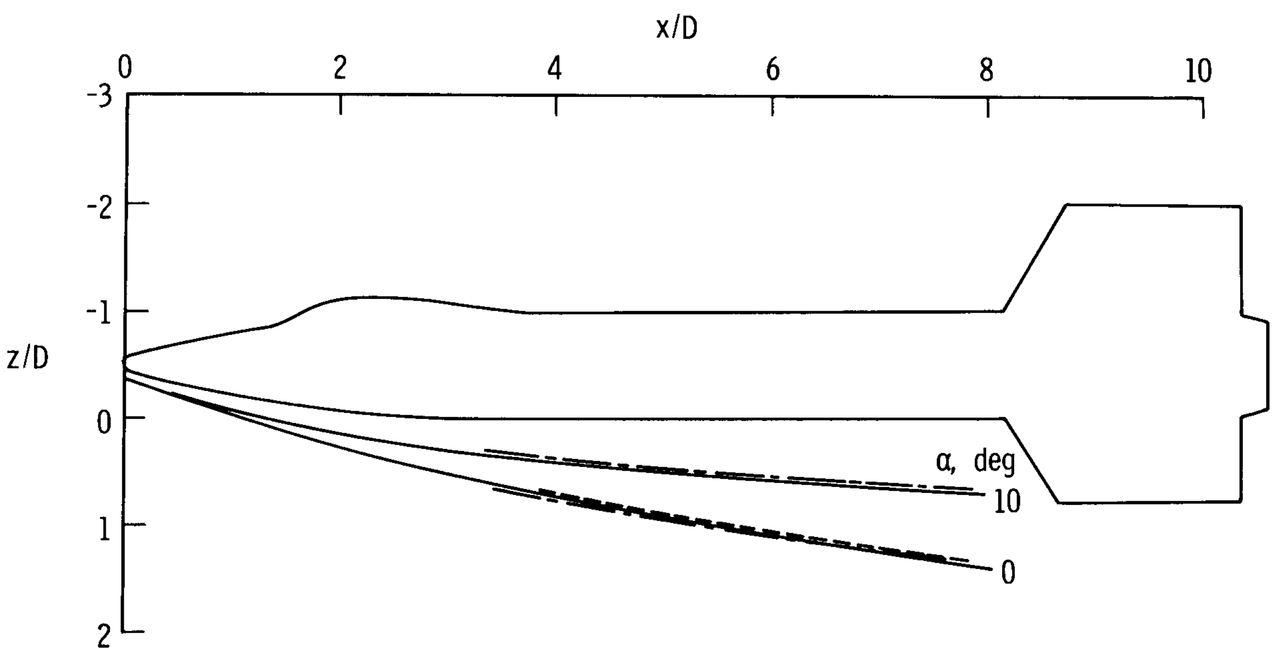

(b) M = 8.

Figure 12. – Comparison of bow-shock location as determined from schlieren, rake, and calculated data. y/D = 0.

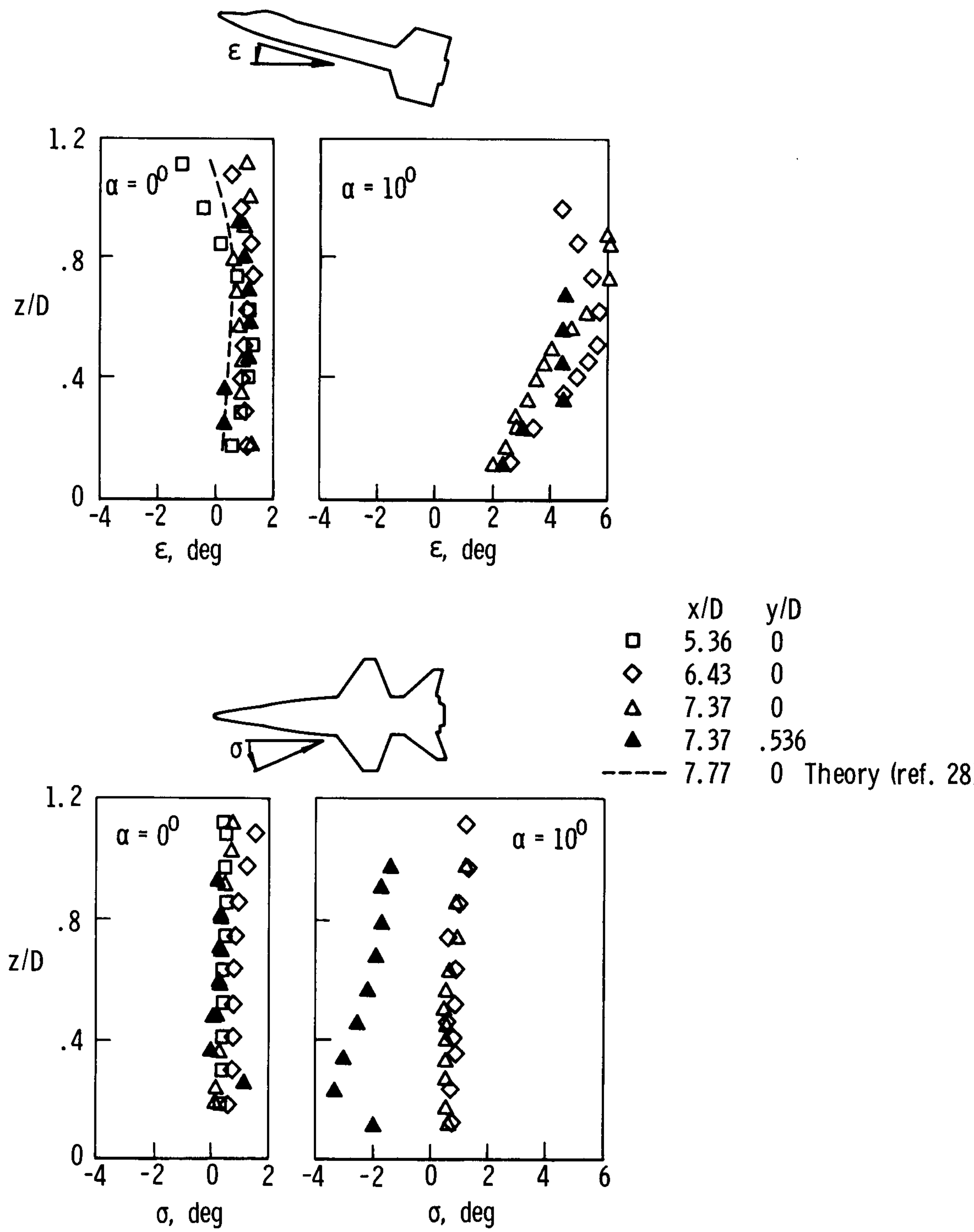

(a) M = 4.

Figure 13. – Flow angles.

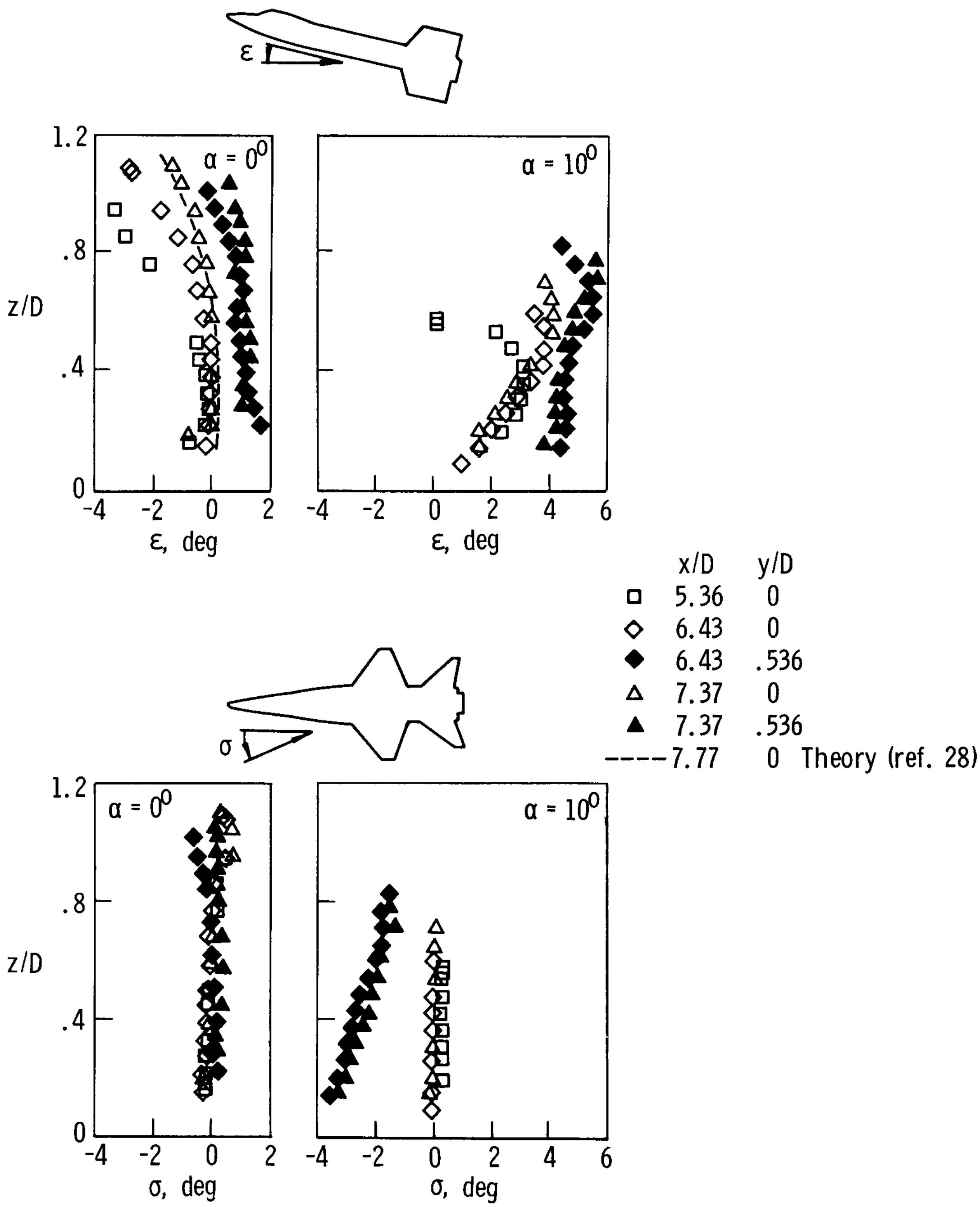

(b) M = 6.

Figure 13. – Continued.

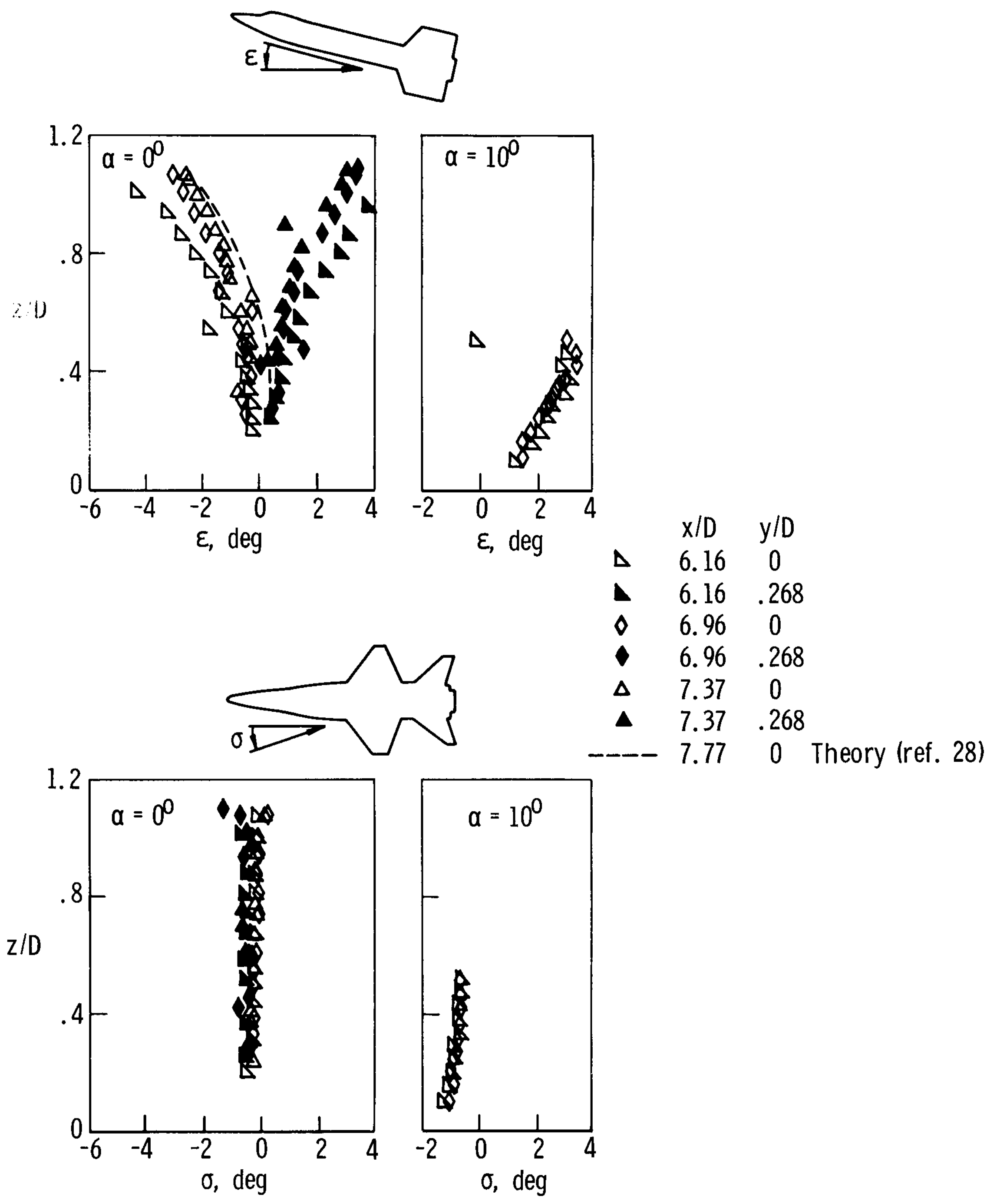

(c) M = 8.

Figure 13. – Concluded.

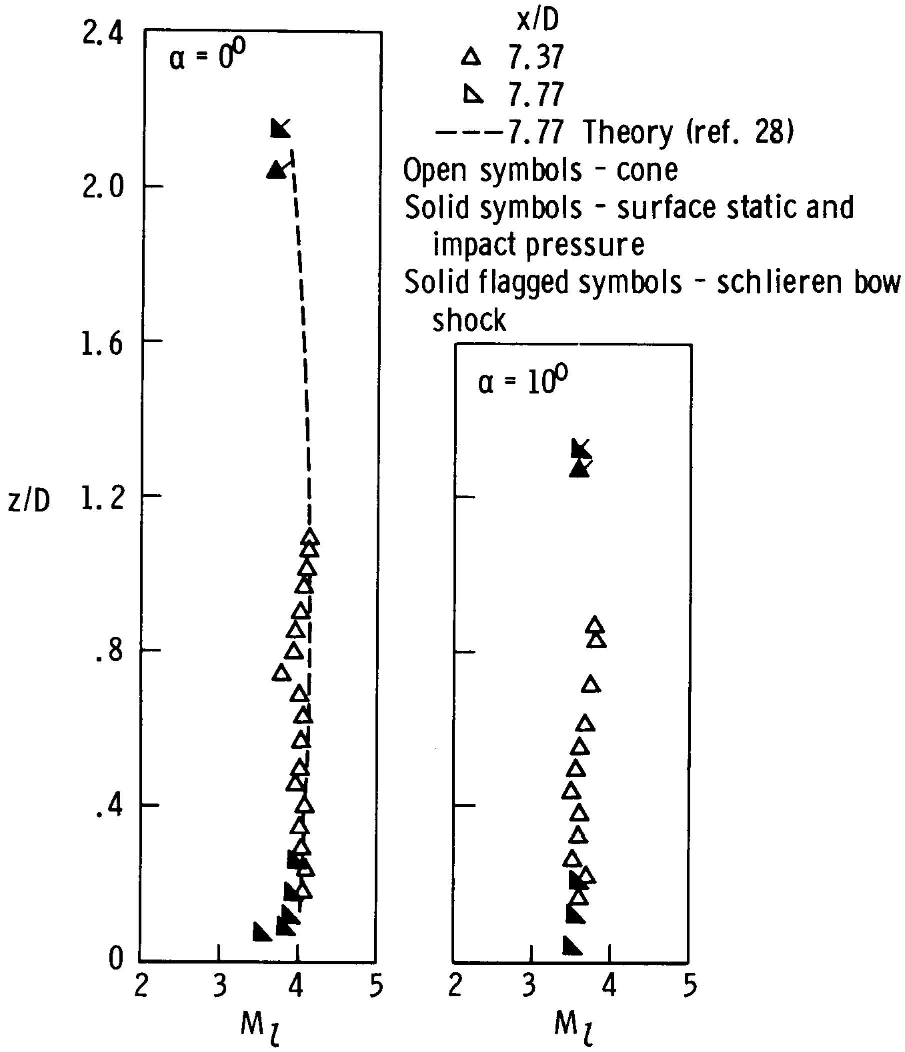

(a) M = 4.

Figure 14.– Comparisons of local Mach number obtained from schlieren photographs and rake and cone surveys at y/D = 0.

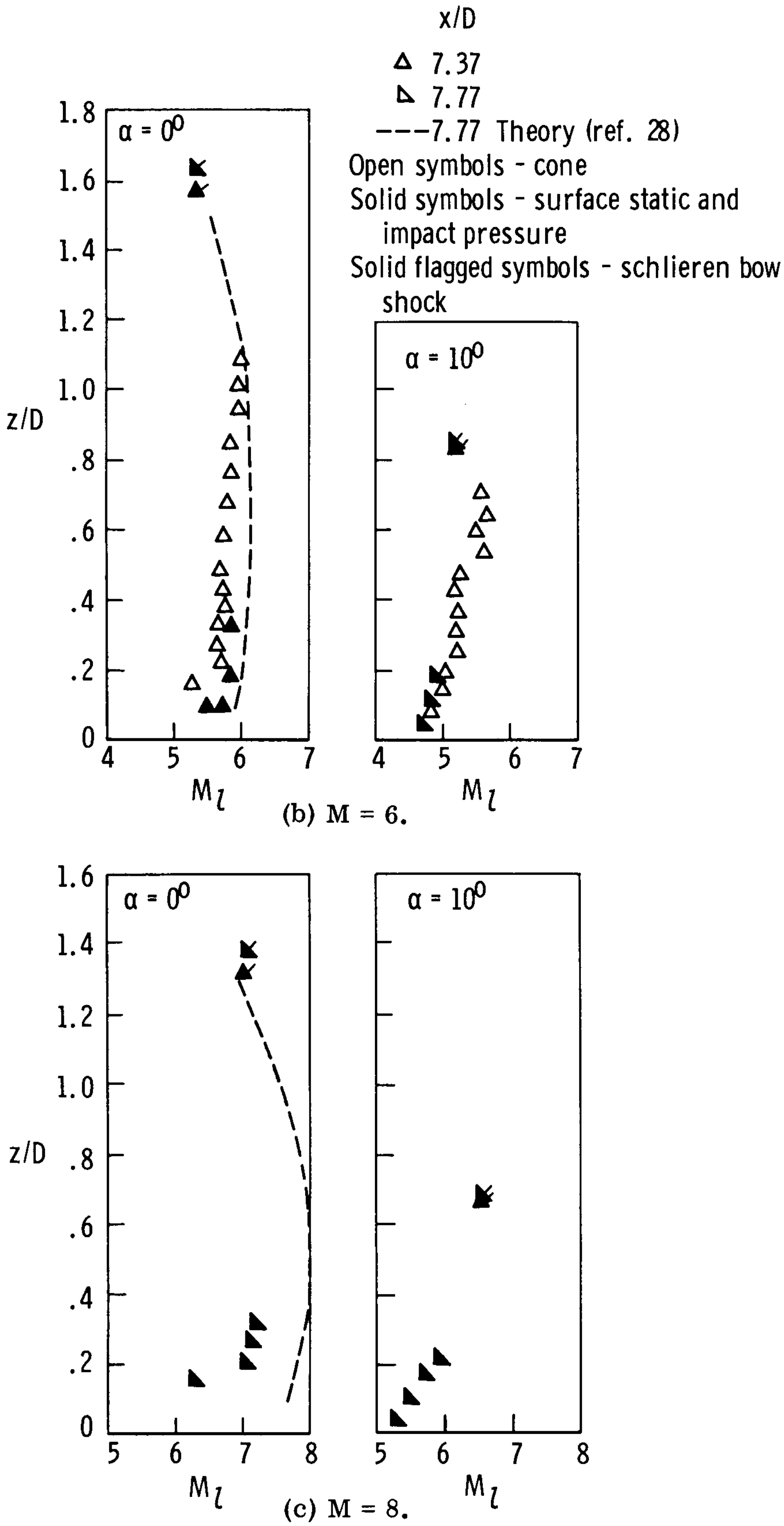

Figure 14. – Concluded.

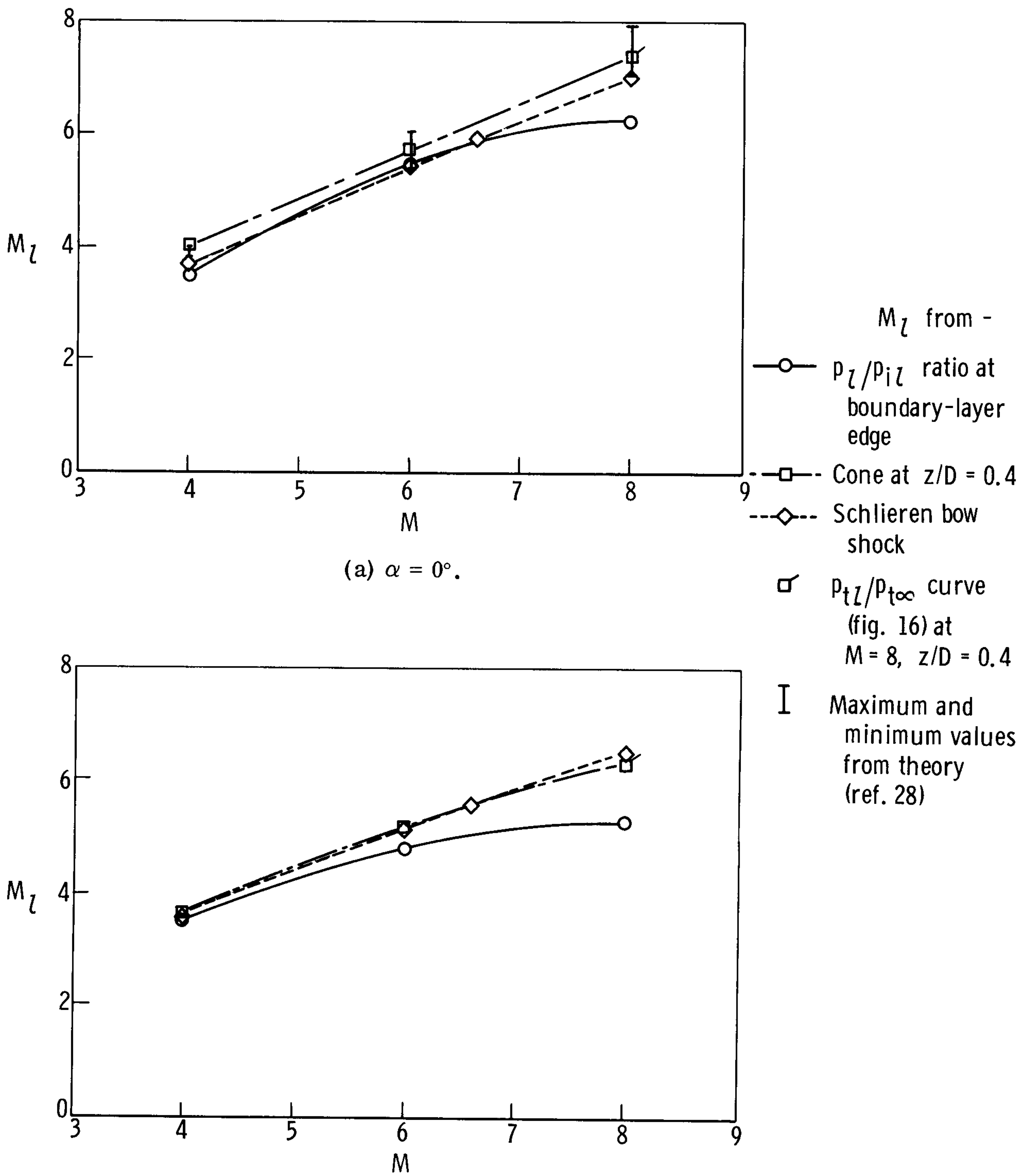

(a) $\alpha = 0°$.

(b) $\alpha = 10°$.

Figure 15. – Comparison of local Mach numbers as a function of free-stream Mach number. $x/D = 7.77$; $y/D = 0$.

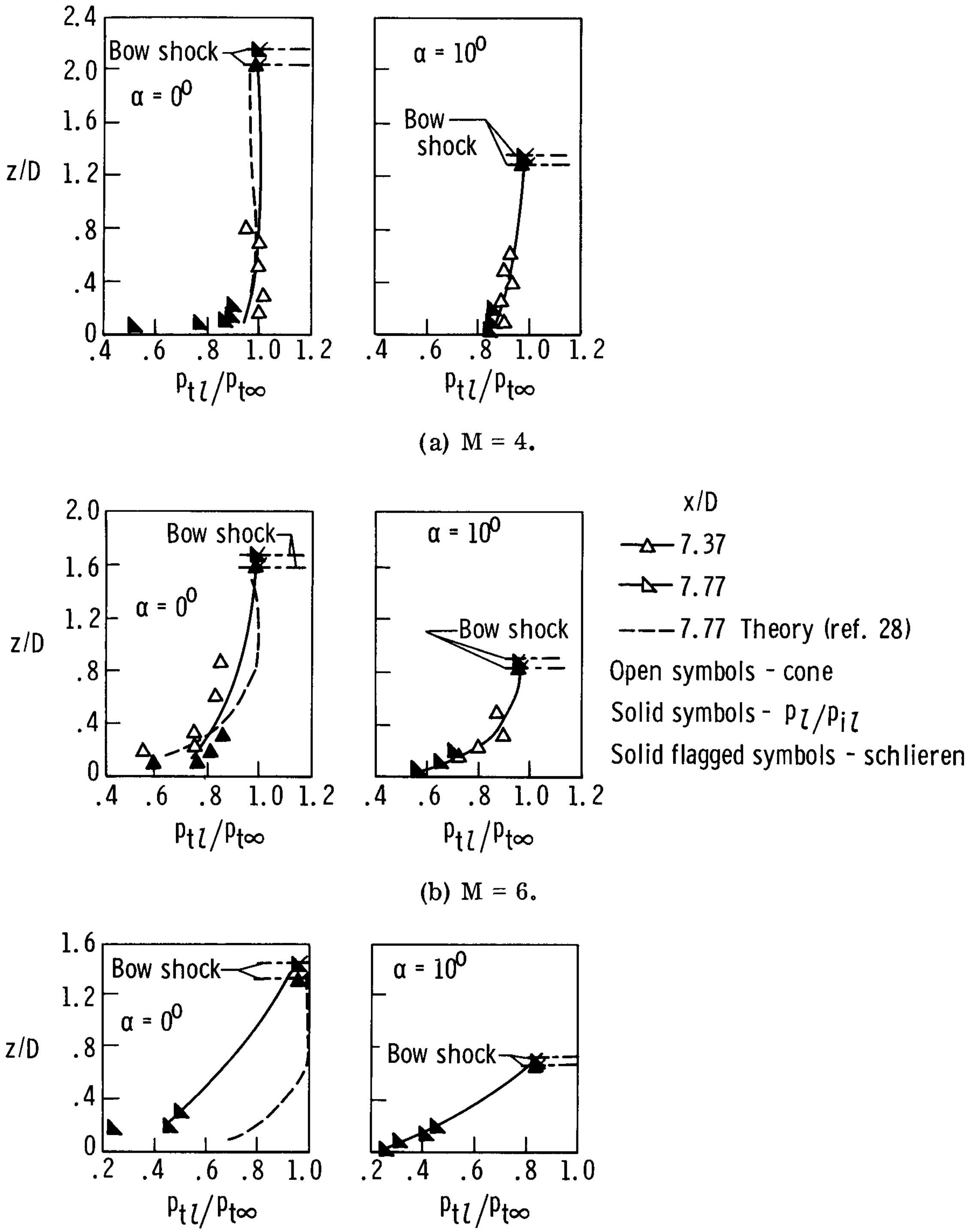

(a) M = 4.

(b) M = 6.

(c) M = 8.

Figure 16. – Comparison of total-pressure recoveries. y/D = 0.

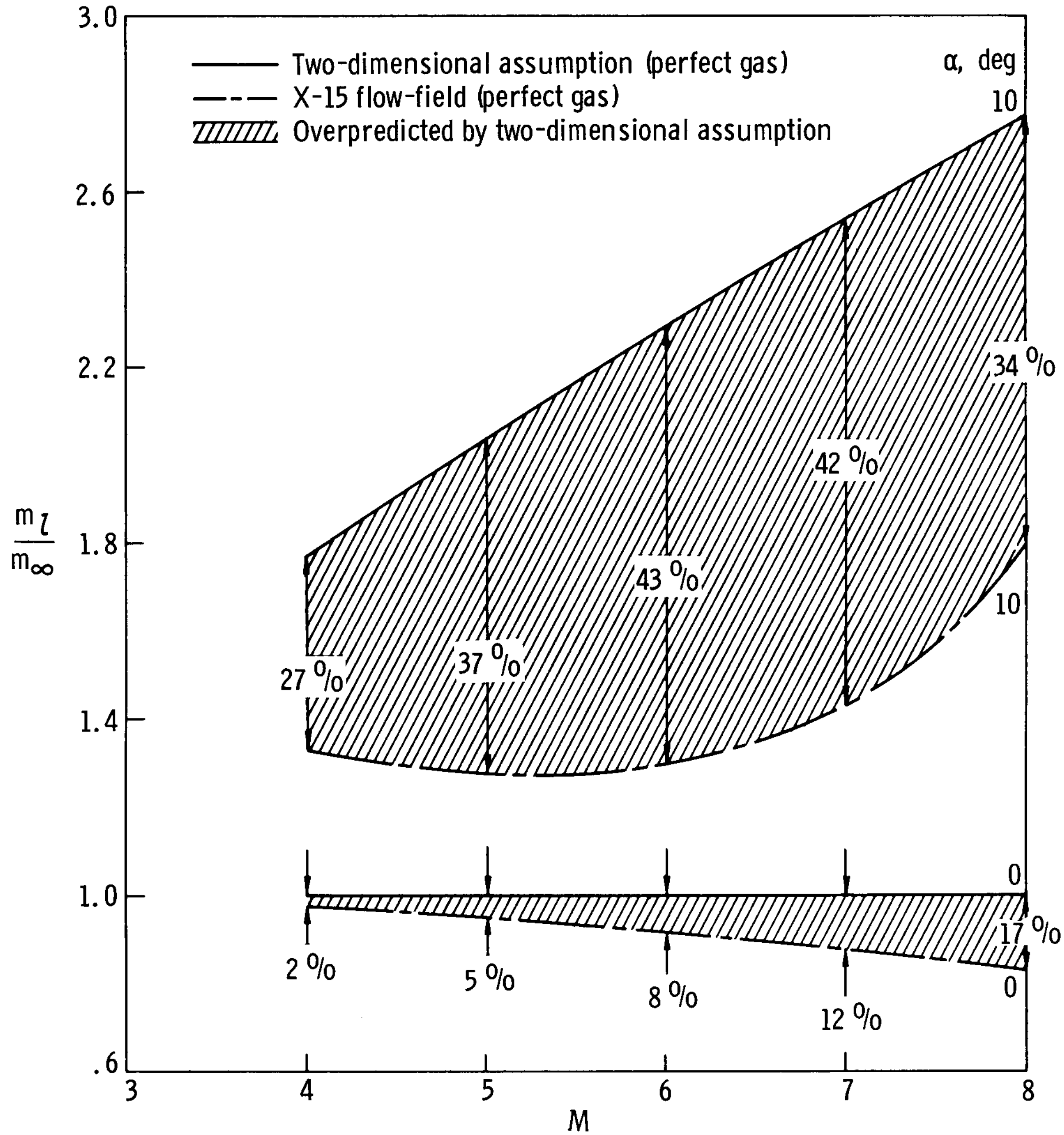

Figure 17. – Comparison of mass-flow ratios obtained from two-dimensional assumption and X-15 wind-tunnel data.

NASA-Langley, 1967 —— 2 H-478